A STUDY OF MECHANICAL PROPERTIES AND PROCESSABILITY OF BLOWN FILMS USING b-LLDPE AND LDPE BLENDS

BY

WAEL SULAIMAN FALLATAH

A Thesis Presented to the

DEANSHIP OF GRADUATE STUDIES

KING FAHD UNIVERSITY OF PETROLEUM & MINERALS

DHAHRAN, SAUDI ARABIA

In Partial Fulfillment of the
Requirements for the Degree of

MASTER OF SCIENCE

In

MECHANICAL ENGINEERING

JULY 2010

KING FAHD UNIVERSITY OF PETROLEUM AND MINERALS

DHAHRAN 31261, SAUDI ARABIA

DEANSHIP OF GRADUATE STUDIES

This thesis, written by **Wael Sulaiman Fallatah** under the direction of his thesis advisor and approved by his thesis committee, has been presented to and accepted by the Dean of Graduate Studies, in partial fulfillment of the requirements for the degree of **MASTER OF SCIENCE IN MECHANICAL ENGINEERING**.

Thesis Committee

Dr. Khaled Mezghani (Advisor)

Dr. Nesar Merah (Member)

Dr. Rached Ben-Mansour (Member)

Dr. Abdul-Ghani Al-Farayedhi

Department Chairman

Dr. Salam Zummo

Dean of Graduate Studies

19/7/10

Date

DEDICATED TO

MY BELOVED PARENTS, WIFE, SISTER AND BROTHER

ACKNOWLEDGMENTS

All praise and thanks are due to Allah (subhanahu wa ta'ala), who created the chance, created me and guided me to get the work completed.

Acknowledgment is due to the King Fahd University of Petroleum and Minerals for supporting this research. Thanks go, also, to King Abdul Aziz City for Science and Technology for supporting and funding this research.

I worked with many people during this research and to all of them I am very grateful. My thesis advisor, Dr. Khaled Mezghani, is the first. I got a lot from him and could feel very clearly the sharp improvement in my research experience after spending three years working with him. His persistent concern and continuous advices were really supportive. His help to make this work completed will not be forgotten. I would like also to acknowledge my committee members, Dr. Nesar Merah and Dr. Rached Ben-Mansour, for their guidance and encouragements. Their comments and observations were really helpful and thankful.

I would like to thank my colleague, Mr. Sarfaraz Furquan; his help started at the first day of the work and has not ended. He helped me a lot to get the experimental work completed. Thanks are extended, also, to Mr. Saleh Al-Abbasi, KFUPM Materials Science lab engineer, for his help in learning the instruments operations.

Thanks, before all of them, to my beloved parents. Their love and pray gave me a great support. I cannot forget my wife, also, who supported me significantly during the last

stages of the work. To all of my friends, I would say thank you so much for your moral encouragements and support.

TABLE OF CONTENTS

LIST OF TABLES

LIST OF FIGURES

THESIS ABSTRACT (ENGLISH)

NAME: WAEL SULAIMAN FALLATAH

TITLE: A STUDY OF MECHANICAL PROPERTIES AND PROCESSABILITY OF BLOWN FILMS USING b-LLDPE AND LDPE BLENDS

MAJOR: MECHANICAL ENGINEERING

DATE: JULY 2010

Butene based linear low density polyethylene (b-LLDPE) is a locally made polymer that has superior mechanical properties, but lower processability compared to low density polyethylene (LDPE). In the present study, the aim is to blend the two polymers at different blend ratios to enhance the processability of b-LLDPE. Effects of draw ratio (DR) and blow ratio (BR) on the mechanical properties of b-LLDPE and LDPE films were investigated. Different mechanical tests, such as tensile, impact and tear resistance were studied. Crystallinity and orientation tests of the produced films were carried out for characterization purposes. It was found that a draw ratio of 21 and a blow ratio of 1.6 are optimum selections.

Using the abovementioned draw and blow ratios, the effect of blending on the mechanical properties and processability was investigated. Blend ratios of 5, 10, 15, 20 and 50% of LDPE were used. Having a blend ratio of up to 20% of LDPE with b-LLDPE brought a great achievement. Blending with LDPE reduces the torque needed to turn the motor, which lowers the energy consumption and lowers the cost of the process, in turn. From the mechanical tests results, many mechanical properties improved dramatically. Adding up to 20% of LDPE enhanced the yield strength in machine direction except for the 5% LDPE. The tensile strength in MD increased up to 15% LDPE. In both directions, the ductility profiles are similar. There was an enhancement in ductility at blend ratios of 5

and 10 %. At 15 and 20% of LDPE the ductility was almost unaltered. There was an enhancement of about 45% at blend ratios of 15 and 20% in the toughness of the films in machine direction. In the transverse direction, the toughness increased by 50% when adding only 10% of LDPE. The impact properties were affected greatly with the addition of LDPE. With the addition of only 5% of LDPE, the failure energy and the energy to peak force were increased by almost 25%. Adding 10% of LDPE, showed deterioration in the failure energy but the energy to peak force was enhanced. The effect of blend ratio on the Elmendorf tear resistance was carried out. If 5 or 10% of LDPE is added, the enhancement of TD tear resistance will be around 90%. At 15 and 20% of LDPE the enhancement was amazingly 115 and 100%, respectively.

In general, the study of blend effect on mechanical properties showed improvement up to 20% LDPE. Furthermore, the torque requirement was reduced with the increase of blend ratio.

MASTER OF SCIENCE DEGREE

KING FAHD UNIVERSITY OF PETROLEUM AND MINERALS

Dhahran, Saudi Arabia

THESIS ABSTRACT (ARABIC)

الاسم: وائل سليمان يحي فلاته

عنوان الرسالة: دراسة الخصائص الميكانيكية وسهولة التصنيع للأغشية المصنعة بواسطة النفخ الهوائي باستخدام خليط من البولي إيثيلين المنخفض الكثافة الخطي والبولي إيثيلين منخفض الكثافة

التخصص: الهندسة الميكانيكية

التاريخ: يوليو ٢٠١٠

البولي إيثيلين منخفض الكثافة الخطي هو مبلمر مصنع محليا ويمتلك خصائص ميكانيكية ممتازة إذا ما قورن بالبولي إيثيلين منخفض الكثافة، لكنه أصعب منه تصنيعا. الهدف من هذه الرسالة هو خلط هذين المبلمرين لتحسين وتسهيل تصنيع البولي إيثيلين المنخفض الكثافة الخطي. قبل البدء بخلط المبلمرين تمت دراسة أثر قوة الشد وقوة نفخ الهواء على الخصائص الميكانيكية لكل منهما على حدة، ثم تم خلطهما بالنسب التالية: ٥، ١٠، ١٥، ٢٠ و ٥٠ % من البولي إيثيلين منخفض الكثافة. تم دراسة تحمل الأغشية للشد وللتصادم وللشق، واتضح أنه بإضافة إلى ٢٠% من البولي إيثيلين منخفض الكثافة تحسنت قابلية المبلمر على التصنيع كما كان متوقعا. الخصائص الميكانيكية تحسنت أيضا بشكل ملفت وغير متوقع خصوصا مقاومة المبلمر للشق بالاتجاه المعاكس لاتجاه الشد وأيضا صلابة الأغشية بنفس اتجاه الشد. تعتبر هذه النتائج إنجازا جديدا لأنه من المعتاد في حالة تحسن التصنيع فإن الخصائص الميكانيكية ستضعف ولكنها تحسنت بالعموم في هذه الدراسة.

درجة الماجستير في العلوم

جامعة الملك فهد للبترول والمعادن

الظهران، المملكة العربية السعودية

CHAPTER ONE

INTRODUCTION

1.1 Polyethylene.

Polyethylene is the largest produced thermo-plastic polymer in the world. Its monomer (Ethylene) can be polymerized in different ways to produce different types of polyethylene. A polyethylene molecule consists of a long backbone of an even number of covalently bonded carbon atoms, each having a pair of hydrogen atoms attached to it; chain ends are terminated by methyl groups (figure1.1).

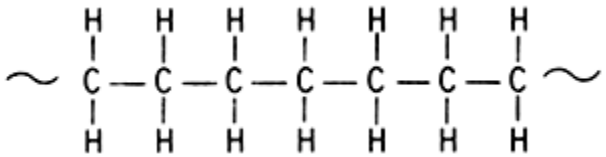

Figure1.1. Chemical Structure of pure polyethylene [1].

Polyethylene can be assembled in many ways; for instance, the main chain may have some branches. They may be short branches (2-6 carbons) or long branches (more than 7 carbons) depending on the polymerization process and conditions. Several types of polyethylene are present: (i) low-density polyethylene (LDPE); (ii) high-density polyethylene; (iii) linear low-density polyethylene.

Low-density polyethylene (LDPE) is the largest of the thermoplastics produced in the world. LDPE is produced by free radical bulk polymerization using traces of oxygen or peroxide (benzoyl or diethyl) and sometimes hydroperoxide compounds as the initiator. This results in the production of branched polymer molecules. LDPE is a partially crystalline solid with melting temperature range of 100 to 120°C, densities around 0.910-0.935 g/cm3 with crystallinities of 40-60% [1]. Branches act as imperfections, and as such the level of side chain branching determines the degree of crystallinity, which in turn affects polymer properties. The number of branches in LDPE may be as high as 20 per 1000 carbon atoms [1].

Polyethylene with limited branching, that is, linear or high-density polyethylene (HDPE), can be produced by the polymerization of ethylene with supported metal-oxide catalysts or in the presence of co-ordination catalysts. They are highly crystalline, with a melting point over 127°C (usually about 135°C), densities in the 0.94-0.97 range and crystallinity about 70-90% [1].

Linear low density polyethylene (LLDPE) is a copolymer of ethylene and alpha olefin, such as 1- butene, 1-hexene, and 1-octene. The presence of small amounts of an alpha olefin introduces short chain branches on the polymer backbone. The major commercial use of LLDPEs is in blown film applications, and the mechanical properties of LLDPE films are generally known to be influenced by molecular structural parameters such as molecular weight, molecular weight distribution, and the type, amount, and distribution of short chain branches.

Since its emergence, linear low-density polyethylene (LLDPE) has been challenging low-density polyethylene LDPE for market share due to the economic and technological advantages of the manufacturing process as well as to the more superior end-use performance compared with LDPE. However, the supremacy of LLDPE over LDPE, particularly in film applications, has been diminished to some extent by difficulties during the processing of LLDPE [1].

1.2 Film Blowing Process.

The majority of polymer films are manufactured by film blowing (blown film extrusion). A screw extruder is used to melt the polymer and pump it into a tubular die. Air is blown into the center of the extruded tube and causes it to expand in the radial direction. Extension of the melt in both the radial and down-stream direction, stops at the freeze line (frost line) due to crystallization of the melt. The nip rolls collect the film, as well as sealing the top of the bubble to maintain the air pressure inside (Figure1.2) [2].

Film blowing is the main processing of polyethylene. During the past decades, numerous efforts have been devoted to its modeling. However, there is no model that can successfully predict the film blowing process so far. First, film blowing is a very complex process with simultaneous effects of heat transfer, melt rheology, aerodynamics, and free-surface kinematics. Second, one needs complete and reliable data to assess the different models; these are rather sparse in the open literature [2].

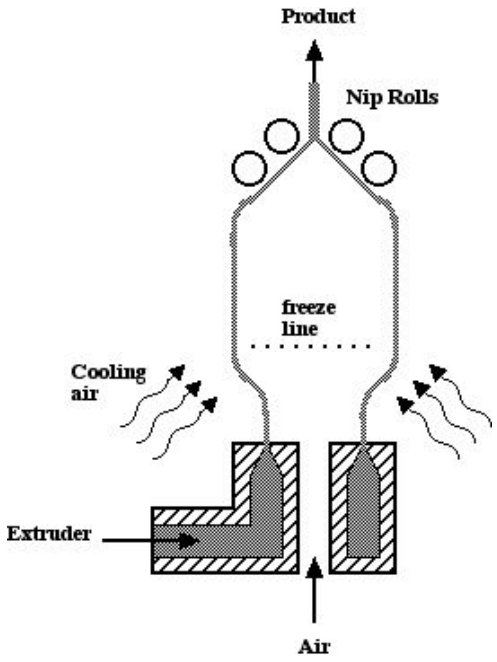

Figure1.2. Film Blowing Process schematic [1].

1.3 Polyethylene Blends

Polymer blends are of interest for generating mechanical properties that cannot be obtained from single component materials. This field is driven commercially by the demand for ever-increasing physical, mechanical, thermal and other properties. Faced with this situation, there are two general responses. The first would be to synthesize a new polymer to meet the desired specifications. This approach has two major drawbacks. Firstly, polymer science has yet to reach the state of maturity that allows the design and synthesis of materials with prescribed properties. The other problem is that the cost of developing and manufacturing a new polymer from scratch is very high. The

second approach, which is less expensive, is to blend polymers, usually not more than two, which provide the desired properties.

Polymer blends can be miscible, immiscible or partially miscible. The term compatible is used to describe polymer blends that have useful practical properties, regardless of whether they are miscible or immiscible whereas the term miscible is used to describe polymer blends that have thermodynamic miscibility down to the segmental level [2].

1.4 Mechanical Properties

Mechanical properties of a polyethylene can be defined as those attributes that involve the physical rearrangement of its constituent molecules or distortion of its initial morphology in response to an applied load. The nature of a specimen's response to applied stress can be correlated with its morphological and molecular characteristics. The mechanical properties of a specimen are controlled by its processing history within the limits imposed by its molecular characteristics. The typical mode of polyethylene deformation is one of yielding and necking followed by strain hardening. Localized yielding is especially noticeable in samples with higher degrees of crystallinity. The mechanical properties of polyethylene may be divided into two broad categories :(1) low strain properties such as yield stress and initial modulus and (2) high strain properties, characterized by ultimate tensile strength and strain at break. To a first approximation, the low strain properties are controlled by sample's morphological features and the high strain properties by its molecular characteristics [1].

1.4.1 Tensile Properties

Tensile properties of polymers are measured on instruments that record the force required to elongate a sample as a function of applied elongation (figure1.3). It is common to plot the load as “engineering stress”, that is, the force per unit area based upon the original cross-section of the specimen versus the engineering strain calculated as the elongation divided by original gauge length. The polymer chain length and its distribution are important molecular parameters in controlling the physical, mechanical and processing characteristics of polymers. Tensile testing of the specimen is carried out following the ASTM D 638 standard. Stress and strain are sample dependent. The stress on any element of the sample is equal to the force experienced by the element divided by its effective cross-sectional area. If the cross-sectional area of the specimen varies along its length, the stress will vary accordingly, i.e., stress is not necessarily uniform along the length or across the width of the specimen.

Most tensile samples start off as a “dogbone” (or dumbbell), the enlarged regions of which are gripped by the jaws of the tensile tester. Initially the gauge region elongates homogenously until it reaches a point at which one cross-sectional slice yields independently of the rest of the specimen. The onset of heterogeneous elongation corresponds to the yield point. As elongation continues, the incipient neck becomes better established until it forms a sharply defined region. Upon further elongation the neck propagates, growing to encompass the entire gauge length. The force required for neck propagation is essentially invariant, resulting in a “plateau” in the force versus elongation curve. Subsequent deformation, termed “strain hardening”, is homogenous, with the necked region elongating uniformly until the sample breaks. Depending on

molecular weight (MW) and its distribution (MWD), polyethylene can exist under a variety of formulations, each one with tailored properties for specific applications. The influence of MW on mechanical properties is clearly depicted in figure1.4 [2].

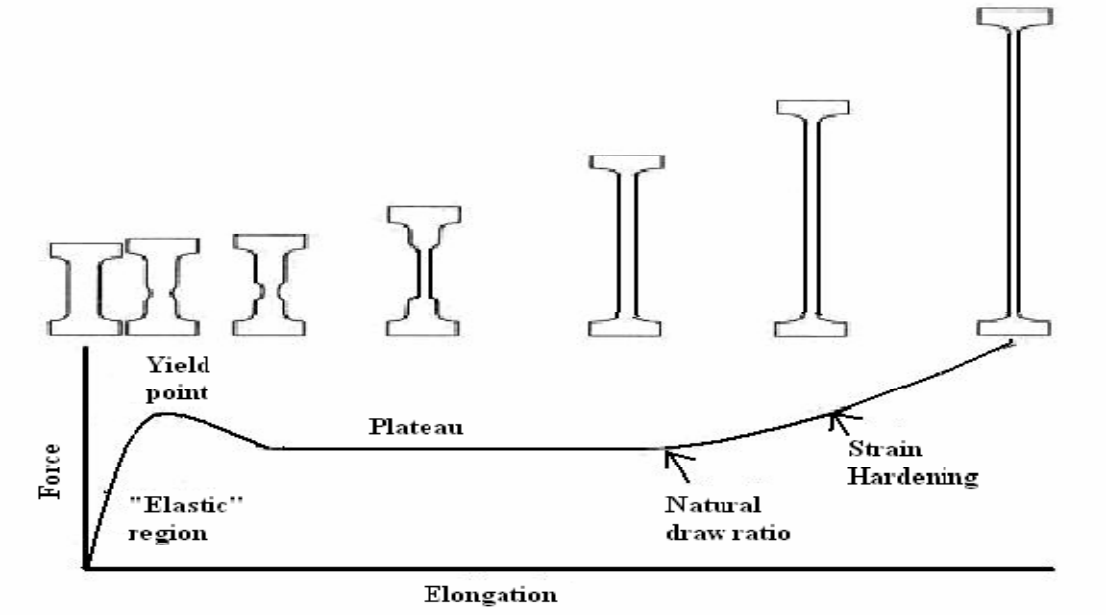

Figure1.3. Generalized force versus elongation curve for polyethylene illustrating principal tensile phenomena [29].

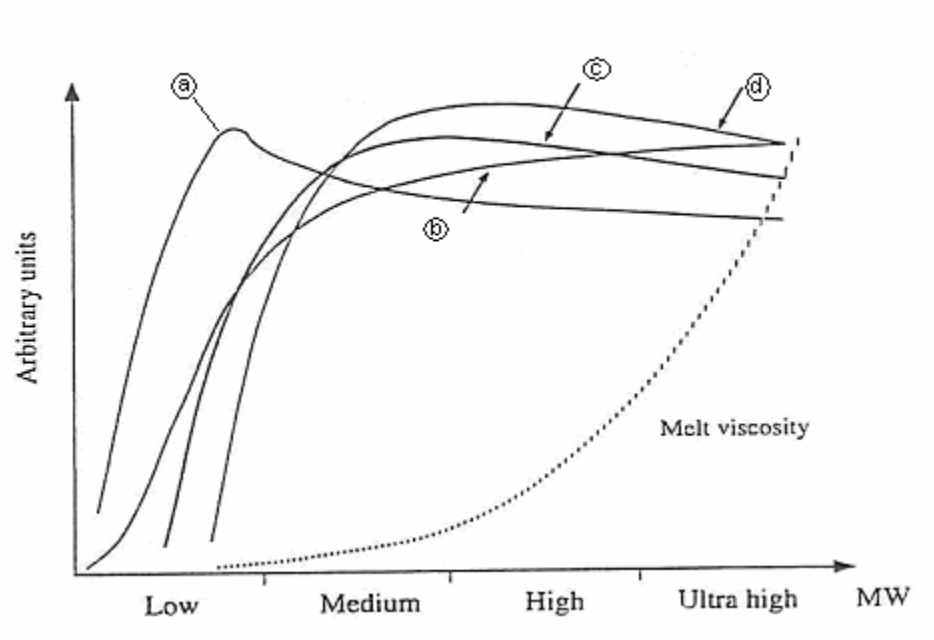

Figure1.4. Effect of molecular weight on the mechanical properties of polymers [1].

It is also important to note that some polymers may have different failure modes for different modes of deformation. In general all polymers at temperatures significantly below their glass transition temperatures (Tg –T >100°C) undergo brittle fracture. In the region above the brittle fracture regime, but below Tg , polymers usually yield and undergo plastic deformation as the modulus decreases (figure1.5).

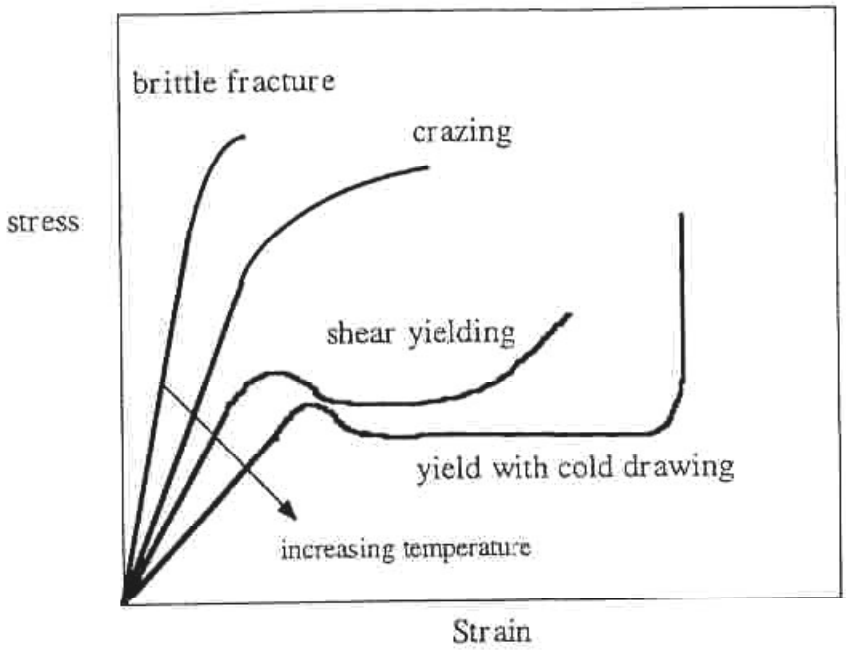

Figure1.5. Schematic of some failure modes of glassy polymers [29].

1.4.2 Elastic Modulus

When a polyethylene sample is subjected to external stress, there is an initial deformation prior to yield that is homogenous and is largely recoverable when the stress is removed. The value of elastic modulus is normally derived from the initial slope of the stress versus strain plot. The elastic modulus of a sample is a measure of its rigidity; the higher the modulus, the stiffer the sample. For the majority of isotropic samples, the

increase of elastic modulus is approximately linear with the degree of crystallinity. The two most commonly used units are pounds per square inch (psi) and mega Pascal (MPa) [2].

1.4.3 Yield Phenomena

Yielding occurs in a polyethylene specimen when it finishes deforming homogenously and starts to deform heterogeneously. Up to the yield point, deformation is principally elastic, whereas afterwards the sample takes on a permanent set. The nature of yield point varies greatly with the type of polyethylene examined and the conditions under which it crystallized. In LLDPE and LDPE samples, two distinct maxima may occur in close succession. In other cases, an inflection may be followed by a diffuse maximum. The mechanisms associated with multiple yield-peaks are the subject of speculation but may correspond to the yielding of bimodal distributions of lamellar populations.

The sharpness of the yield peak exhibited during stress versus strain measurements reflects the distinctness of usually observed neck. Samples with very low levels of crystallinity exhibit neither localized necking nor a distinct yield peak. For isotropic samples, the yield stress at room temperature is closely correlated to the degree of crystallinity and thus to the sample density. The yield stress of a specimen is of great interest from a practical point of view. In many cases it represents the maximum allowable load that a sample can withstand while still performing its assigned role. Once a sample has yielded, its dimensions are irrevocably changed, and it may no longer meet the requirements for continued service. In cases, where there is a distinct yield maximum in the stress-strain curve, the force required to propagate a neck along the

length of a sample is lower than the yield stress. Once such a sample has yielded, it will continue to elongate unless the applied load is removed [2].

1.4.4 Ultimate Tensile Strength

The ultimate tensile stress also known as the "tensile strength" of a sample is the force required to break it divided by its original cross-sectional area. The values of ultimate strength of LDPE samples are generally lower than that of LLDPE samples largely because of the higher percent elongation values obtained for the LLDPE samples. Actually, this is the property that gives LLDPE an advantage over LDPE in blown film packaging application [2].

1.4.5 Elongation at Break

This term refers to the strain of the sample at the point of tensile failure. The strain at break of the polyethylene sample is a function of its molecular nature and its initial orientation. The molecular characteristics that facilitate drawing are similar to those that promote the development of high degrees of crystallinity. Features that hinder the slippage of chains past one another during crystallization also inhibit the drawing process. The two principal inhibitors to chain movement are entanglements and branch points. Thus high molecular weight linear polyethylene resins and branched samples have lower strain at break values than low molecular weight unbranched samples. For ductile samples at a given MW, the strains at break values fall as their comonomer

content increases. Similarly, for a given comonomer content, the strain at break of ductile samples falls as the molecular weight increases. The molecular weight corresponding to the transition between brittle and ductile behavior increases as the comonomer content increases [2].

1.5 Thermal Properties

Semicrystalline polymers in general differ from most crystalline solids in that they display a melting range rather than a discrete melting point. The melting range is a consequence of the expected distribution of lamellar thickness in the solid state.

1.5.1 Melting Range

Polyethylene undergoes a transition from the semicrystalline to the molten state that takes place over a temperature range that can span from less than 10°C up to 130°C. As it passes through this transition the semicrystalline morphology gradually takes on more of the characteristics of the amorphous state at the expense of the crystalline regions. The melting range is broad because it consists of a series of overlapping melting points that correspond to the melting of lamellae of various thicknesses. A dispersion of lamellar thicknesses is a natural consequence of entanglements and chain branching that divides chain backbones into a series of discrete crystallizable sequences with a distribution of lengths. The broadest melting ranges occur in branched samples crystallized during rapid cooling.

The melting characteristics of polymers are commonly investigated by means of Differential Scanning Caloriemetry (DSC). DSC provides a trace, called a thermogram that consists of the instantaneous heat capacity of a specimen plotted as a function of temperature. The greater the volume of crystallites that melt at a given temperature, the higher the sample's instantaneous heat capacity. There is an approximately inverse relationship between the position of the peak maximum and the overall breadth of the melting peak. Samples with lower molecular weights, lower levels of branching, and slower crystallization rates tend to have narrower melting distributions and elevated peak melting temperatures. The normalized area under the peak, which is a measure of degree of crystallinity, can be approximately correlated with the temperature of the peak maximum and the sharpness of the melting range [1].

1.5.2 Heat of Fusion and Crystallinity.

The heat of fusion (ΔH_f) of a sample is a measure of the amount of heat that must be introduced to convert its crystalline fraction to the disordered state. It is thus uniquely dependent upon the degree of crystallinity of the sample and the theoretical heat of fusion of a 100% crystalline sample. The heat of fusion (ΔH) of 100% crystalline polyethylene sample has been calculated to be 293.6 J/g [1].

$$\% \text{ Crystallinity} = \frac{\Delta H_f}{\Delta H} \times 100$$

The factors that determine the actual degree of ordering realized, and hence the heat of fusion, are principally the rate of crystallization and the degree of orientation. The

slower the crystallization process or the higher the degree of orientation, the greater will be the heat of fusion [1].

CHAPTER TWO

LITERATURE REVIEW

2.1 Investigations on the Film Blowing Process

Pearson and Petrie [2, 3] and petrie [4] have done the first major work dealing with modeling the film blowing process. There are two major processes to produce biaxially oriented polymeric films, namely the flat film extrusion process and the film blowing process. In the former, biaxial orientation is achieved in two steps. The extruded film is first stretched in the machine direction by using two pairs of nip rolls, and then the film is oriented in the transverse direction by use of a tentering machine. On the other hand, film blowing process is a one step method. The film is oriented in the machine and transverse directions at the same time. In this process, a polymer melt is extruded through an annular die. The molten polymer tube exiting the die is drawn by a pair of take-up rolls, thus stretching the film in the machine direction, while the air inflates the tube, thus stretching the film in the transverse direction. There are several advantages of using film blowing process over the flat film method [5, 6]: (i) a simultaneous biaxial stretching, (ii) uniform properties across the film from the axial symmetry of the bubble, and (iii) no edge scrap. Therefore, film blowing process is widely used to manufacture thin films in the industry.

Usually, film blowing is operated with air ring for rapid cooling and stabilization of the bubble. Because a change in temperature affects rheological properties to a great extent, the heat transfer is important in analyzing the process. Dealy and Farber [7] used a radiation pyrometer to measure the thermal history of the fluid. Manges and Predhol [8] studied the effect of the cooling air on the temperature change of the bubble. The properties of the final film are greatly affected by the processing conditions.

2.1.1 Extrudate Swell.

When a polymer melt is extruded in a die, the extrudate swells. For many years, the behavior of extrudate swell has attracted much attention from researchers. Some of them [9, 10] asserted that the extrudate swell occurs from the relaxation of axial normal stress, while the other [11] argued that this occurs from the relaxation of radial normal stresses. It is generally agreed that the extrudate swells as a result of the recovery of the elastic deformation imposed in the die.

2.1.2 Bubble Stability.

The problem of bubble stability was first described by Ast [12]. Han and Park [13] presented detailed description of the instability for a single layer film of LDPE and PS/HDPE blends by recording the bubble behavior through still pictures. They concluded that lowering the extrusion temperature improved the blown film stability for HDPE and LDPE. They observed pulsations of the bubble diameter as the stretch ratio

increased under uniaxial deformation for small blow-up ratio (BUR) less than unity and observed a wavy film under biaxial deformation for BUR larger than 1.5. Kanai and White [14] investigated the kinematics and stability of the tubular film process over a wide range of BURs, Take-up Ratios (TURs) and frost line heights (FLHs) for LLDPE, LDPE and HDPE and suggested that the stability should be in the following order: LDPE > HDPE > LLDPE. Minoshima and White [15] have concluded that in tubular film extrusion, the LDPEs are most stable. They also discussed their results in terms of Maxwell model representation. Following Previous authors, Ghaneh-Fard et al [16] has extensively studied the bubble stabilities for LDPE, HDPE, LLDPE and PP by giving detailed definition of bubble instabilities and suggested the relative order of stability: LDPE > HDPE > LLDPE > PP. LDPE is always the most stable in the polymers investigated during film blowing, it is due to the strain hardening behavior of LDPE in elongation flow.

2.2 Mechanical Analysis and Processability investigations of PE Blends.

Beagan and Malleja [17] have investigated the processability and mechanical performance of metallocene catalyzed polyethylene resins for packaging applications. Blends and co-extruded structures with metallocene catalyzed polyethylene resins and a conventional low-density polyethylene were produced. The effect of processing parameters, resin density, melt flow index, molecular weight, molecular weight distribution and co-monomer type on the viscosity characteristics and mechanical properties were investigated. The glass transition temperatures (T_g) of the films were

measured using dynamic mechanical thermal analysis techniques and these T_g's were found to be much lower than the conventional linear low-density polyethylenes. The structural compatibility of the blends was determined using differential scanning calorimetry and dynamic thermal analysis. All blends were found to be compatible in the amorphous phase.

Shishesaz and Donatelli [18] studied the tensile properties of binary and ternary blends of low, medium and high-density polyethylene. The tensile properties of these materials indicated that the blends formed either compatible or semicompatible mixtures.

Krishnaswamy and Lamborn [19] have prepared various LLDPE resins that encompassed those polymerized using Ziegler-Natta, metallocene and chromium oxide based catalysts. These resins were blown into film at similar process conditions, and the tensile properties of the resulting films were investigated in relation to the orientation characteristics.

The tensile properties were observed to be significantly different from those of isotropic/un-oriented polyethylene specimens of similar density. These were explained in terms of lamellar organization and orientation characteristics of LLDPE blown films. Investigation of the temperature dependence (between –50ºC to +50ºC) of these tensile properties indicated an increase in modulus, yield stress and break stress with decreasing temperature pointing to the possible role played by the decreased mobility of the noncrystalline phase at lower temperatures.

Jafari et al [20] have prepared morphologically distinct binary polymer blends by melt mixing of HDPE and various LLDPEs for the entire range of blend composition under

identical processing conditions. The morphology of the tensile fracture surfaces of blend, the parent polymers and their blends are quite interesting and show good correlation with thermal and mechanical properties. The HDPE forms linear and interpenetrating fibrils with a large number of interfibrillar separation, whereas, octane containing LLDPE (O-LLDPE) with almost equal number of branching to that of HDPE shows nicely formed twisted fibrils. On the other hand, pentene containing LLDPE (P-LLDPE) manifests a straight fibrillar with well-defined boundary comprising many thin fibrils with alternative thick and thin regimes and perfection, whilst butane containing LLDPE (B-LLDPE) showed thick comparatively smooth and well-defined imperfect boundary of the tensile fracture.

Kim and Park [21] studied three linear low density polyethylene (LLDPE) resins of similar melt index and density. The resins were synthesized with different comonomers in the Unipol pilot-plant scale reactor. The molecular structure, blown film morphology, and film strength properties of the resins have been comprehensively characterized. The film dart drop impact strength of the LLDPEs increases in the order of ethylene/l-butene, ethylene/l-octene, and ethylene/ 1-hexene copolymers; whereas the Elmendorf tear strength of them increases in the order of ethylene/l-butene, ethylene/l-hexene, and ethylene/l-octene copolymers. The mechanical properties seem to be highly associated with the length and distribution of short chain branches and, consequently, the lamellar thickness distribution of the resins. Films were prepared using 40 mm Yoo Jin Engineering tubular blown LLDPE film equipment under a commercially typical processing condition. It consists of a full flight screw with an L/D of 25 to 1, a 50 mm spiral die with a die gap of 2.3 mm, an air ring, nip rolls, and take-up device. The

extrusion motor speed was fixed at 810 rpm; and the extrusion temperature was fixed at 160, 170, 180, 190. The film thickness, blow-up ratio, and frost-line height were 30 μm, 2.5 : 1, and 25 cm, respectively.

Hong et al. [22] investigated the use of hyperbranched polymer (HBP) as a processing aid for linear low-density polyethylene (LLDPE) in the tubular film blowing process. Through the addition of HBP, sharkskin was successfully eliminated without significantly changing the overall physical properties of LLDPE films. Also, there was a minimum of 40% enhancement in processing rate with addition of 0.5 wt% HBP. The study showed that HBP and LLDPE are immiscible, and HBP has a tendency to migrate to the surface, subsequently, it seems to form a lubricating layer between the metal surfaces and the bulk material. This phase separation between HBP and LLDPE results in an HBP-rich surface, which has a high potential to create unique surface properties tailored to various applications. Rheological analysis indicated that excessive slip was present in HBP/LLDPE suggesting that the onset of slip is not the cause of sharkskin. On the contrary, it may be partially responsible for the elimination of sharkskin.

Y. Fang, et al. [23] evaluated the inline birefringence of two blend systems in film blowing. The first system consisted of a metallocene catalyzed linear low density polyethylene (mLLDPE-1) and a low density polyethylene (LDPE-1); the second one was made of a metallocene catalyzed polyethylene containing sparse long chain branches (mLLDPE-2) and another low density polyethylene (LDPE-2). Experimental data show that before the crystallization starts, the birefringence of the mLLDPE-2/LDPE-2 blends is a linear function of blend composition, suggesting miscibility of the mLLDPE-2/LDPE-2 blends. However, the birefringence of the mLLDPE-1/LDPE-1

blends shows positive deviations with respect to a linear function of blend composition. This is caused by the existence of form birefringence, suggesting immiscibility of the mLLDPE1/LDPE-1 blends. The non-uniform biaxial elongational viscosity (NUBEV) at the reference temperature of 175°C for LDPE-1 was evaluated for different operating conditions. The results show that NUBEV is approximately a unique function of the deformation rate, confirming the validity of the assumptions and technique used for the NUBEV calculation. The NUBEV and the non-uniform biaxial Trouton ratio (NUTR) of the mLLDPE-2/LDPE-2 blends was also evaluated using the same technique. The NUBEV of all mLLDPE-2/LDPE-2 blends shows a strain-thinning behavior within the deformation rates investigated. Furthermore, the NUTR results show that LDPE-2 deviates largely from the Newtonian fluid behavior, whereas mLLDPE-2 is quite close to the Newtonian behavior. Nevertheless, the NUTR of the mLLDPE-2/LDPE-2 blends is almost a linear function of blend composition.

R. Krishnaswamy and A. Sukhadia [24] characterized the orientation features of several linear low-density polyethylene (LLDPE) blown films; and significant insights into the morphological origin of Elmendorf tear resistance were developed. The orientation features of all the LLDPE blown films investigated were described in terms of the Keller–Machin “row” structure. The machine direction (MD) tear resistance was observed to be higher when the non-crystalline chains were closer to equi-biaxial in the plane of the film. Further, the transverse direction (TD) tear resistance was observed to be high when the crystalline lamellae were minimally curved and oriented closer to the film TD. These results indicated that deformations in the interlamellar region and the

stresses borne along the lamellar long axes play important roles in distinguishing the MD and TD tear resistances, respectively, of LLDPE blown films.

Gupta et al. [25] utilized Three nearly identical linear low density polyethylene resins based on copolymers of ethylene with 1-butene (B), 1-hexene (H) and 1-octene (O) to investigate the effect of short chain branch length on the mechanical properties of blown and compression molded (quenched and slow cooled) films. The content of short chain comononer in the three copolymers was ca. 2.5–2.9 mol% that corresponded to a density of 0.917–0.918 g/cm3. Within a given series, the tensile properties of these films do not show any significant difference at slow deformation rates (up to 510 mm/min), even though the DSC and TREF profiles of 'H' and 'O' differed slightly in comparison to 'B'. However, at higher deformation rates (ca. 1 m/s), the breaking strength of these films was found to increase with increasing short chain branch length. In addition, the Spencer impact and Elmendorf tear strength of the blown films were also observed to increase with increasing short chain branch length. Further, dart impact strength and high-speed puncture resistance (5.1 m/s) of 1-octene and 1-hexene based samples was also observed to be higher than that based on 1-butene. The blown films displayed low and comparable levels of equivalent in-plane birefringence and crystalline orientation by wide angle X-ray scattering. This confirms that the differences in mechanical properties in the blown film series are not attributable to differences in molecular orientation. The deformation behavior of both the compression molded and blown films were also investigated in a well-defined controlled regime by analyzing their essential work of fracture. It was found that the essential work of fracture of films based on 1-hexene and 1-octene was higher than that of films based on 1-butene. While the origin of these

differences in mechanical properties with increasing short chain branch length is not fully understood, the present investigation confirms this effect to be pronounced at high deformation rates for both the blown and compression molded quenched films. Blown films were made from each of the three resins under the following conditions: 100 mm (4 in.) die diameter, 1.5 mm die gap, 37.5 mm diameter single-screw extruder (L/D=24, compression ratio 2.2:1), 115 rpm screw speed (ca. 27 kg/h output rate), 2.5:1 blowup ratio (BUR) and barrel and die temperatures set to 190^{o}C. The freeze line height (FLH) was between 20 and 28 cm and cooling was accomplished with a dual lip air ring using ambient air that had a temperature of ca. 20^{o}C. Films with different thicknesses (12.5–100 μm or 0.5–4 mil) were produced this way.

S. Furquan [27] studied the effect of blend ratio of h-LLDPE with LDPE on the mechanical properties and the processability of blown films. He found that with addition of up to 20% LDPE, there was a 20% enhancement in MD yield strength without any decrement in the MD ductility. The MD toughness also observed an increment of around 43%. The enhancement in TD tensile strength was more than 75%. The TD ductility improved slightly in comparison to pure h-LLDPE. There was 20% enhancement in failure energy due to 5% blend ratio. The TD tear resistance improved by almost 100% by adding 20% of LDPE. With addition of up to 20% LDPE, many mechanical properties improved. This was of great importance because the processability was improved with the addition of LDPE.

2.3 Objectives of the Present Work.

From the previous literature review it was observed that the influence of blend ratio between b-LLDPE and LDPE needs to be studied. Furthermore, a comprehensive correlation between processability and mechanical properties of the films should be investigated. A similar approach was done by A. Sarfaras [27] with hexene based LLDPE. In this study a butene based LLDPE will be used which is another type of locally made LLDPEs. The b-LLDPE has lower cost and better thermal properties [28].

The objectives are as follows:

- Study the effect of blend ratio of 1-Butene LLDPE and LDPE on the processability of the blown films.
- Examine the effect of blend ratio on tensile and impact properties and tear resistance of the films.
- Determine optimum blend ratio that gives optimum processability and mechanical properties.
- Compare b-LLDPE with h-LLDPE in terms of the effect of blending on the mechanical properties and processability of blown films.

CHAPTER THREE

EXPERIMENTAL PROCEDURE

3.1 Film Blowing Process.

3.1.1 The Extruder.

In this study, a twin screw extruder, manufactured by Thermo Haake Co., as shown in figure 3.1 was used to melt and process the polymers. The extruder has an L/D ratio of 40 and seven controllable heating zones. A temperature profile of 120/ 150/ 180/ 200/ 200/ 200/ 200 ^{o}C was maintained throughout the extruder. This temperature profile was chosen by putting into account the machine limitations, processability and the degradation of the polymer. The torque needed to turn the screw, the temperature of the molten polymer at different heating zones and the pressure at the extruder exit are monitored, controlled and reported by a computer. The screws are driven by a motor with variable speeds. The extruder has two metered feeders; one of them has been manufactured locally at KFUPM shop. One feeder is supplied with b-LLDPE and the other is fed with LDPE pellets. With the help of the metered feeders, the polymer pellets are continuously supplied to the extruder barrel with constant mass flow rate. Upon entering the heating zones inside the extruder barrel, the pellets melt and are pushed towards a die at the extruder exit.

3.1.2 The Film Blowing Unit

A film blowing unit is attached to the extruder, as shown in figure 3.2. It consists of a tubular die, an air ring attached to it, nip rolls and a pick up unit. A melt pump figure 3.3 connects the extruder exit with the die to assure constant mass flow rate. When the molten polymer departs the extruder it is pushed through the tubular die with the aid of the melt pump. While exiting the die, the molten polymer is exposed to a cooled air from the air ring. Air is blown into the center of the extruded tube causing it to expand in the radial direction. Extension of the melt in both the radial and down-stream directions stops at the freeze line (frost line) due to crystallization of the melt. The nip rolls collect the film and seal the top of the bubble to maintain the air pressure inside. As discussed above, the temperature profile was chosen as to produce maximum mass flow rate complying with the degradation of the polymer and the equipment constraints. Other parameters are optimized while maintaining the temperature profile as constant. The optimized screw speed was 12 rpm. This speed provides the maximum flow rate without overwhelming the motor torque limitation. The pressure at the extruder exit was around 16 bars. The melt pump speed of 10 rpm was optimum as to maintain constant flow rate. Conforming to the abovementioned parameters, the maximum flow rate was around 8 grams/min.

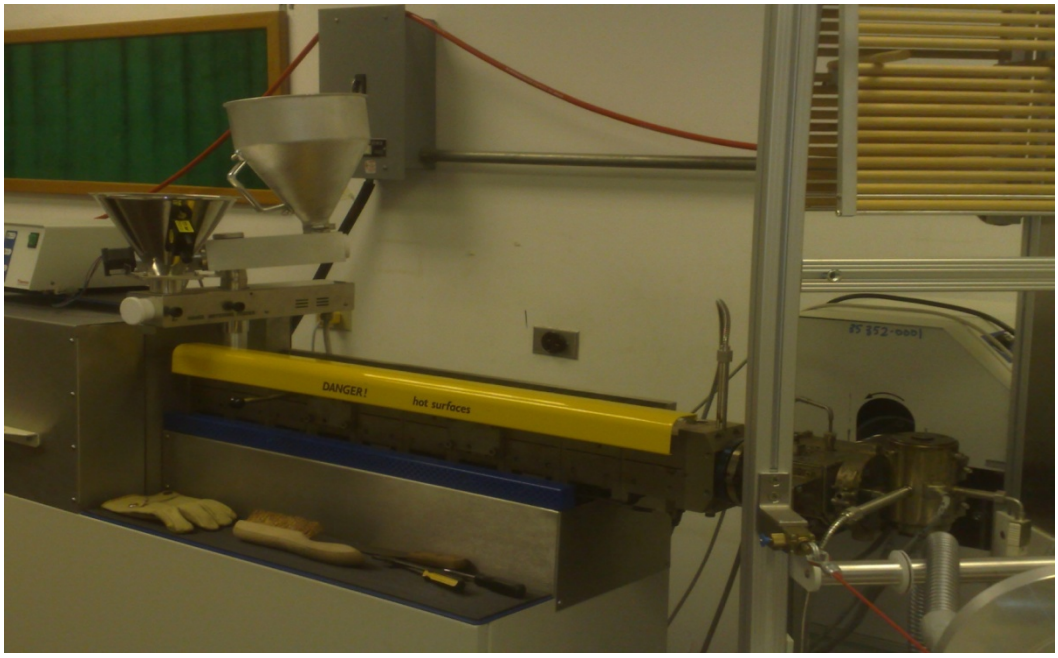

Figure3.1. Thermo Haake twin screw extruder.

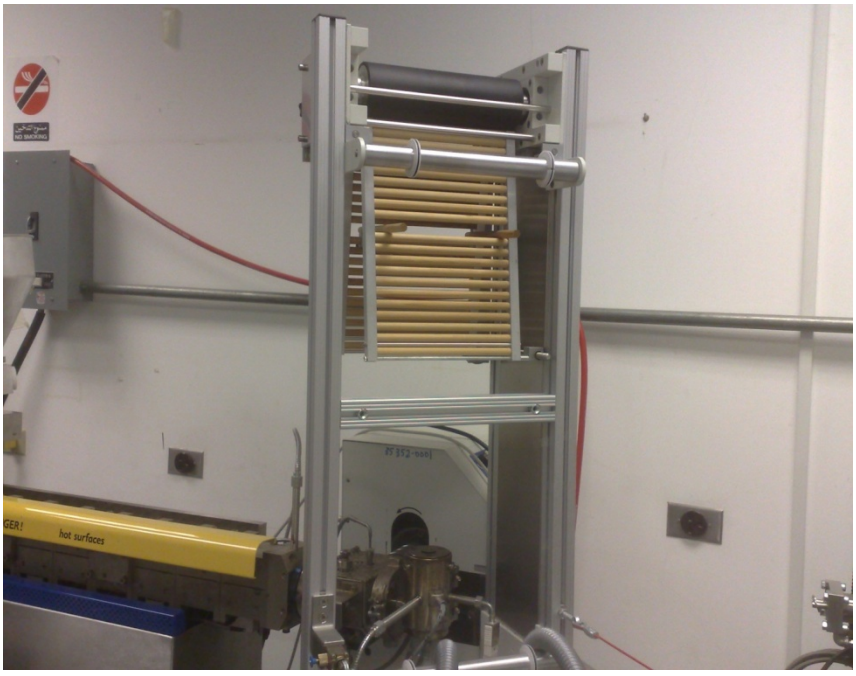

Figure 3.2. The Film Blowing Unit.

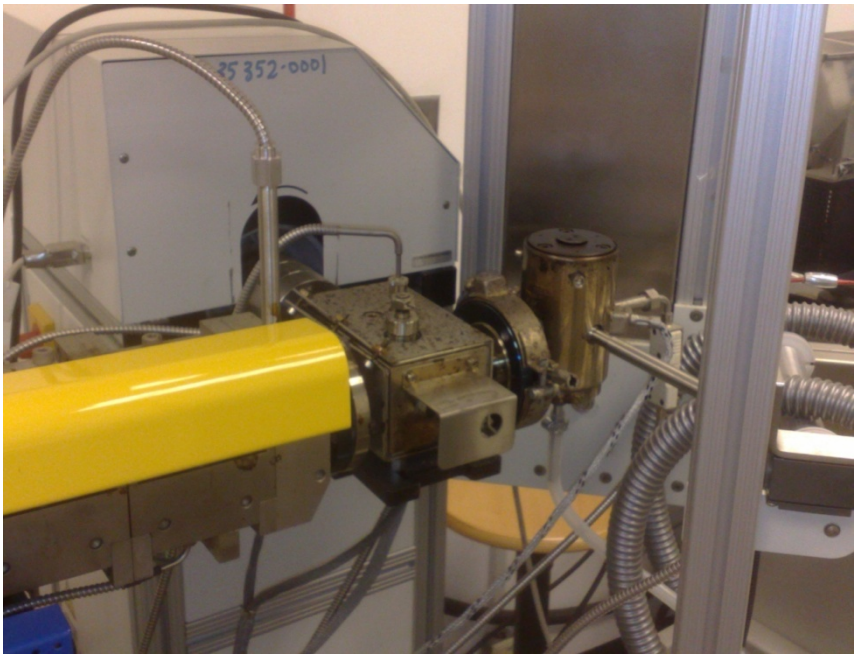

Figure 3.3. The melt pump.

3.1.3 Calibrating the Feeders.

The extruder has two metered feeders; one of them has been manufactured locally at KFUPM shop. Blending using two feeders with the same point of entry provides a highly homogenized mixture. The first feeder was used to feed b-LLDPE Pellets, while the second one was used for LDPE. The calibration plots for the two feeders are shown in figures 3.4 and3.5.

3.1.4 Draw Ratio and Blow Ratio Calculations.

Two important parameters that affect the properties of the produced films are the draw ratio (DR) and the blow ratio (BR). The draw ratio is the ratio between the nip rolls speed and the speed of the molten polymer while departing the die. The melt velocity can be calculated simply by taking into account the mass flow rate of the polymer, the density and the area of the die exit:

$$\text{Draw Ratio (DR)} = \frac{nip\ rolls\ speed}{melt\ velocity}$$

$$\text{Melt velocity (m/min)} = \frac{mass\ flow\ rate\ (g/min)}{density\left(\frac{g}{cm^3}\right) \times area(cm^2)} \times (10^{-2} m/cm)$$

$$\text{Area} = \frac{\pi}{4}(D_0^2 - D_i^2)$$

Where $D_0 = 2.5\ cm$ and $D_i = 2.3\ cm$ are the outer and inner diameters of the die, respectively. Therefore, Area = 0.7536 cm^2. The mass flow rate was fixed to be 8.3 grams/min. For LLDPE, the density (g/cm^3) can be calculated by the following equation [29]:

$$\rho_{LLDPE@T} = 0.8674 - 6.313 \times 10^{-4} \times T + 0.367 \times 10^{-6} \times T^2 - 0.055 \times 10^{-8} \times T^3$$

The die temperature is 230°C. Therefore:

$$\rho_{LLDPE@230} = 0.7349\ (\frac{g}{cm^3})$$

For LDPE, the density (g/cm^3) is calculated by [29]:

$$\rho_{LDPE} = 0.868 \times e^{-6.73\times10^{-4}\times T}$$

The die temperature is 230°C. Therefore:

$$\rho_{LDPE@230} = 0.7435\ (\frac{g}{cm^3})$$

The blow ratio (BR), on the other hand, is the ratio between the diameter of the bubble and the diameter of the die.

$$BR = \frac{Bubble\ Diameter}{Average\ Die\ Diameter}$$

The draw ratio can be varied by changing the nip rolls speed, while the blow ratio can be varied by adjusting the pressure inside the bubble with the help of the compressed air line.

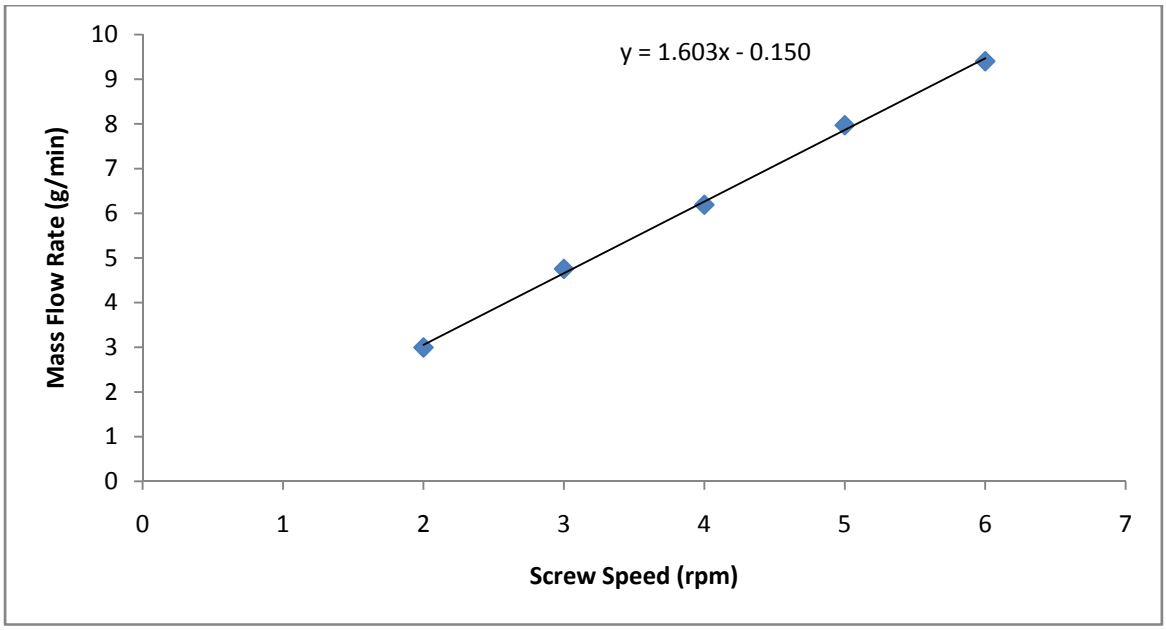

Figure 3.4. b-LLDPE Feeder Calibration.

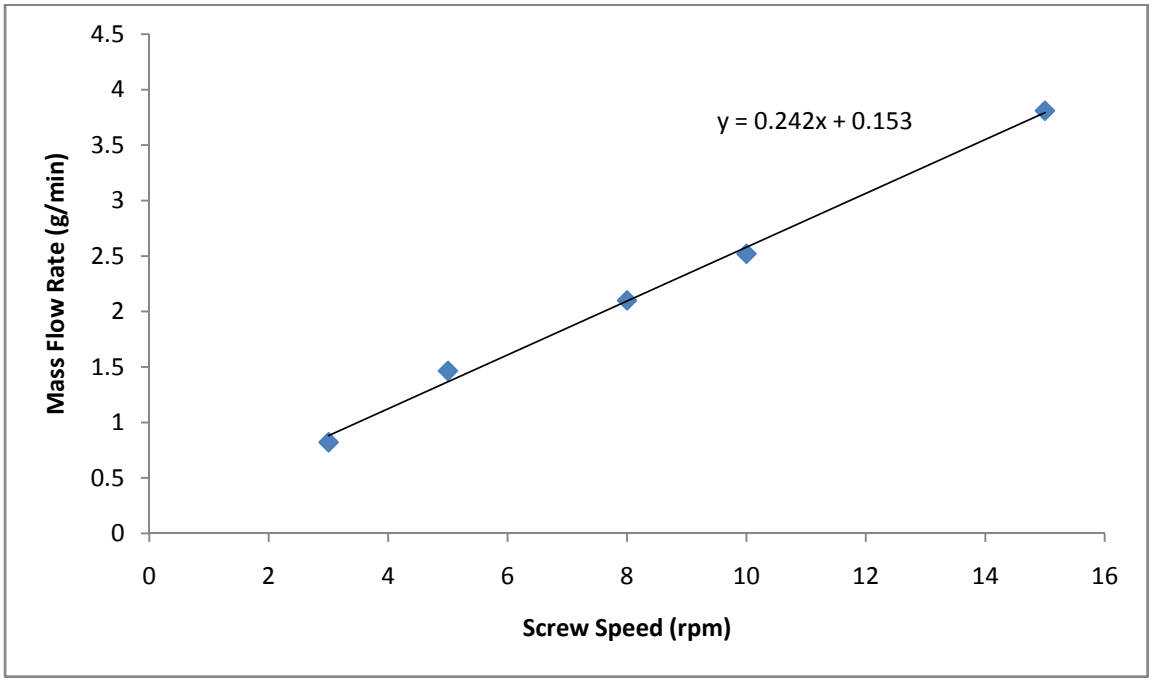

Figure 3.5. LDPE Feeder Calibration.

3.2 Tensile Test.

The films were tested using the Instron tensile machine, as shown in figure 3.6. ASTM D 882 standard was followed. Rectangular cross section specimens (figure 3.7) were cut in both machine and transverse directions (MD&TD). The gage length was 15 mm and the width was 3.14 mm. the thickness was measured using a high precision micrometer with an accuracy of 0.001 mm. the machine pulled the specimens with the rate of 50 mm/min. Tensile properties such as yield strength, tensile strength, ductility and toughness were determined from stress-strain plot. The stress is the force needed to pull the specimen divided by the cross sectional area of the specimen, while the strain is the elongation of the specimen divided by the original gage length.

3.3 Impact Test.

Instron Dynatup 9250 G impact tester (figure 3.8) was used to determine the impact properties of the produced films. The tests were conducted in accordance to ISO 7765-2 standard. The machine is connected to a computer with impulse data acquisition and analysis system. A locally made fixture with a 40 mm inner diameter was used to clamp the samples. The films were cut to a circular shape with a diameter of 80 mm and stacked together to compose a thickness of 0.8 mm. A dart with 0.78 inch diameter and a weight of 9.4 kg was used. The velocity of the dart while coming in touch with the specimen was fixed to be 2 m/s. The force-deformation diagram (figure 3.9) obtained from this test reveals several impact properties such as peak force, energy to peak force and failure energy.

Figure 3.6. Instron 5569 tensile machine.

Figure 3.7. Tensile rectangular specimen.

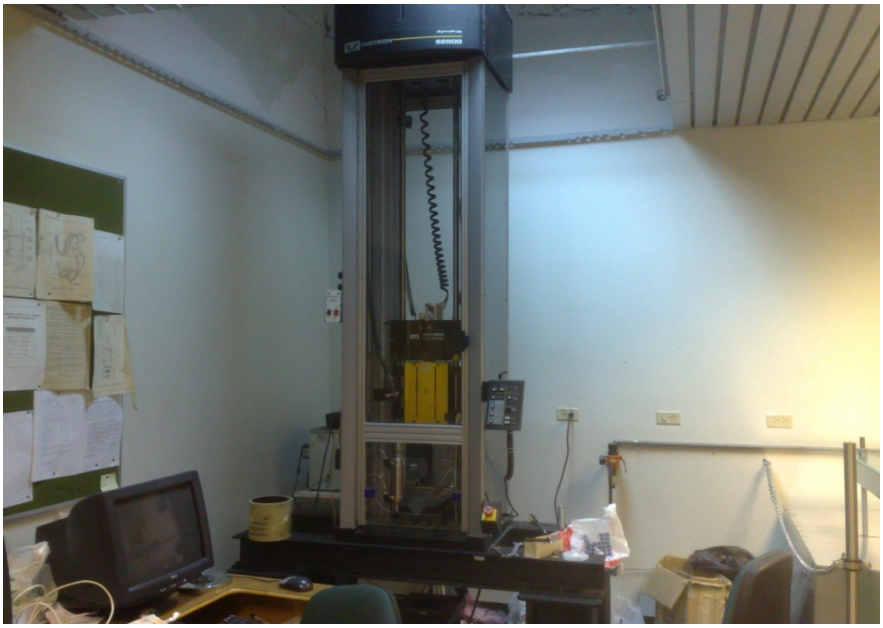

Figure 3.8. Instron Dynatup 9250 G impact tester.

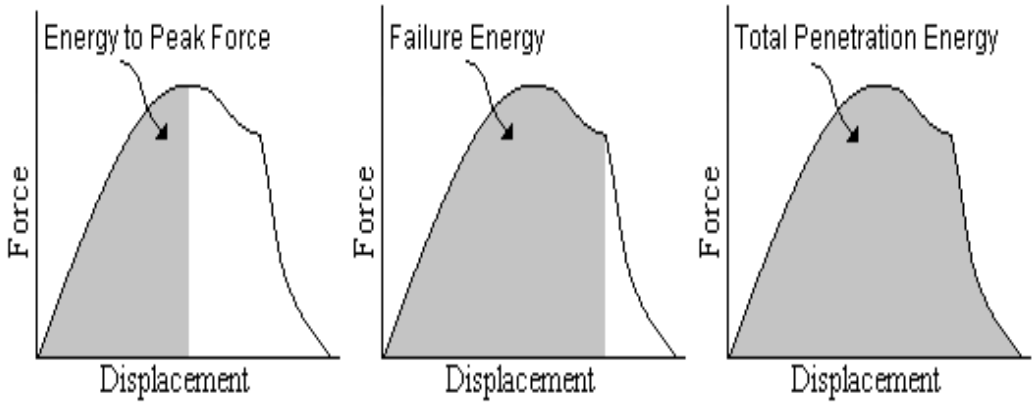

Figure 3.9. Force-deformation diagram.

3.4 Elmendorf Tear Resistance Test.

A Thwing-Albert Elmendorf tear tester (figure 3.10) was used to test films tear properties in both machine and transverse directions. ASTM 1922 standard was followed. The force in grams was measured using a calibrated pendulum. The specimen is fixed by automatic pneumatic jaws. The specimen is then precut with a knife attached to the instrument. After releasing the pendulum, it falls down in an angular motion and tears the specimen. The energy loss is the energy needed to tear the specimen. The tear resistance (in grams) is, then, normalized by dividing by the thickness of the tested film.

3.5 Crystallinity.

The crystallinity of the produced films was determined by the differential scanning calorimetry (DSC) technique. Mettler DSC 882 (figure 3.11) was used. Temperature calibration of the instrument was done with an indium sample. Samples are cut to form small circular disks and stacked together. The weight of the stack should be in the range from 3 to 5 mg. The stack is placed inside a small aluminum pan and sealed. The specimens were scanned from 20^{o}C to 180^{o}C at a rate of 10^{o}C/min. For b-LLDPE, the enthalpy of the 100% crystalline polymer is 293.6 J/g [29].

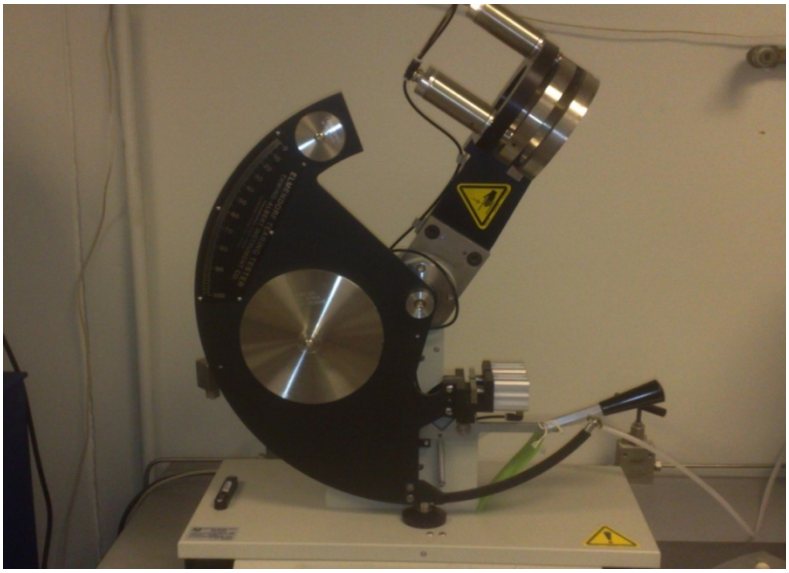

Figure 3.10. Thwing-Albert Elmendorf tear tester.

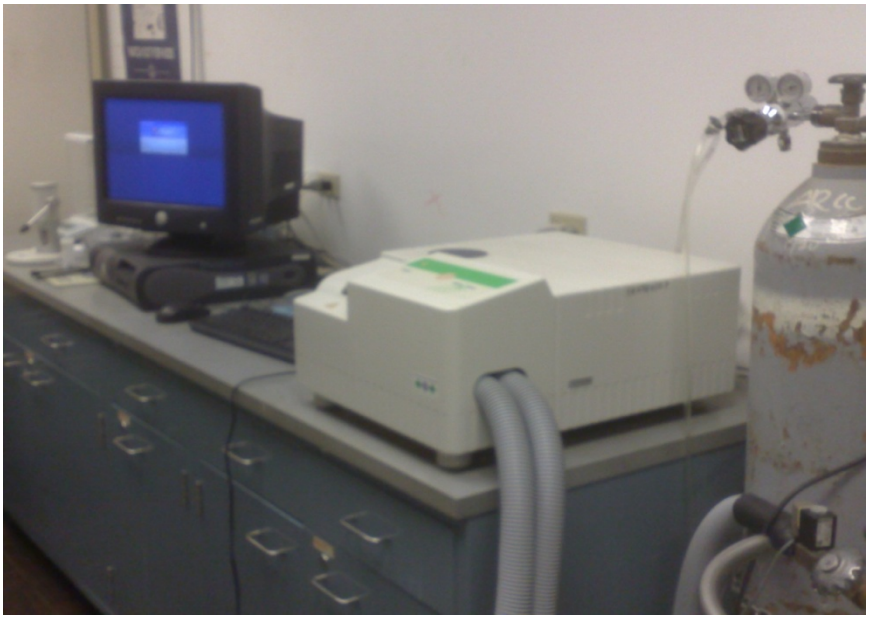

Figure 3.11. Mettler DSC 882.

3.6 Orientation.

The degree of orientation in the films in both directions was determined using an optical microscope with a compensator. The microscope is set in a dark field transmission mode with the lens axis visible on the screen. A glass plate is kept between the polarizer and the analyzer, while the compensator is placed between the sample and the analyzer. The first reading of the compensator at this position is recorded. Rectangular specimens are prepared and placed between two glass plates. The base is turned to an angle of 45^0. The orientation is represented by the retardation wavelength with respect to the dial increment of the compensator, taking into account the thickness of the film. The birefringence (Δn) is calculated by the following equation which is provided with the compensator manual:

$$\Delta n = \frac{r - r_0}{t}$$

where $\boldsymbol{r}$ and $\boldsymbol{r}_0$ are the phase differences or the retardation times for the glass plates with and without the film, respectively. The phase difference can be calculated by the following equation:

$$r = \frac{c}{10{,}000} \times 10{,}000\, f(i)$$

where *c/10,000* is prescribed to be 6.5. The value of *10,000 f(i)* is given by:

$$10{,}000\, f(i) = 2.824\ (i)^2 + 2.399\ (i)$$

where *i* is the compensator angle.

CHAPTER FOUR

RESULTS

4.1 Effect of Draw Ratio on Mechanical Properties of b-LLDPE Films.

The draw ratio is the ratio between the nip rolls speed and the speed of the molten polymer while departing the die. As discussed earlier, the optimized screw speed was 12 rpm. This speed provides the maximum flow rate without overwhelming the motor torque limitation. The pressure at the extruder exit was around 16 bars. The melt pump speed of 10 rpm was optimum as to maintain constant flow rate. Conforming to the abovementioned parameters, the maximum flow rate was around 8 grams/min. The draw ratio can be varied by changing the nip rolls speed. In this study, draw ratios of 21, 36, 49 and 64 were used. These values are limit to the machine constraints.

4.1.1 Tensile Test.

Tensile tests were conducted using ASTM D882 standard. Five samples were tested in machine and transverse directions for each draw ratio. The average and standard deviation were then calculated. Stress-strain curves at different draw ratios in both directions are shown in figures 4.1-8.

The tensile properties of b-LLDPE at different draw ratios (DRs) in both directions are listed in tables 4.1 and 4.2.

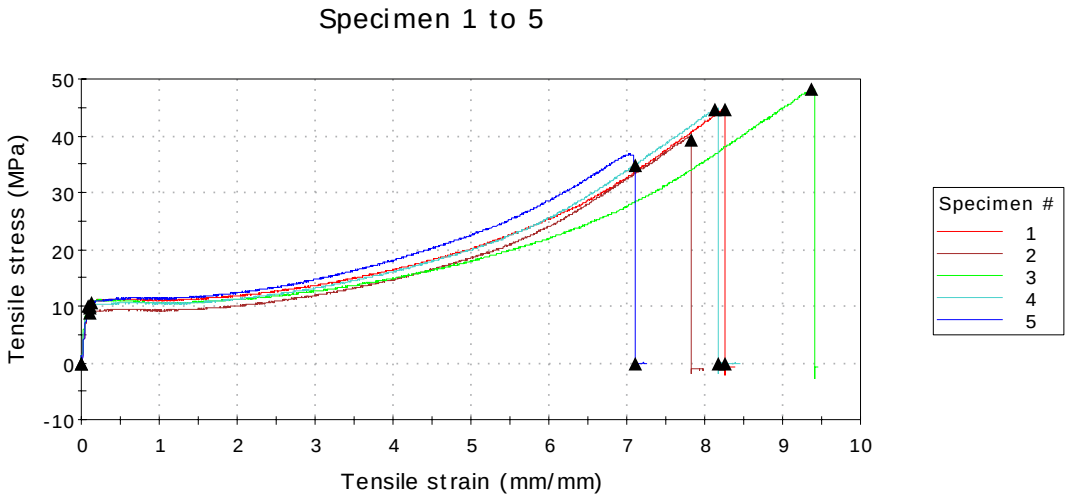

Figure 4.1. Machine direction stress-strain curves at a draw ratio of 21.

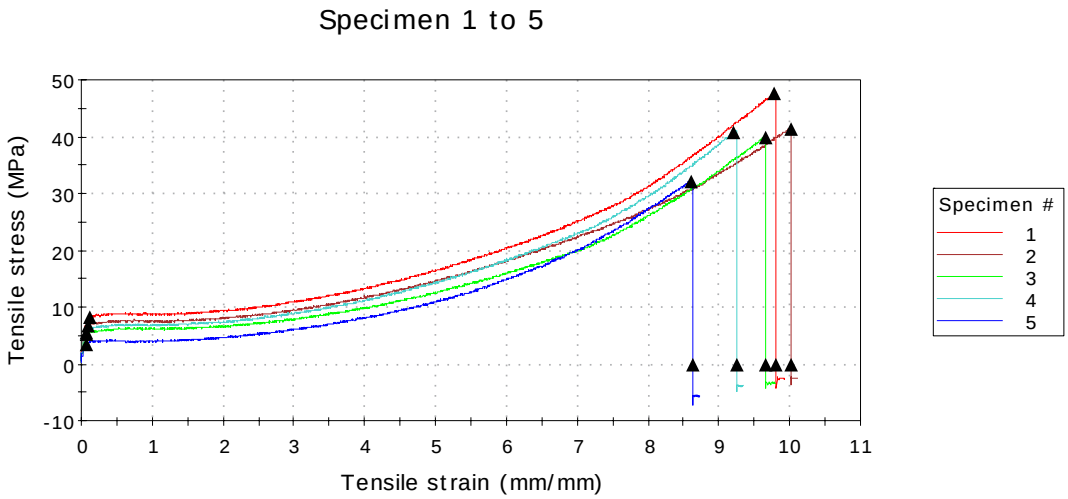

Figure 4.2. Transverse direction stress-strain curves at a draw ratio of 21.

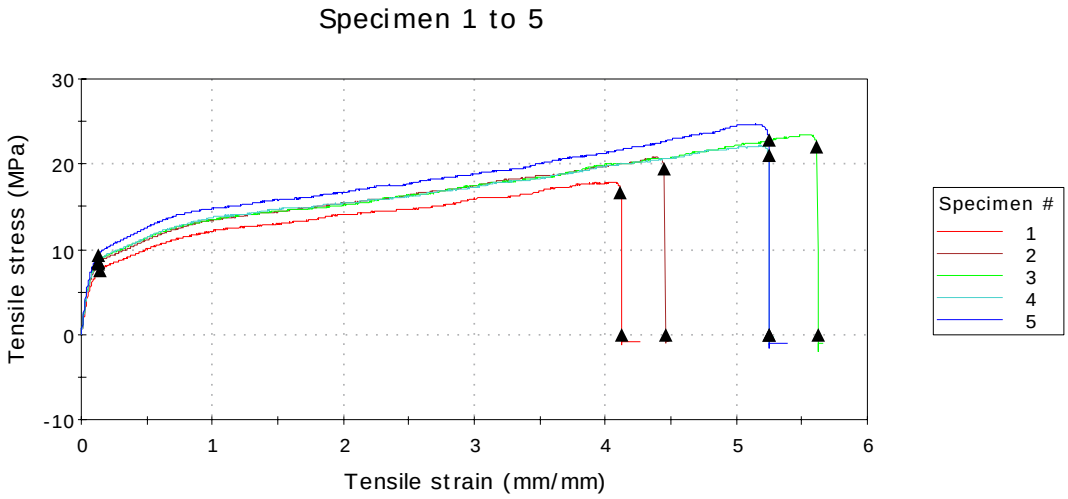

Figure 4.3. Machine direction stress-strain curves at a draw ratio of 36.

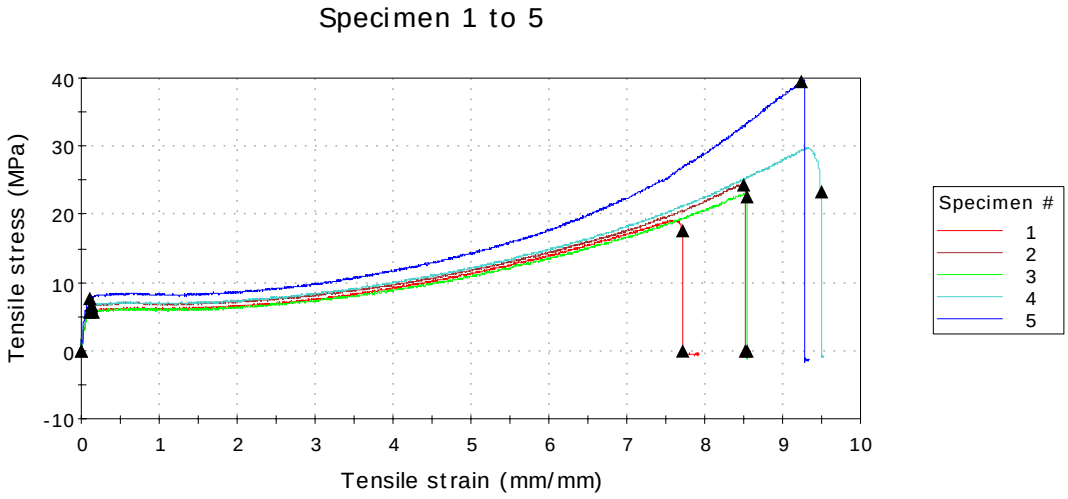

Figure 4.4. Transverse direction stress-strain curves at a draw ratio of 36.

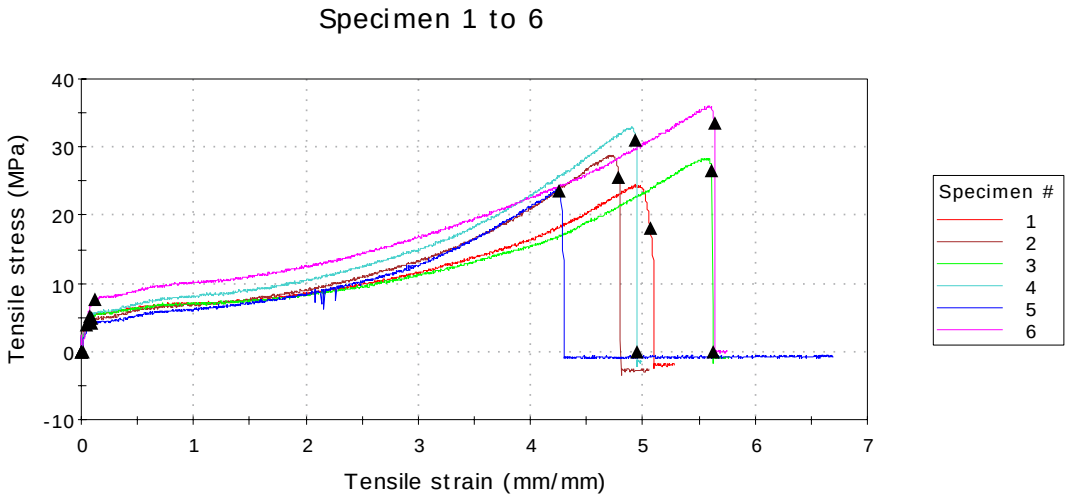

Figure 4.5. Machine direction stress-strain curves at a draw ratio of 49.

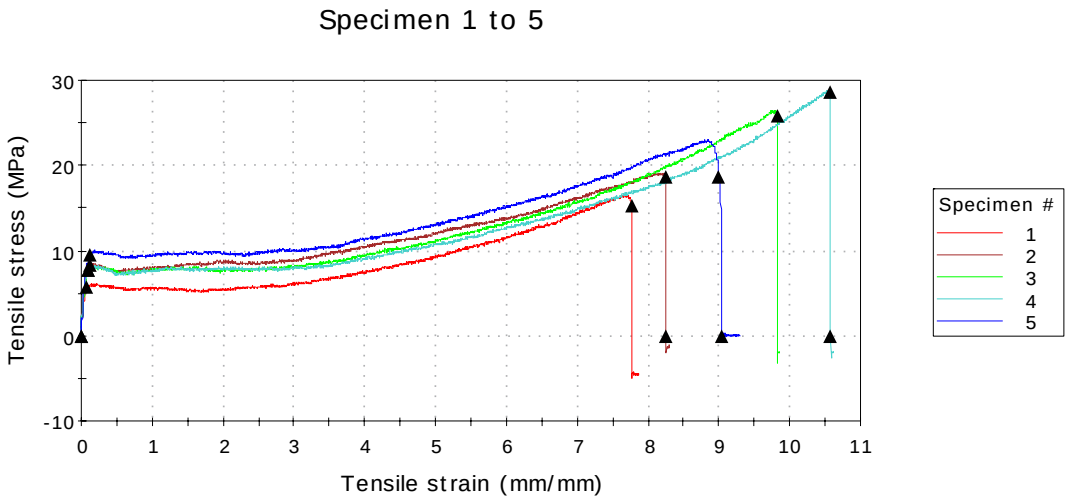

Figure 4.6. Transverse direction stress-strain curves at a draw ratio of 49.

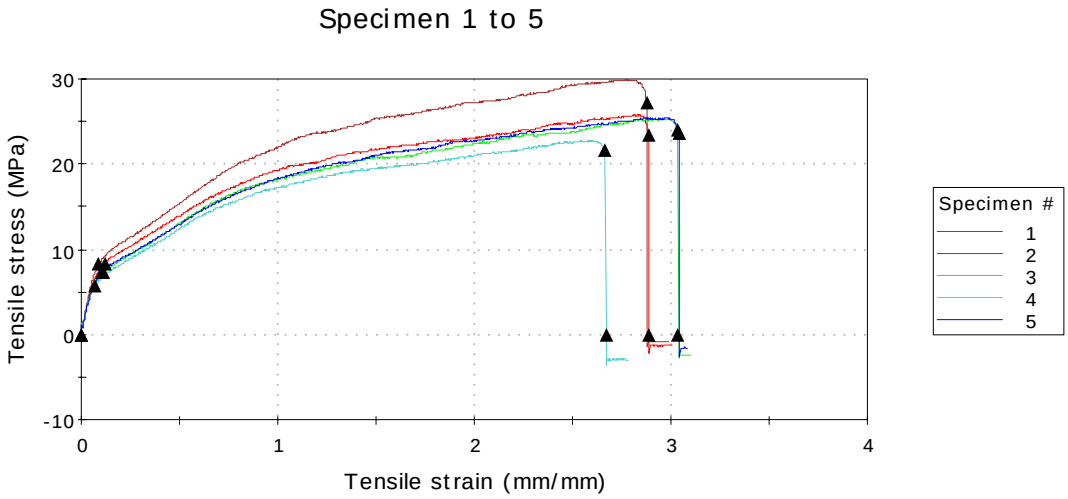

Figure 4.7. Machine direction stress-strain curves at a draw ratio of 64.

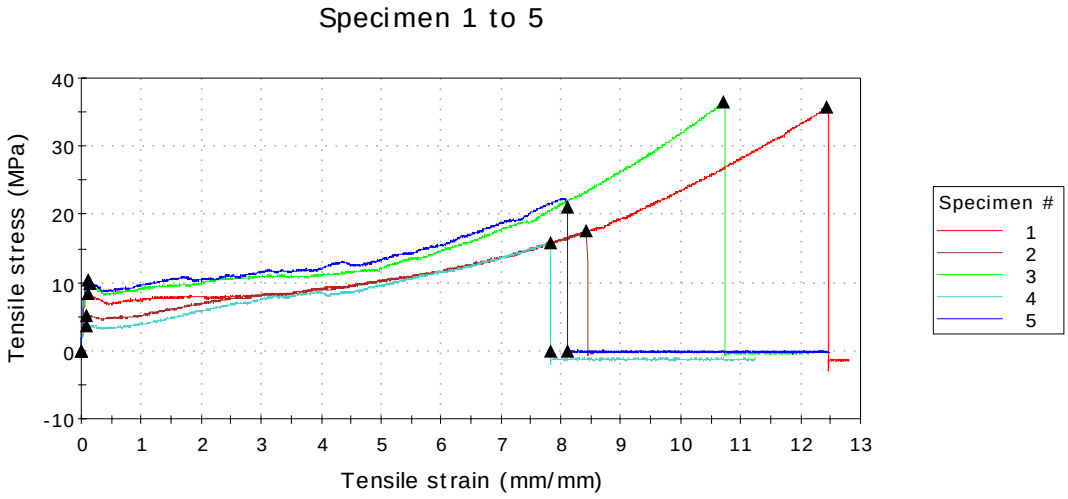

Figure 4.8. Transverse direction stress-strain curves at a draw ratio of 64.

Table 4.1. MD tensile properties of b-LLDPE at different DRs

DR	Yield strength (MPa)	Std Dev	Tensile strength (MPa)	Std Dev	Ductility (%)	Std Dev	Toughness (MPa)	Std Dev
21	9.6	0.9	40.2	4.3	821	72.8	140	22.3
36	8.8	0.6	21.1	2.8	490	62.5	120	19.3
49	5.3	0.9	28.6	4.0	505	52.0	118	26.3
64	7.3	1.0	25.7	2.6	289	15.6	105	11.1

Table 4.2. TD tensile properties of b-LLDPE at different DRs

DR	Yield strength (MPa)	Std Dev	Tensile strength (MPa)	Std Dev	Ductility (%)	Std Dev	Toughness (MPa)	Std Dev
21	6.6	1.3	40.6	5.4	955	50.8	211	9.2
36	6.2	0.8	27.1	7.8	887	70.2	160	19.3
49	7.8	1.4	23.7	5.1	876	93.3	145	8.3
64	8.8	2.9	27.2	9.2	950	180.3	181	20.7

4.1.2 Impact Test.

Impact tests were conducted using ISO 7765-2 standard. Five samples were tested for each draw ratio and the average and the standard deviation were calculated. Impact test diagrams for one of the tested samples at different draw ratios are shown in figures 4.9-12. The peak force, energy to peak force and failure energy values at different draw ratios are presented in table 4.3.

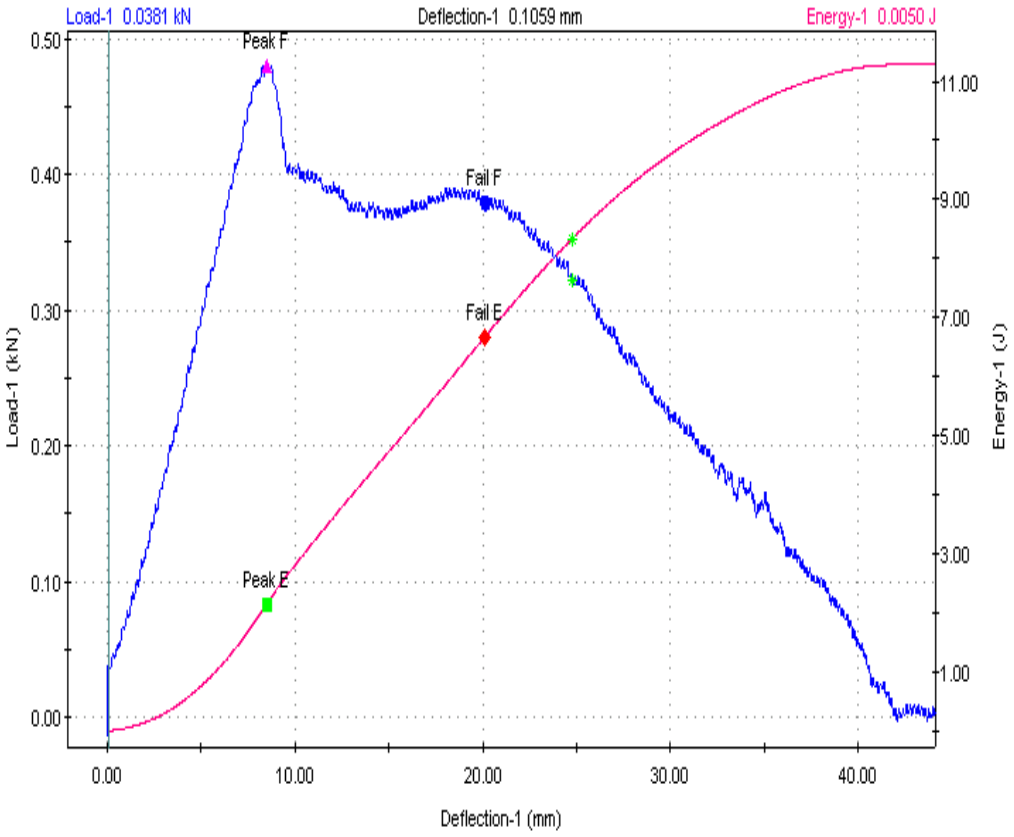

Figure 4.9. Impact test diagram at a draw ratio of 21.

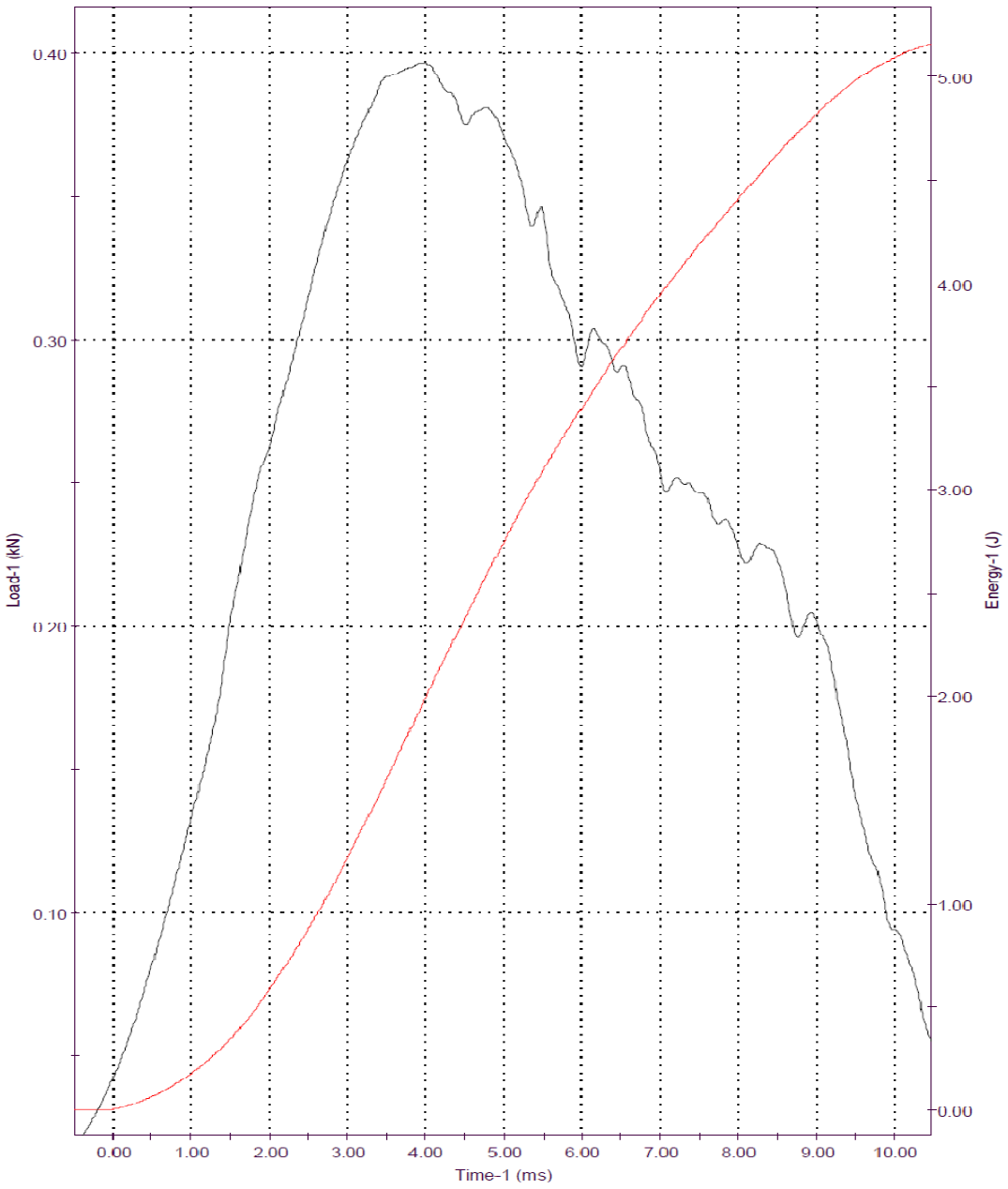

Figure 4.10. Impact test diagram at a draw ratio of 36.

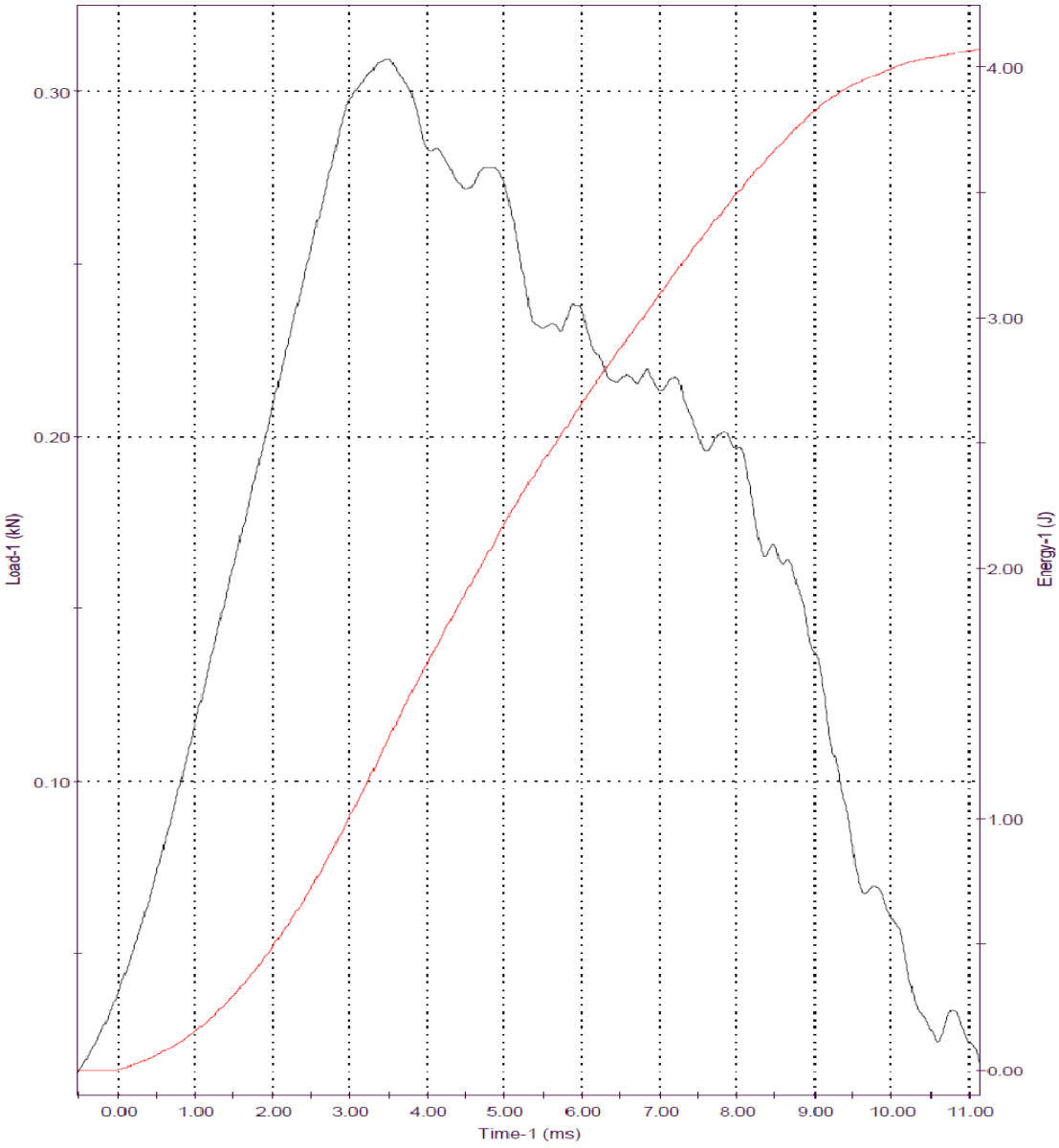

Figure 4.11. Impact test diagram at a draw ratio of 49.

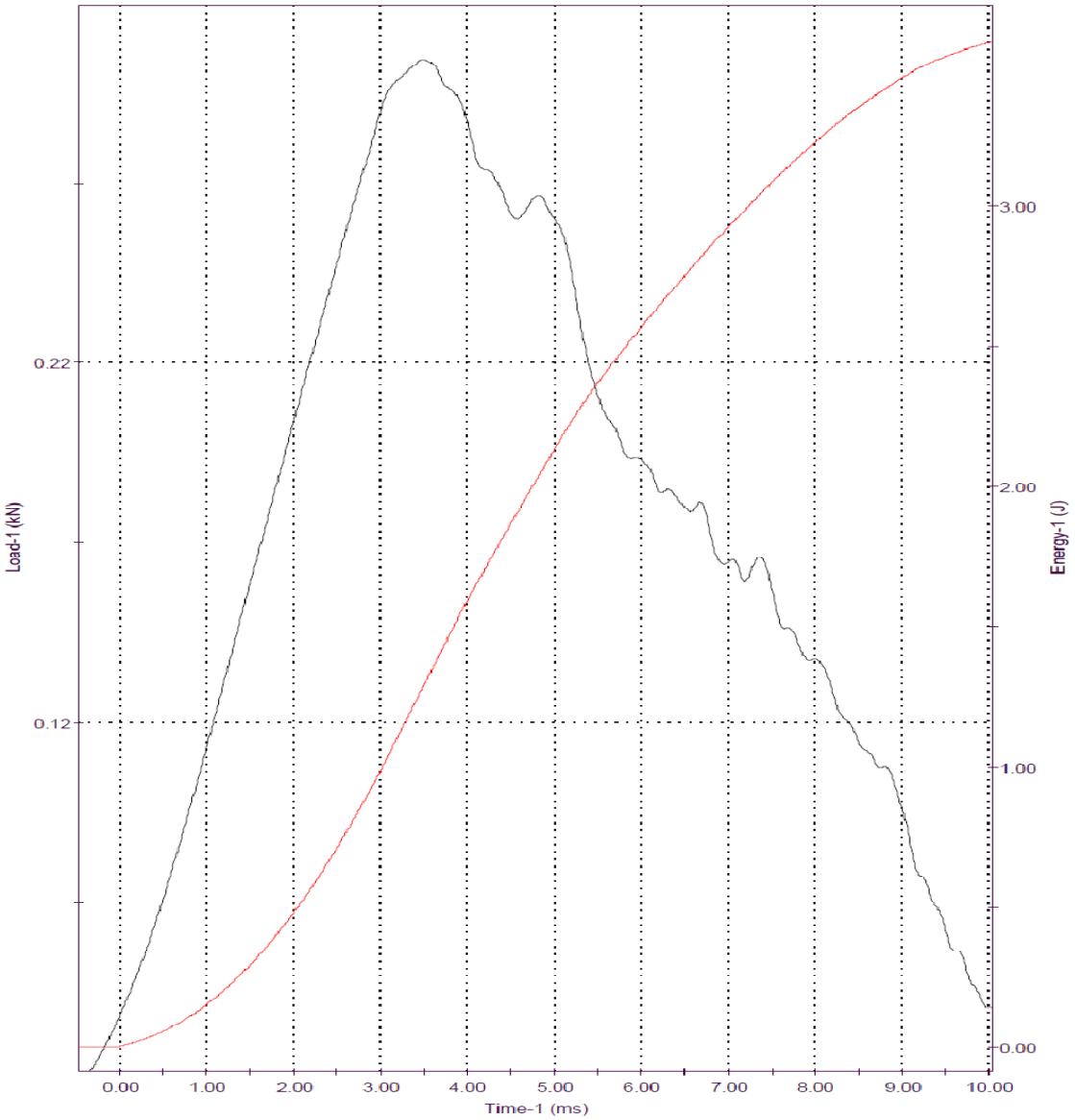

Figure 4.12. Impact test diagram at a draw ratio of 64.

Table 4.3. Impact test data for different draw ratios.

DR	Peak Force (N)	SD	Energy to Peak Force (J)	SD	Failure Energy (J)	SD
21	498	31.6	2.25	0.20	6.04	0.8
36	422	20.1	1.92	0.19	5.01	0.9
49	292	16.5	1.12	0.21	2.99	1.0
64	290	14.3	1.16	0.09	2.81	1.2

4.1.3 Elmendorf Tear Test.

The normalized tear resistance values in machine and transverse directions are listed in table 4.4 and 4.5. The normalized values were obtained by dividing each value by the thickness of the tested film. For each draw ratio, seven to eight samples were tested and then the average and the standard deviations were calculated.

Table 4.4. MD tear resistance at different draw ratios.

DR	Tear Resistance (g)	SD	Normalized Tear Resistance (g/mm)	SD
21	159	11.3	4116	291
36	100	8.6	4965	425
49	60.2	9.3	3537	540
64	30.3	6.3	2428	504

Table 4.5. TD tear resistance at different draw ratios.

DR	Tear Resistance (g)	SD	Normalized Tear Resistance (g/mm)	SD
21	1002	60	25906	1558
36	622	10	30737	509
49	593	15	34331	906
64	517	20	41392	1624

4.1.4 Crystallinity.

The first heating curves of the samples at different draw ratios are shown in figure 4.13. The crystallinity percentages are displayed in table 4.6. For each draw ratio, three samples were tested.

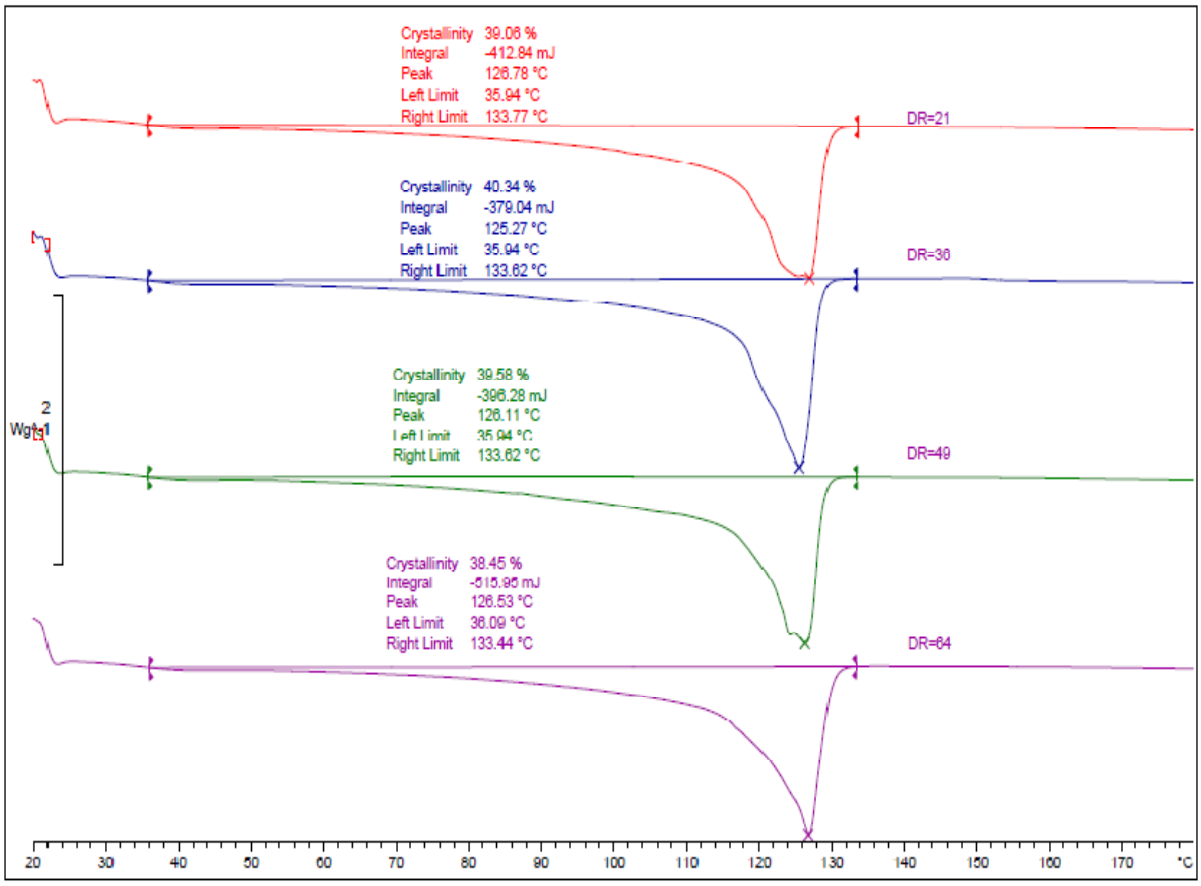

Figure 4.13. Heating cycles of samples at different draw ratios.

Table 4.6. crystallinity percentages at different draw ratios.

DR	% Crystallinity	SD
21	39.0	0.66
36	40.3	0.22
49	39.5	0.83
64	38.4	0.35

4.1.5 Orientation.

The birefringence (Δn) values in MD is calculated and listed in table 4.7.

Table 4.7. Birefringence at different DRs.

DR	Birefringence ×1000	SD
21	-2.6	0.19
36	-4.5	0.20
49	-2.4	0.11
64	-2.4	0.32

4.2 Effect of Blow Ratio on Mechanical Properties of b-LLDPE Films.

The blow ratio (BR) is the ratio between the diameter of the bubble and the diameter of the die. Again, the optimized screw speed was 12 rpm. This speed provides the maximum flow rate without overwhelming the motor torque limitation. The pressure at the extruder exit was around 16 bars. The melt pump speed of 10 rpm was optimum as to maintain constant flow rate. Conforming to the abovementioned parameters, the maximum flow rate was 8.3 grams/min. The blow ratio can be varied by adjusting the pressure inside the bubble with the help of the compressed air line. the used blow ratios are 1.1, 1.4 and 1.8. The results of mechanical tests are presented. Blow ratios of more than 1.8 cause the film to fracture.

4.2.1 Tensile Test.

Tensile tests were conducted using ASTM D882 standard. Five samples were tested in machine and transverse directions for each blow ratio. The average and standard deviation were then calculated. Stress-strain curves at different blow ratios of 1.1 in both directions are shown in figures 4.14-19. Tensile properties of b-LLDPE at different blow ratios (BRs) in both directions are listed in tables 4.8 and 4.9.

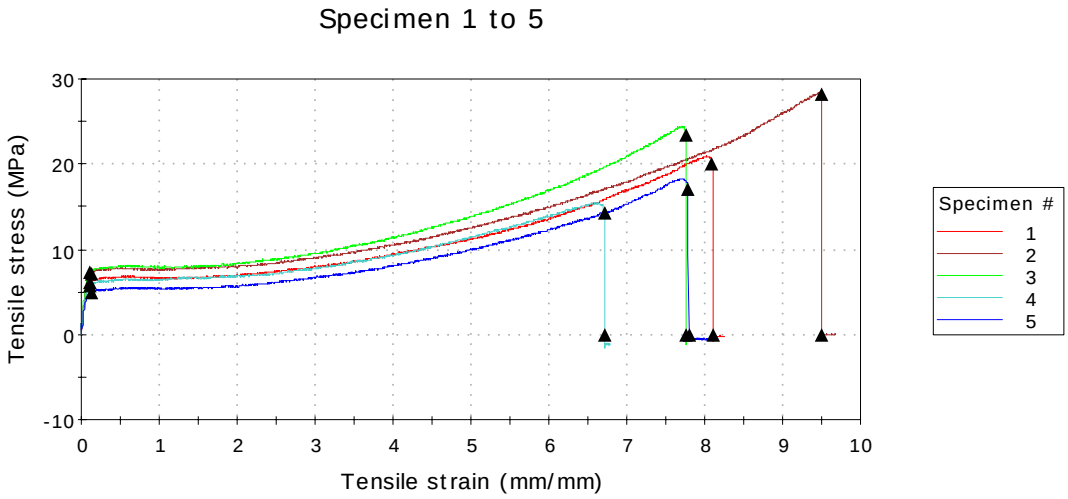

Figure 4.14. Machine direction stress-strain curves at a blow ratio of 1.1.

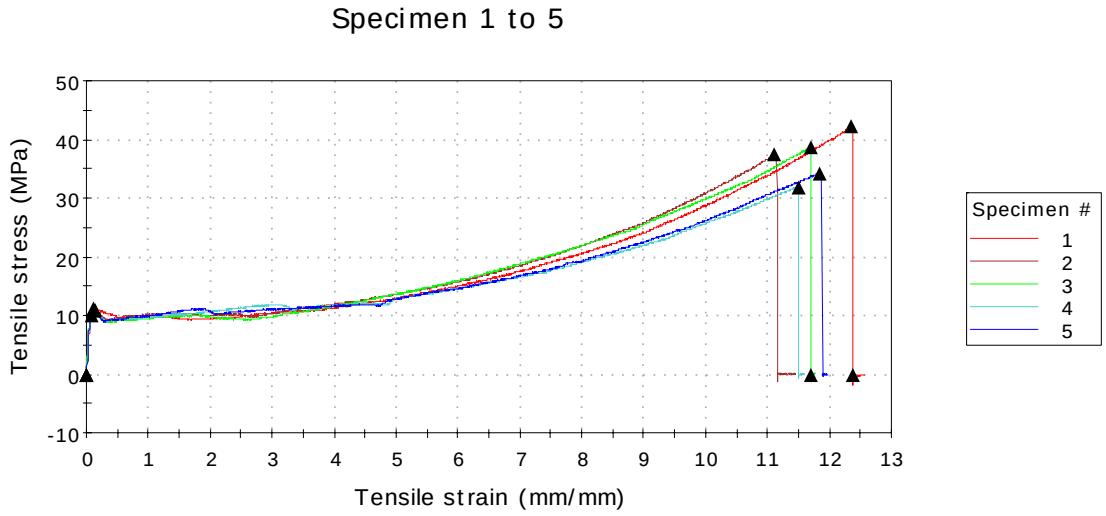

Figure 4.15. Transverse direction stress-strain curves at a blow ratio of 1.1.

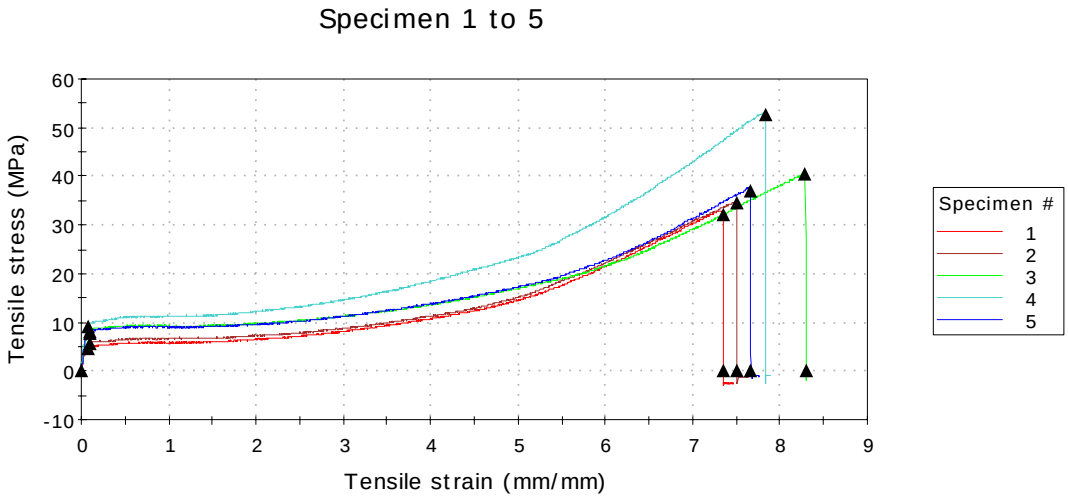

Figure 4.16. Machine direction stress-strain curves at a blow ratio of 1.4.

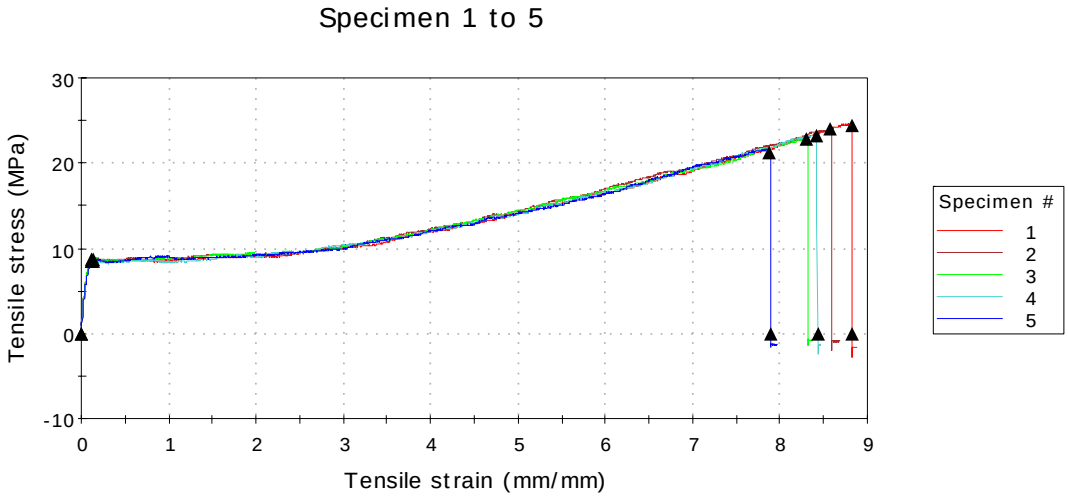

Figure 4.17. Transverse direction stress-strain curves at a blow ratio of 1.4.

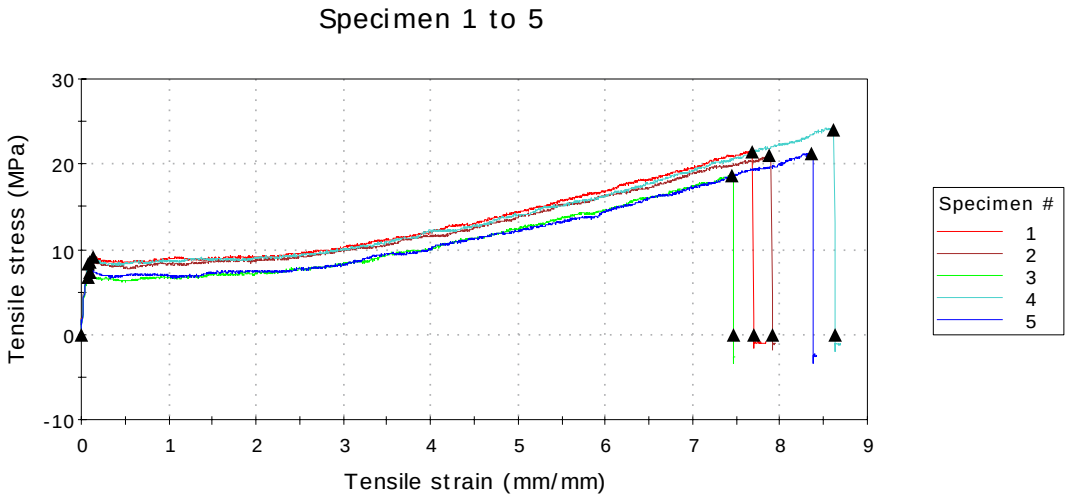

Figure 4.18. Machine direction stress-strain curves at a blow ratio of 1.8.

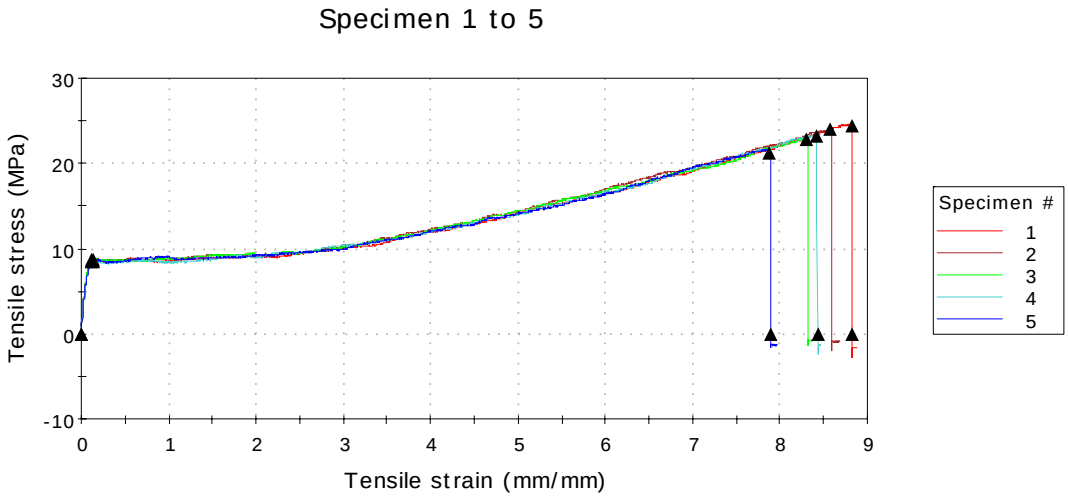

Figure 4.19. Transverse direction stress-strain curves at a blow ratio of 1.8.

Table 4.8. MD tensile properties of b-LLDPE at different BRs.

BR	Yield strength (MPa)	Std Dev	Tensile strength (MPa)	Std Dev	Ductility (%)	Std Dev	Toughness (MPa)	Std Dev
1.1	6.2	1.6	20.2	2.6	797	90.3	152	18.6
1.4	7.3	1.8	39.7	6.9	772	22.4	168	12.3
1.8	8.9	1.0	21.3	1.9	800	38.3	159	20.0

Table 4.9. TD tensile properties of b-LLDPE at different BRs.

BR	Yield strength (MPa)	Std Dev	Tensile strength (MPa)	Std Dev	Ductility (%)	Std Dev	Toughness (MPa)	Std Dev
1.1	10.3	0.4	35.3	3.9	1201	40	211	10
1.4	8.6	0.1	23.5	1.1	850	34	197	18
1.8	8.2	0.1	22.1	1.0	829	45	193	17

4.2.2 Impact Test.

Impact tests were conducted using ISO 7765-2 standard. Five samples were tested for each blow ratio and the average and the standard deviation were calculated. Impact test diagrams for one of the tested samples at different draw ratios are shown in figures 4.20-22. The peak force, energy to peak force and failure energy values at different Blow ratios are presented in table 4.10.

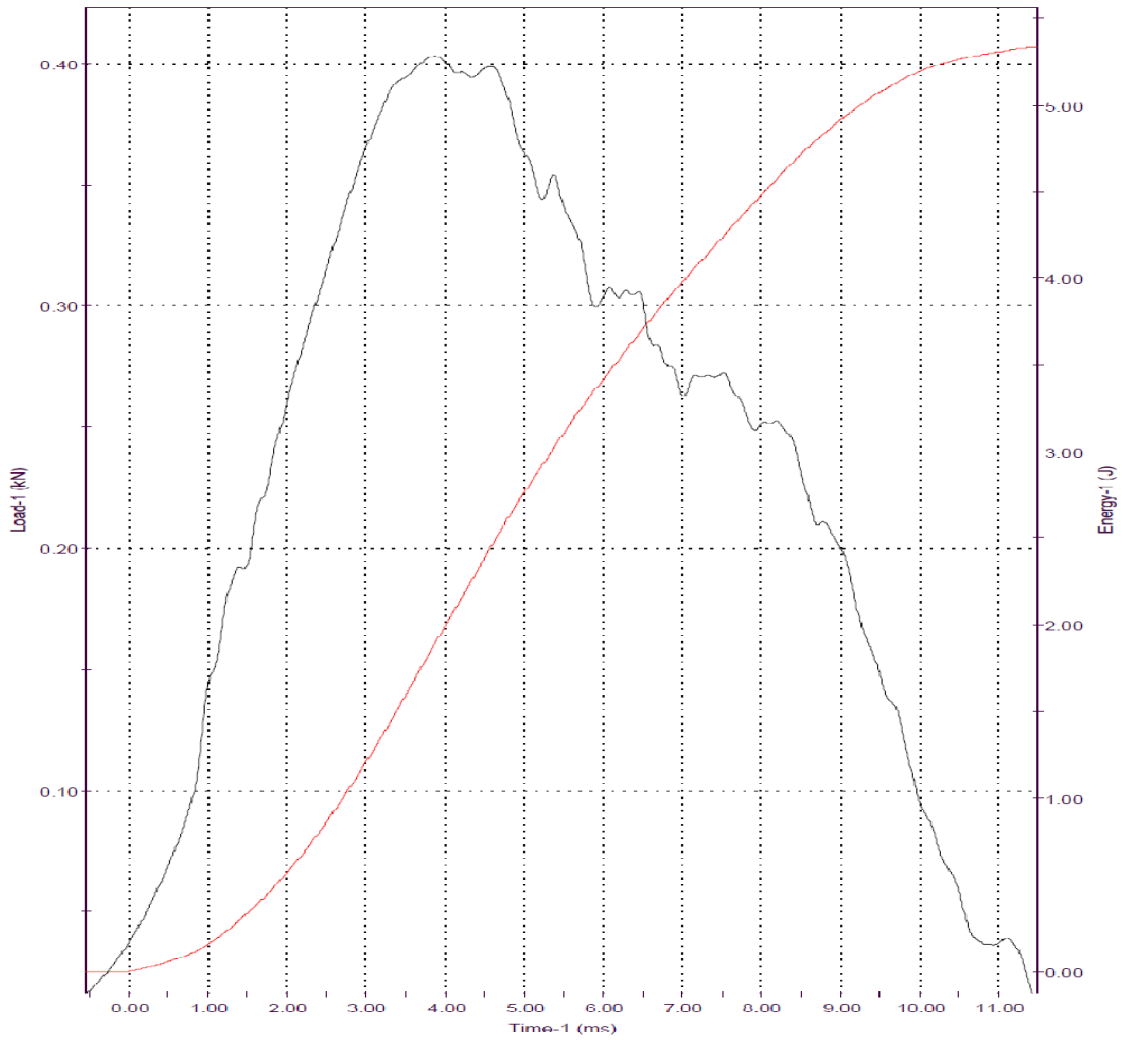

Figure 4.20. Impact test diagram at a blow ratio of 1.1.

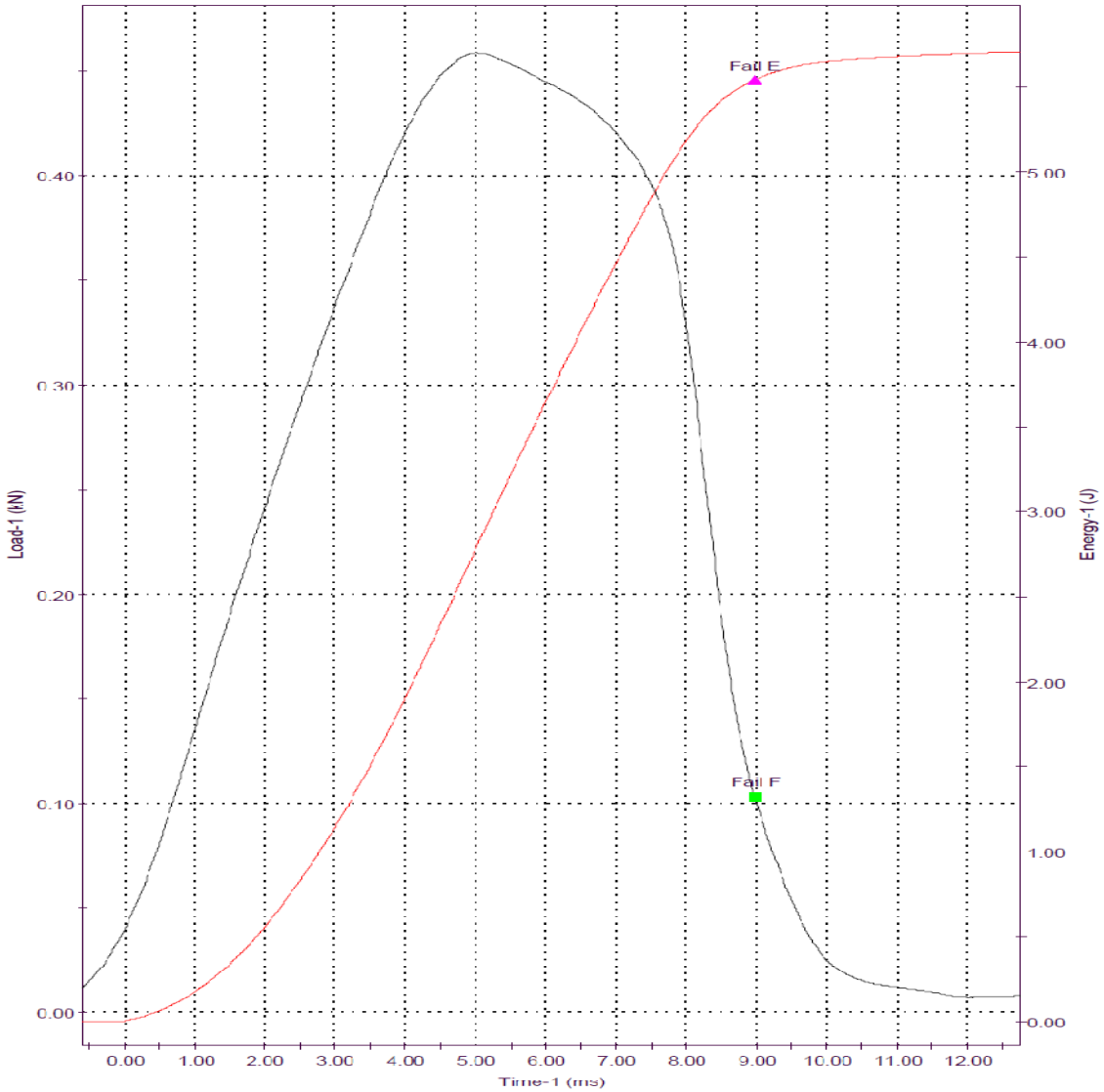

Figure 4.21. Impact test diagram at a blow ratio of 1.4.

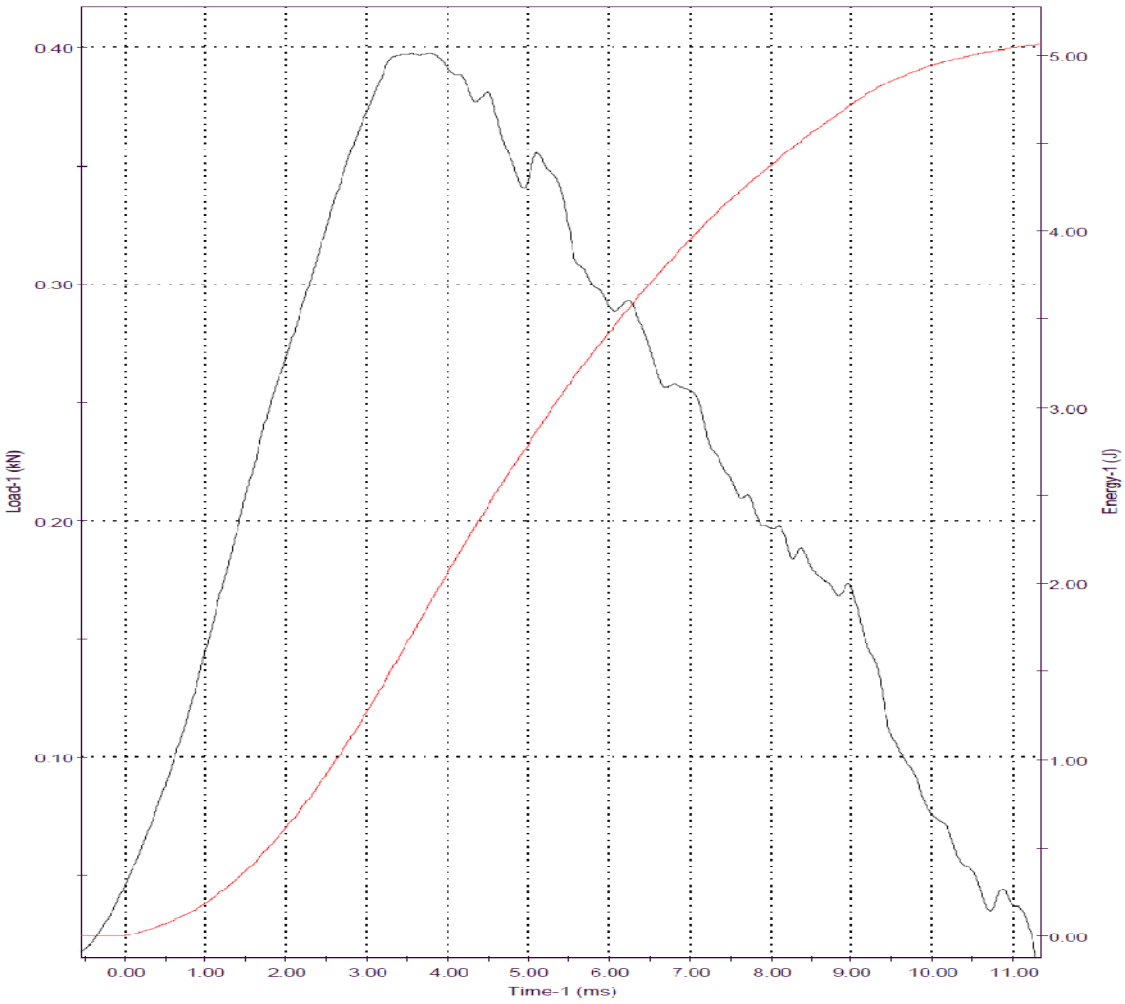

Figure 4.22. Impact test diagram at a blow ratio of 1.8.

Table 4.10. Impact test data for different blow ratios.

BR	Peak Force (N)	SD	Energy to Peak Force (J)	SD	Failure Energy (J)	SD
1.1	421	10.1	1.80	0.01	5.06	0.19
1.4	468	8.3	2.01	0.01	5.88	0.12
1.8	419	9.9	1.84	0.02	4.76	0.15

4.2.3 Elmendorf Tear Test.

The normalized tear resistance values in machine and transverse directions are listed in table 4.11 and 4.12. The normalized values were obtained by dividing each value by the thickness of the tested film. For each draw ratio, seven to eight samples were tested and then the average and the standard deviations were calculated.

Table 4.11. MD tear resistance at different blow ratios.

DR	Tear Resistance (g)	SD	Normalized Tear Resistance (g/mm)	SD
1.1	438	12.0	11288	309
1.4	320	16.4	9377	467
1.8	208	7.9	7658	290

Table 4.12. TD tear resistance at different blow ratios.

DR	Tear Resistance (g)	SD	Normalized Tear Resistance (g/mm)	SD
1.1	999	43	25752	1128
1.4	1100	20	32166	593
1.8	683	18	25139	669

4.2.4 Crystallinity.

The first heating curves of the samples at different blow ratios are shown in figure 4.23.

The crystallinity percentages are displayed in table 4.13.

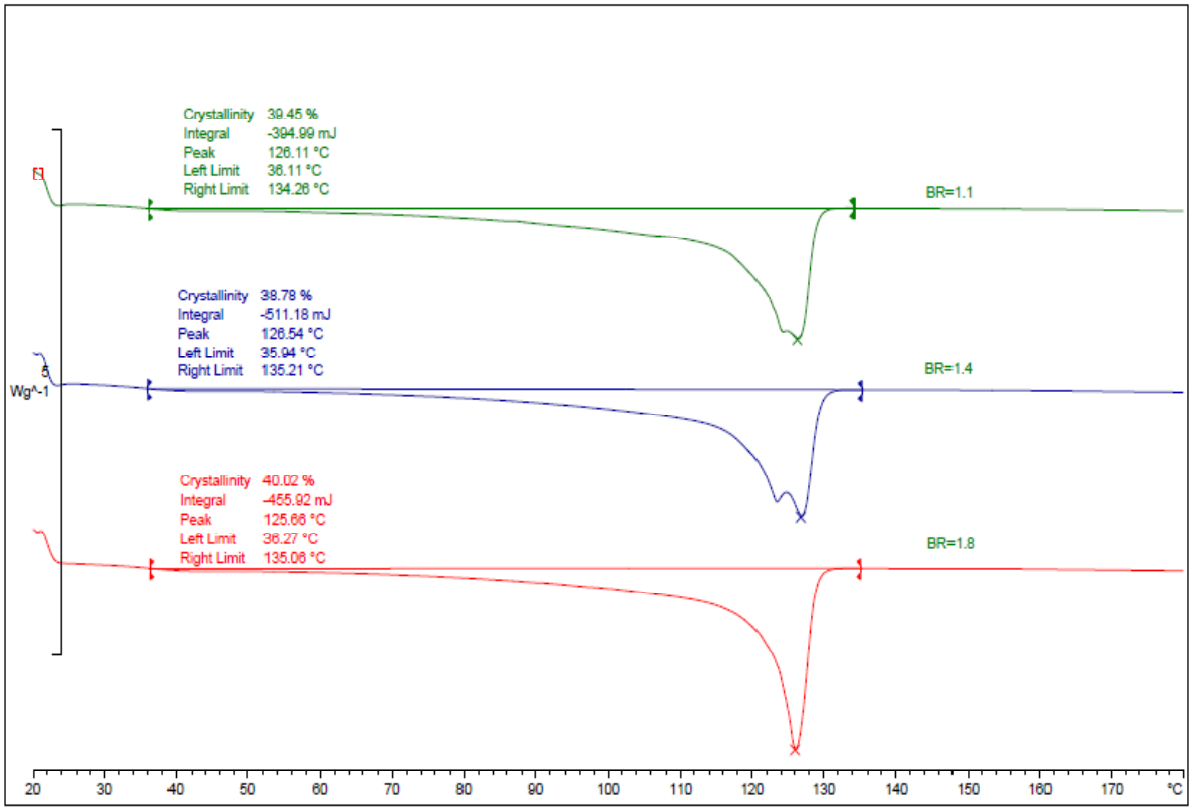

Figure 4.23. Heating cycles of samples at different blow ratios.

Table 4.13. crystallinity percentages at different blow ratios.

BR	% Crystallinity	SD
1.1	39.4	0.06
1.4	38.7	0.40
1.8	40.0	0.12

4.2.5 Orientation.

The birefringence (Δn) values in MD is calculated and listed in table 4.14.

Table 4.14. Birefringence at different BRs.

DR	Birefringence ×1000	SD
1.1	-1.4	0.02
1.4	-3.6	0.01
1.8	-3.9	0.02

4.3 Effect of Blend Ratio on Mechanical Properties of b-LLDPE/LDPE Films.

b-LLDPE and LDPE were blended together with the help of the two controlled feeders. The different blend ratios are listed in table 4.15. The results of thermal and mechanical tests are presented in this section. A blow ratio of around 1.6, a draw ratio of 21 and a mass flow rate of 8 g/min is maintained during the blending process.

Table 4.15. blending percentages of LDPE to b-LLDPE.

Host Material LLDPE		Blending Percentage of LDPE				
Branch Type	ID	5%	10%	15%	20%	50%
Butene	BL	BL5	BL10	BL15	BL20	BL50

4.3.1 Tensile Test.

Tensile tests were conducted using ASTM D882 standard. Five samples were tested in machine and transverse directions for each blend ratio. The average and standard deviation were then calculated. Stress-strain curves at different blend ratios in both directions are shown in figures 4.24-35. The tensile properties of b-LLDPE/LDPE at different blend ratios in both directions are listed in tables 4.16-17.

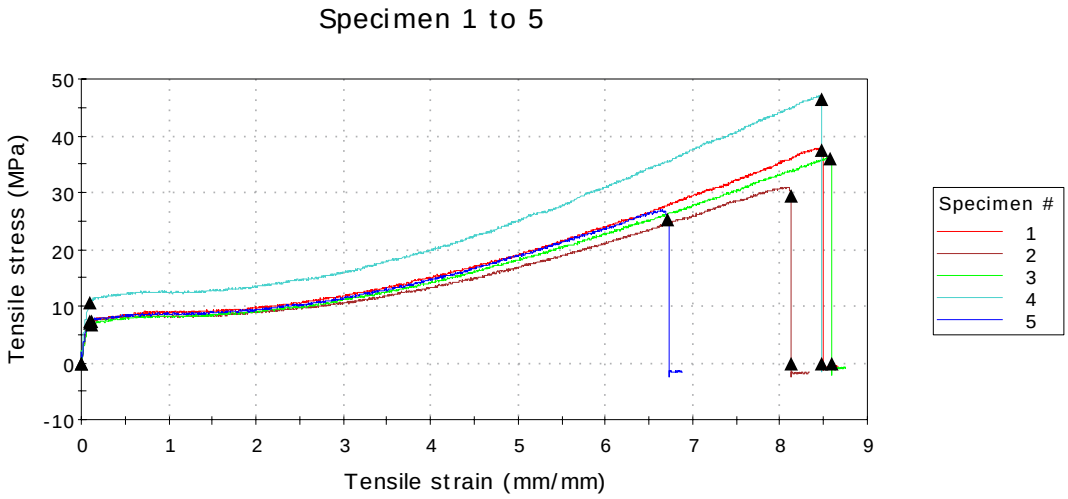

Figure 4.24. Machine direction stress-strain curves for 100% LLDPE.

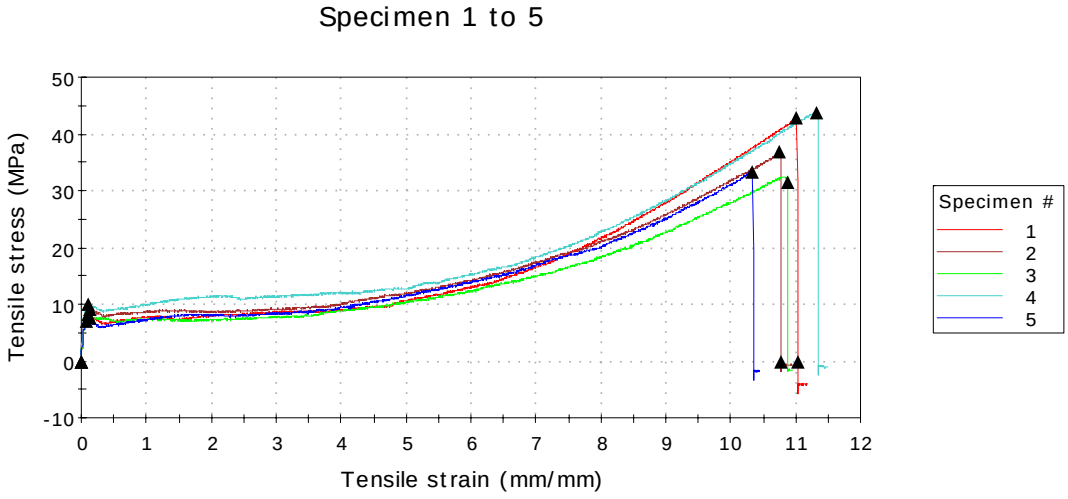

Figure 4.25. Transverse direction stress-strain curves for 100% LLDPE.

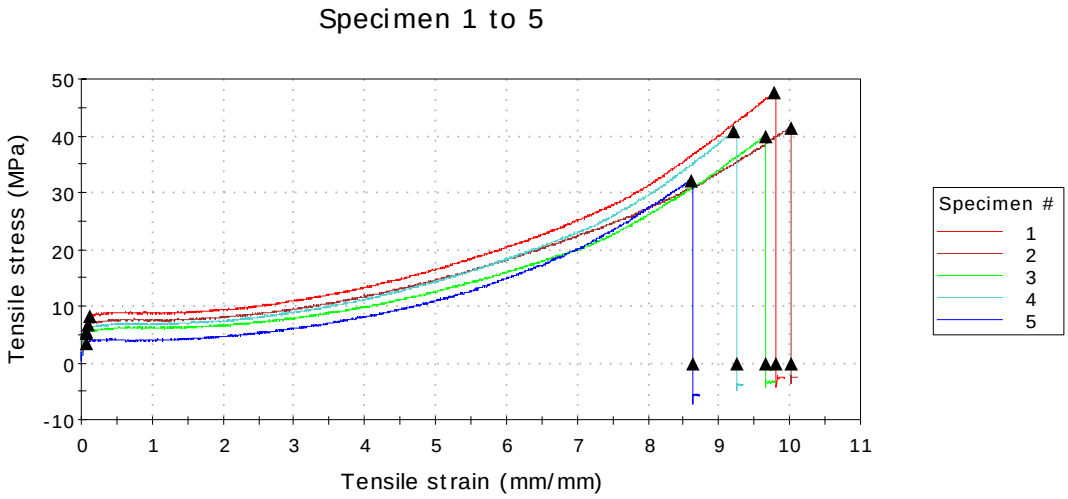

Figure 4.26. Machine direction stress-strain curves for 95% LLDPE/5% LDPE blends.

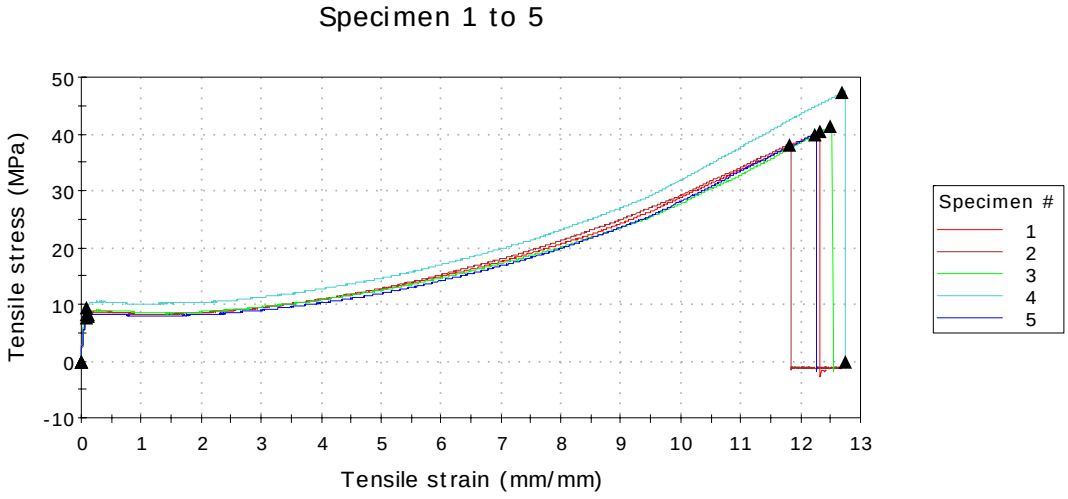

Figure 4.27. Transverse direction stress-strain curves for 95% LLDPE/5% LDPE blends.

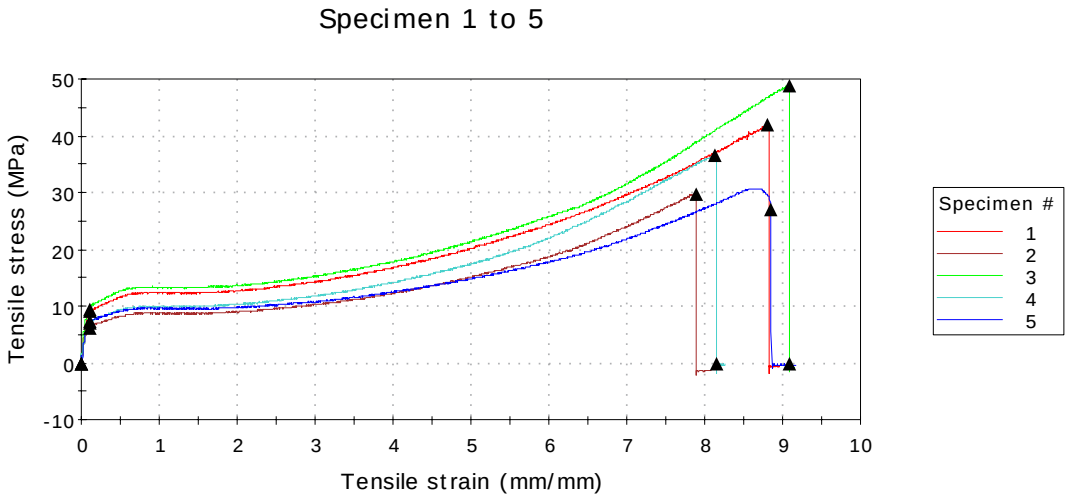

Figure 4.28. Machine direction stress-strain curves for 90% LLDPE/10% LDPE blends.

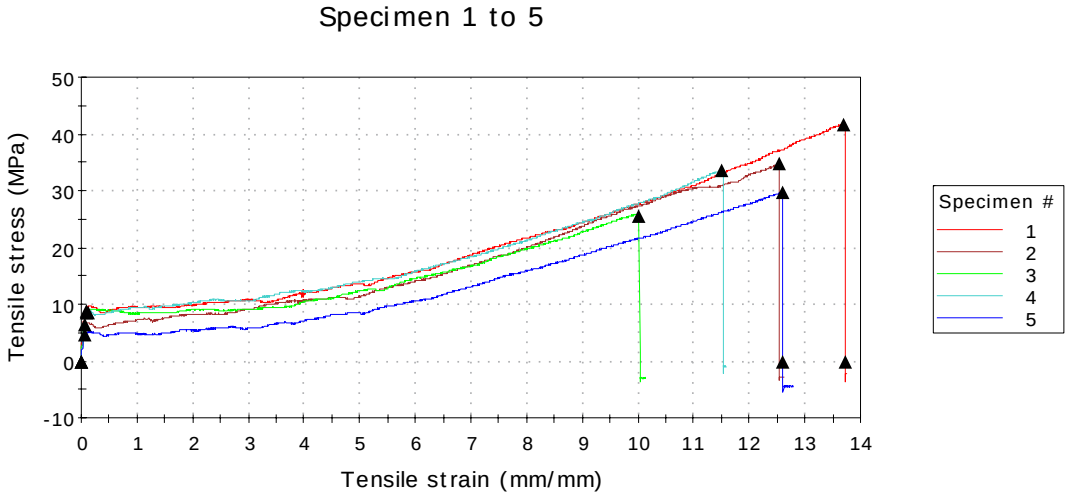

Figure 4.29. Transverse direction stress-strain curves for 90% LLDPE/10% LDPE blends.

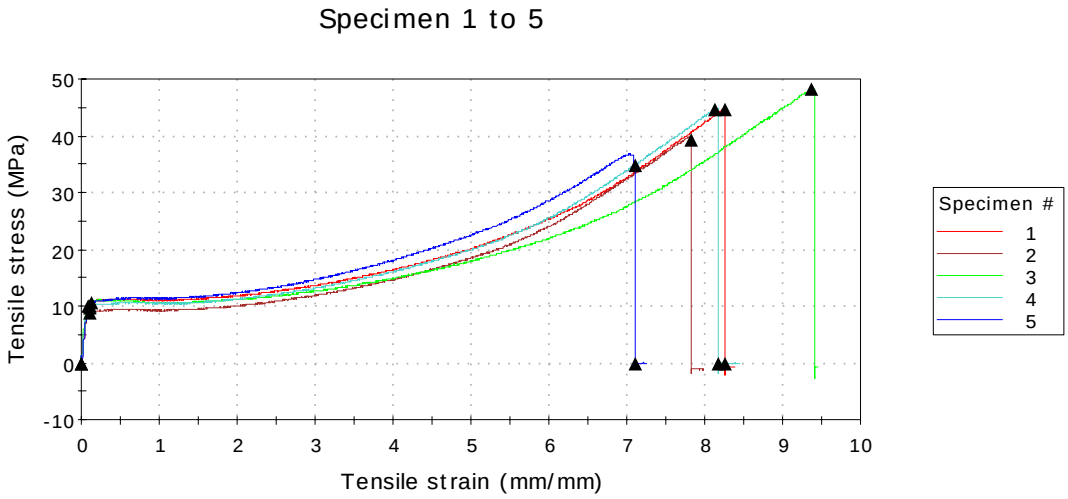

Figure 4.30. Machine direction stress-strain curves for 85% LLDPE/15% LDPE blends.

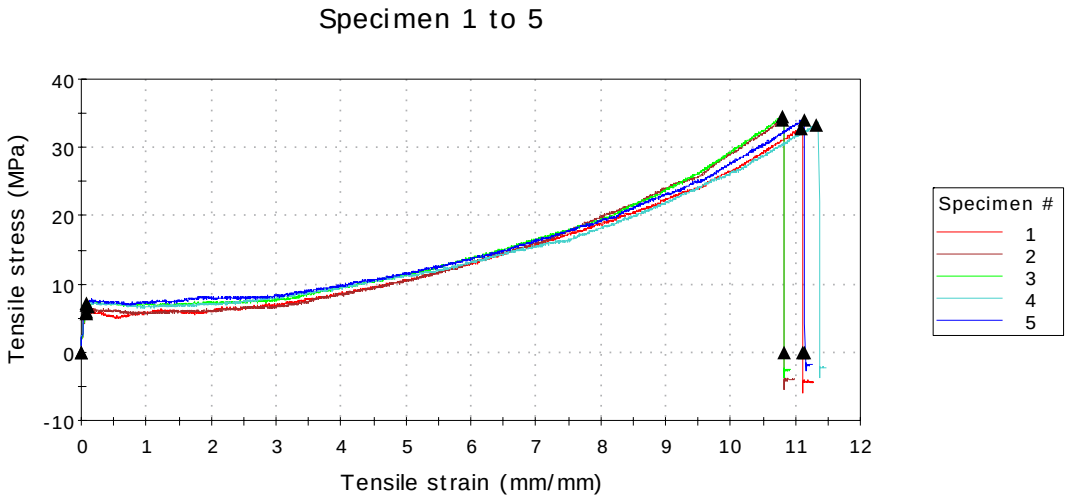

Figure 4.31. Transverse direction stress-strain curves for 85% LLDPE/15% LDPE blends.

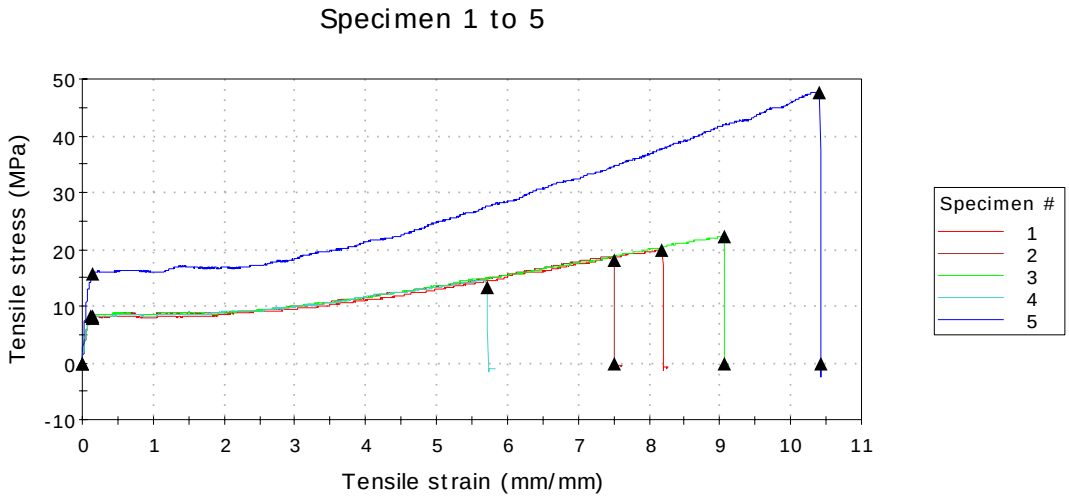

Figure 4.32. Machine direction stress-strain curves for 80% LLDPE/20% LDPE blends.

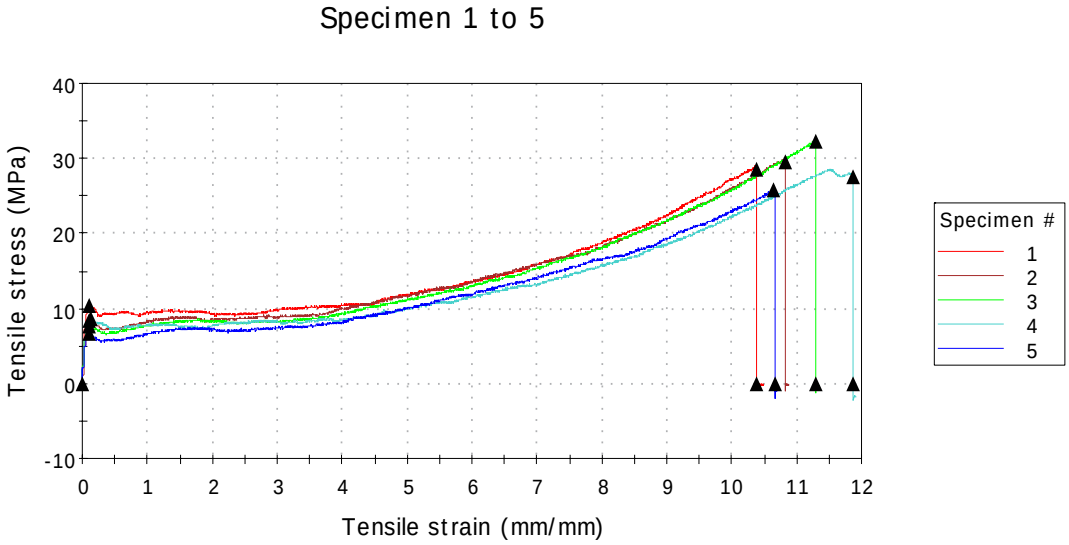

Figure 4.33. Transverse direction stress-strain curves for 80% LLDPE/20% LDPE blends.

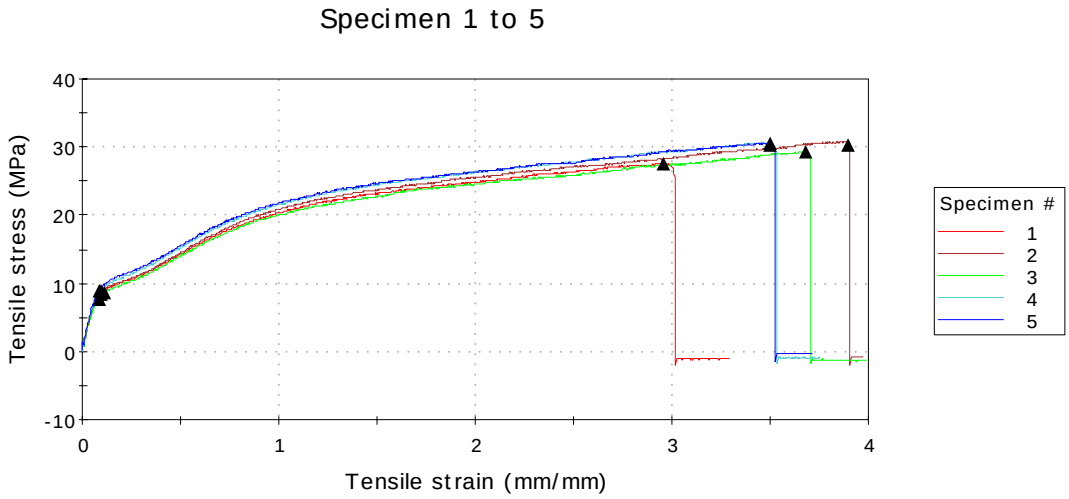

Figure 4.34. Machine direction stress-strain curves for 50% LLDPE/50% LDPE blends.

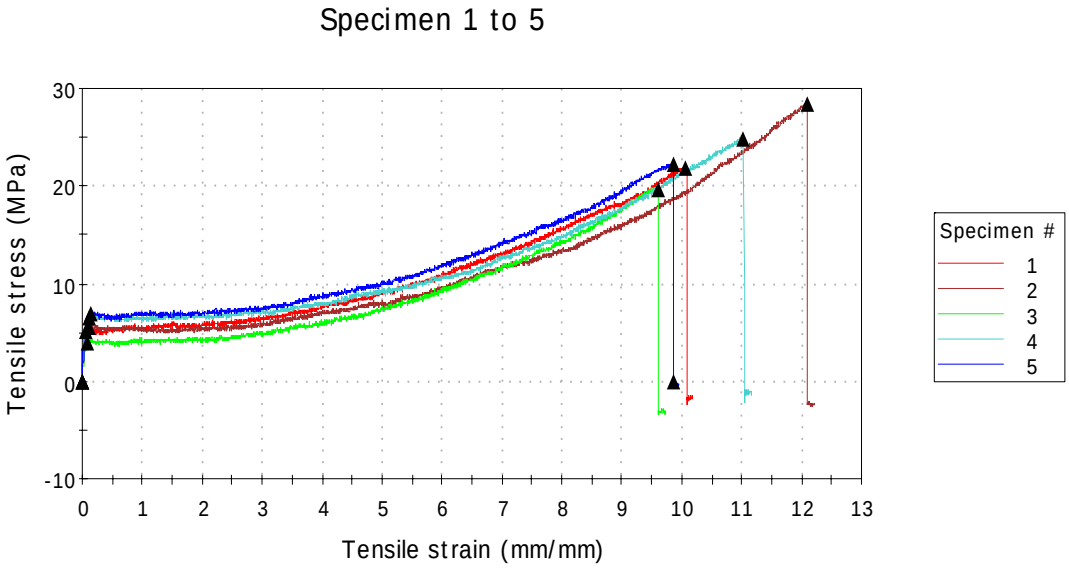

Figure 4.35. Transverse direction stress-strain curves for 50% LLDPE/50% LDPE blends.

Table 4.16. MD tensile properties of b-LLDPE/LDPE blends.

LDPE %	Yield strength (MPa)	Std Dev	Tensile strength (MPa)	Std Dev	Ductility (%)	Std Dev	Toughness (MPa)	Std Dev
0	8.7	1.6	35.7	7.6	841	74.2	136	36.6
5	6.9	1.7	39.7	5.6	940	55.7	151	34.0
10	8.3	1.4	39.3	7.7	879	51.4	204	51.1
15	9.4	0.4	42.8	4.6	813	72.2	228	36.2
20	9.4	2.4	28.2	13.1	815	128.3	219	54.8
50	8.0	0.5	30.2	1.3	352	34.7	110	15.0
100	7.2	1.1	28.8	2.8	163	17.5	33	6.8

Table 4.17. TD tensile properties of b-LLDPE/LDPE blends.

LDPE %	Yield strength (MPa)	Std Dev	Tensile strength (MPa)	Std Dev	Ductility (%)	Std Dev	Toughness (MPa)	Std Dev
0	8.6	1.1	35.3	5.4	1099	36.9	156	24.0
5	8.1	0.6	41.5	3.5	1219	33.0	182	22.2
10	7.4	1.8	31.3	5.5	1235	110.2	189	28.7
15	6.5	0.6	34.0	0.7	1111	22.9	135	6.0
20	8.5	1.4	28.2	2.3	1102	58.9	143	14.2
50	6.1	1.2	23.6	3.5	1059	102.3	127	19.2
100	5.9	0.6	11.9	0.9	699	50.8	54	7.7

4.3.2 Impact Test.

Impact tests were conducted using ISO 7765-2 standard. Five samples were tested for each blend ratio and the average and the standard deviation were calculated. Impact test diagrams for tested samples at different blend ratios are shown in figures 4.36-41. The peak force, energy to peak force and failure energy values at different Blend ratios are presented in table 4.18. For each Blow ratio, five samples were tested.

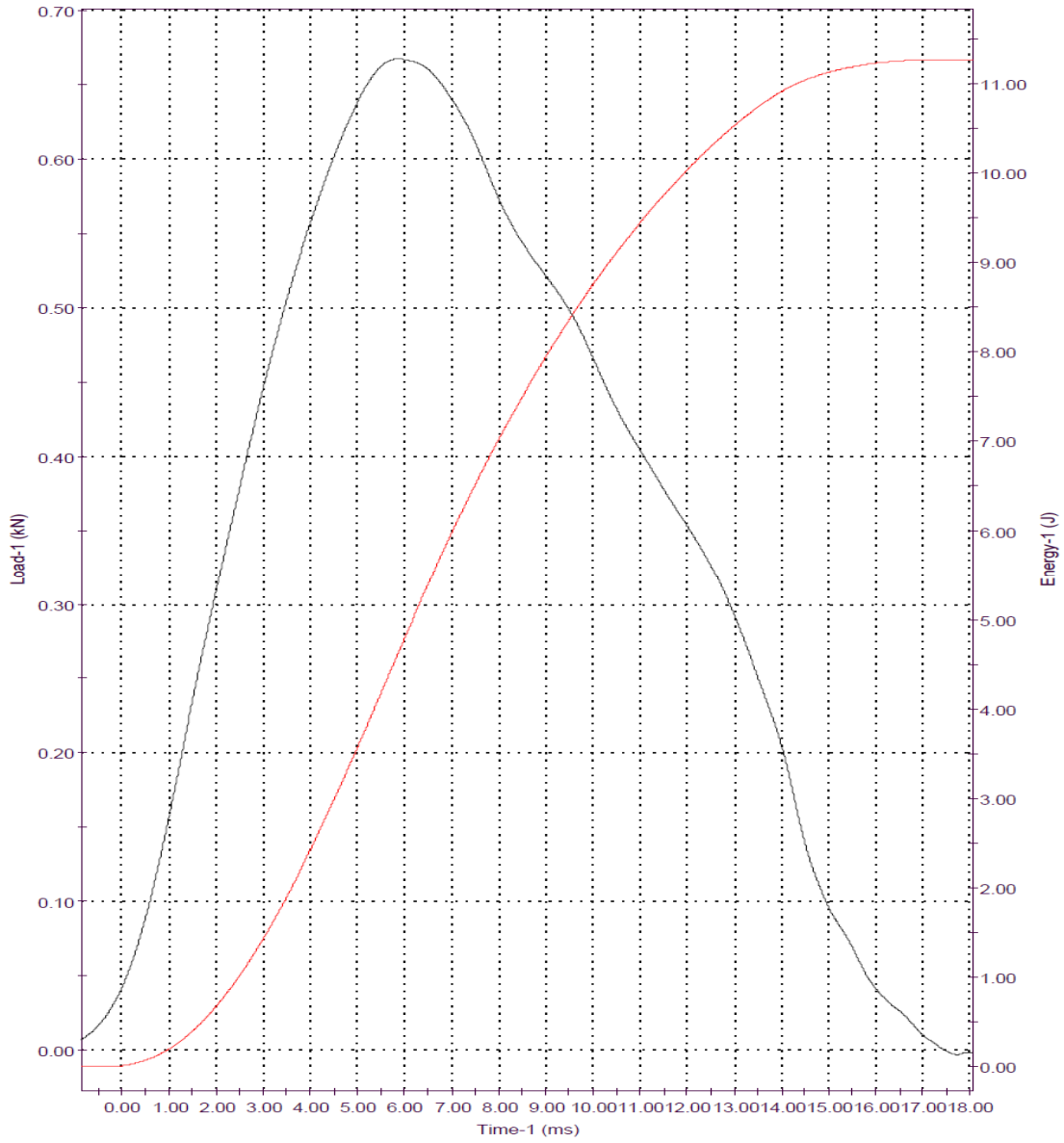

Figure 4.36. Impact test diagram at 100% b-LLDPE.

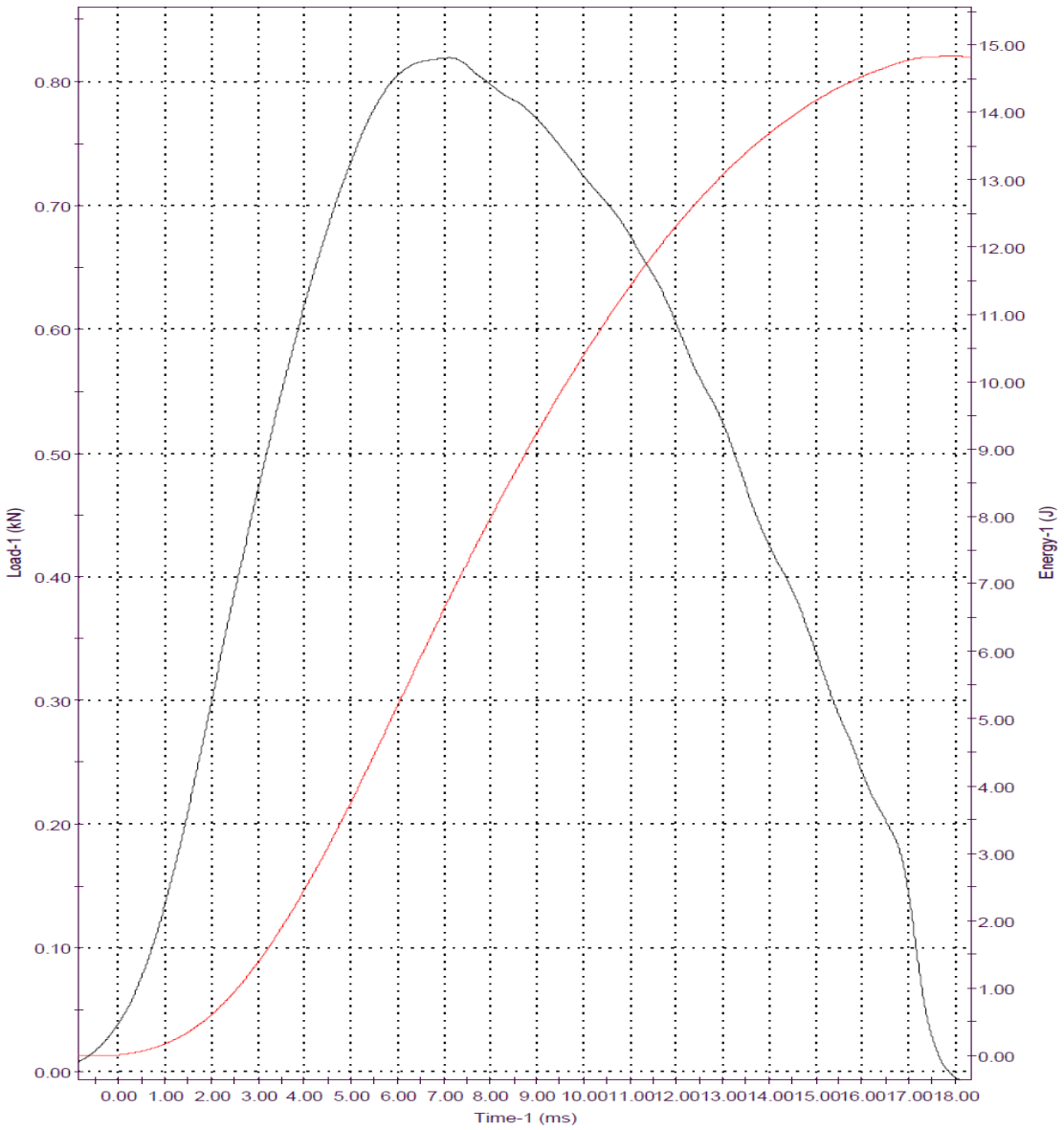

Figure 4.37. Impact test diagram at a blend ratio of 5%.

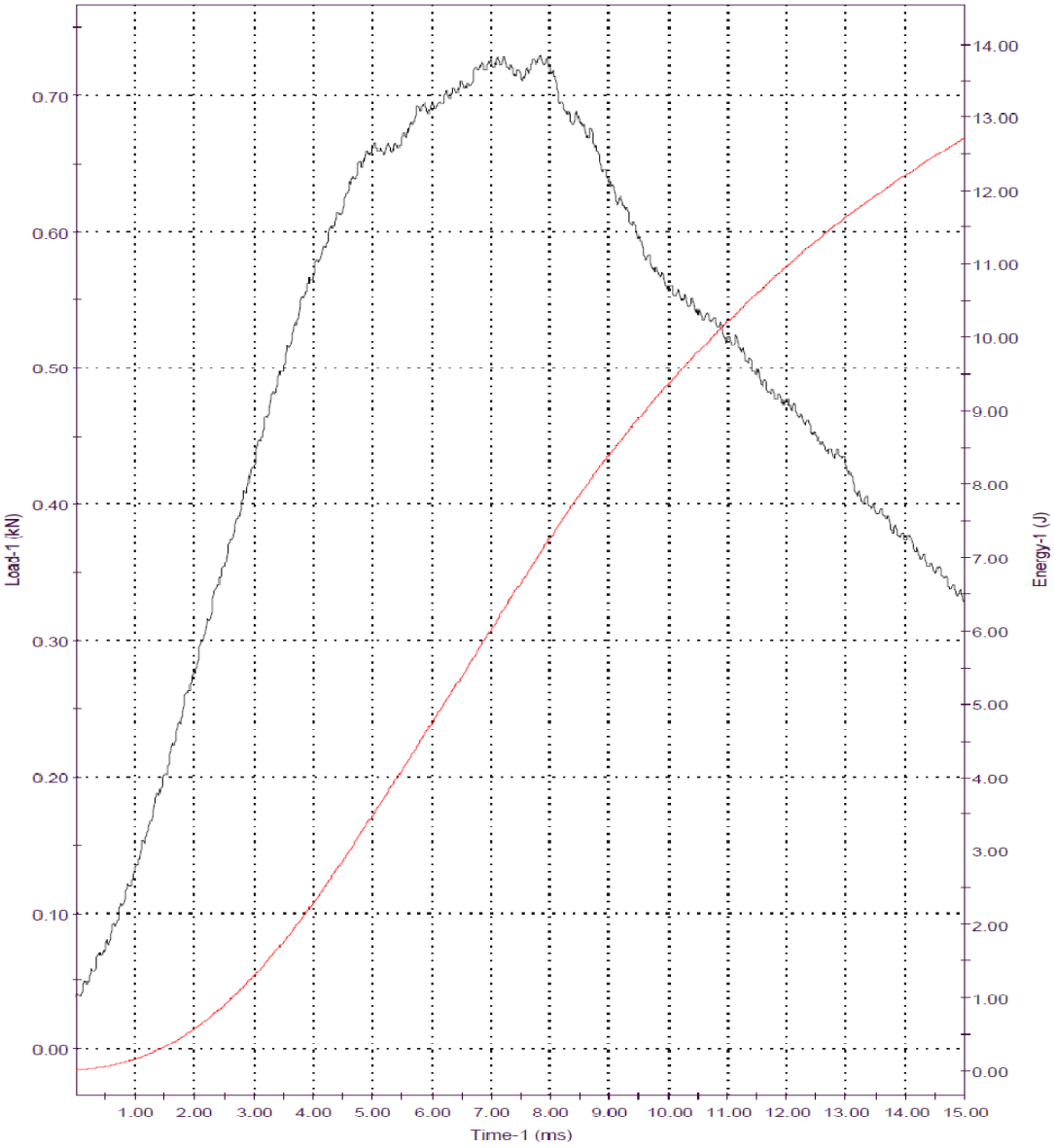

Figure 4.38. Impact test diagram at a blend ratio of 10%.

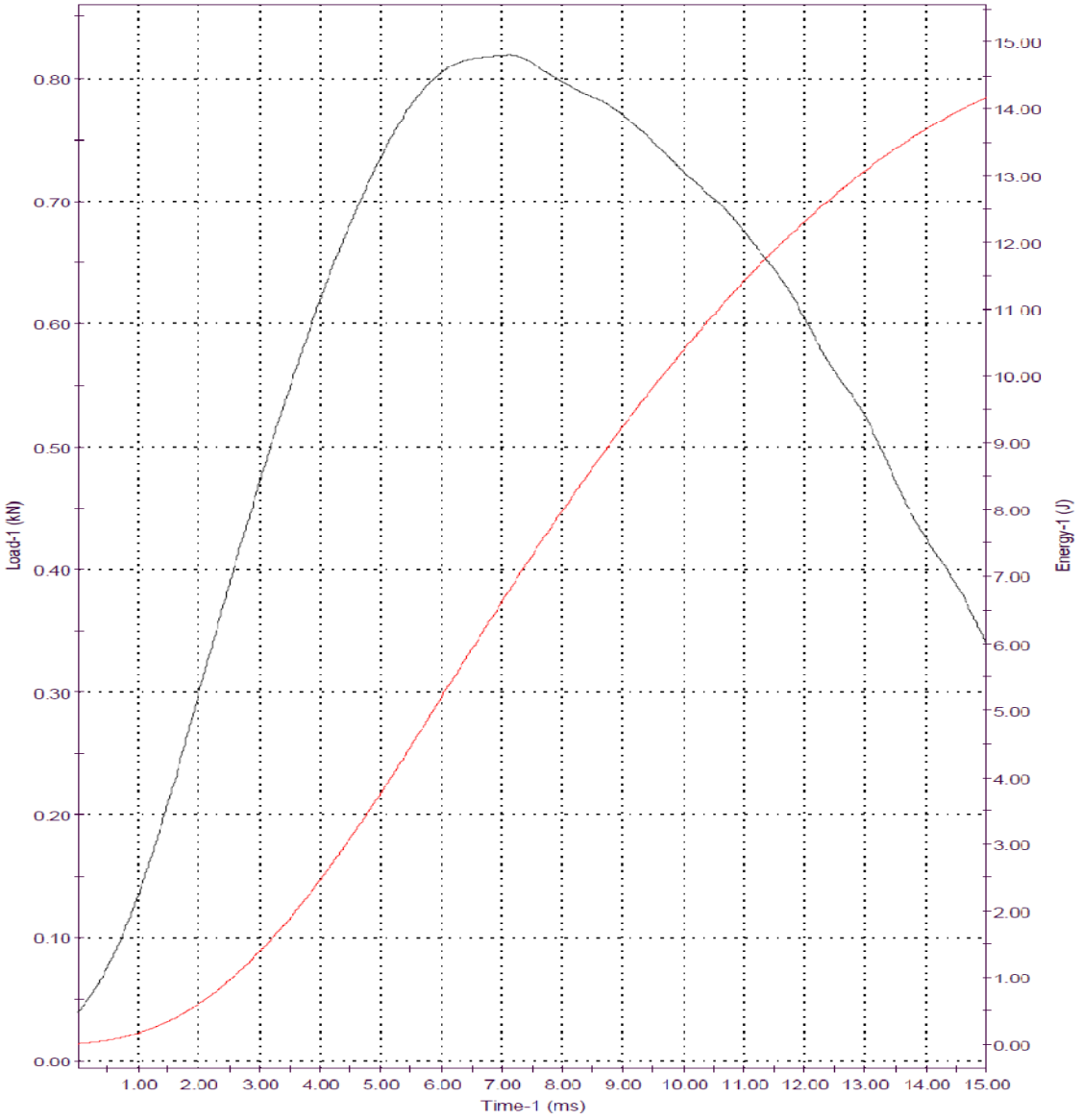

Figure 4.39. Impact test diagram at a blend ratio of 15%.

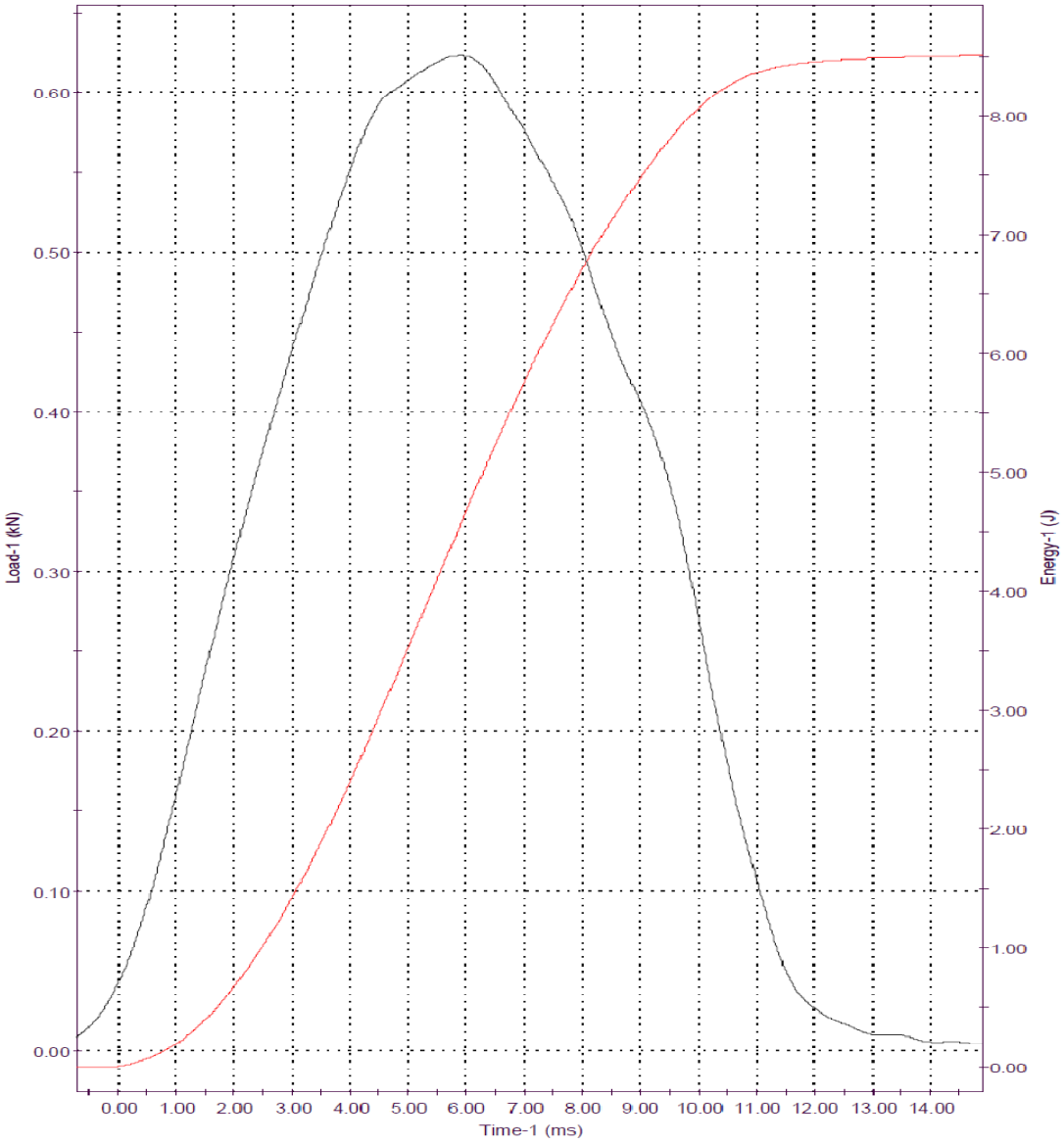

Figure 4.40. Impact test diagram at a blend ratio of 20%.

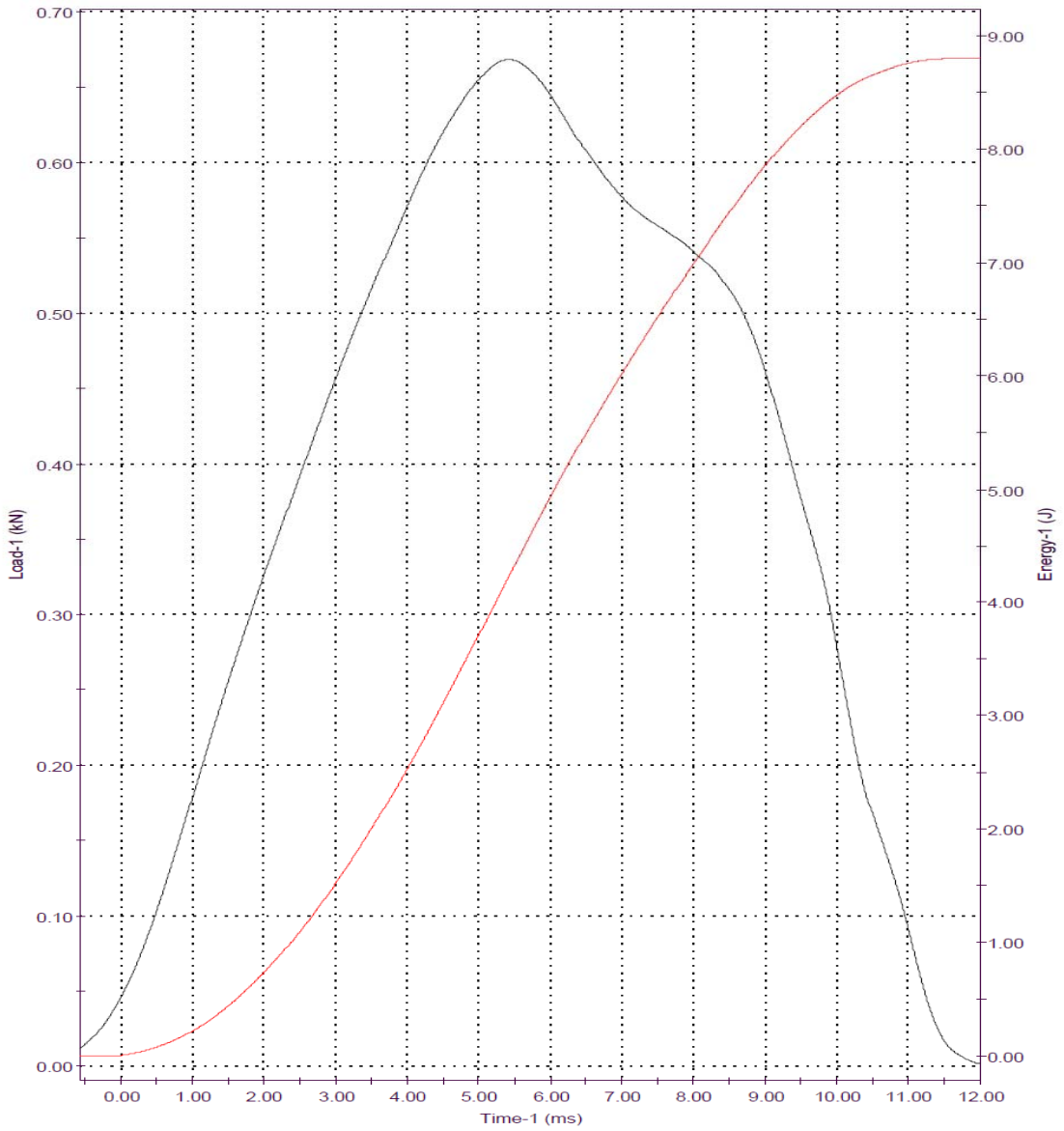

Figure 4.41. Impact test diagram at a blend ratio of 50%.

Table 4.18. Impact test data for different blend ratios.

LDPE %	Peak Force (N)	SD	Energy to Peak Force (J)	SD	Failure Energy (J)	SD
0	620.3	17.5	5.91	0.1	11.3	0.9
5	829.3	9.7	7.63	0.3	14.4	0.8
10	809.3	19.0	7.81	0.2	10.2	0.5
15	820.6	16.3	6.02	0.1	9.9	0.7
20	607.3	29.3	5.29	0.1	7.9	0.8
50	610.3	27.3	4.03	0.1	8.3	0.2
100	615.5	29.3	2.94	0.4	8.7	1.0

4.3.3 Elmendorf Tear Test.

The normalized tear resistance values in machine and transverse directions are listed in tables 4.19-20.

Table 4.19. MD tear resistance at different blend ratios.

LDPE %	Tear Resistance (g)	SD	Normalized Tear Resistance (g/mm)	SD
0	300	19.2	9686.7	619.3
5	202	12.0	6972.4	413.7
10	140	6.9	4687.6	232.6
15	83	20.2	2883.1	696.5
20	78	9.5	2897.4	352.5
50	122	11.3	3144.3	291.2
100	410	90.0	12062.8	2647.6

.

Table 4.20. TD tear resistance at different blend ratios.

LDPE %	Tear Resistance (g)	SD	Normalized Tear Resistance (g/mm)	SD
0	599	17.6	19329	567
5	1005	21.9	34666	757
10	1120	9.8	37344	329
15	1195	11.4	41217	394
20	1055	28.3	39084	1048
50	499	31.8	12803	815
100	136	10.5	4050	312

4.3.4 Crystallinity.

The second heating cycles of virgin b-LLDPE and LDPE pellets are shown in figure 4.42. The first heating curves of the samples at different blend ratios are shown in figure 4.43. The crystallinity percentages are displayed in table 4.21.

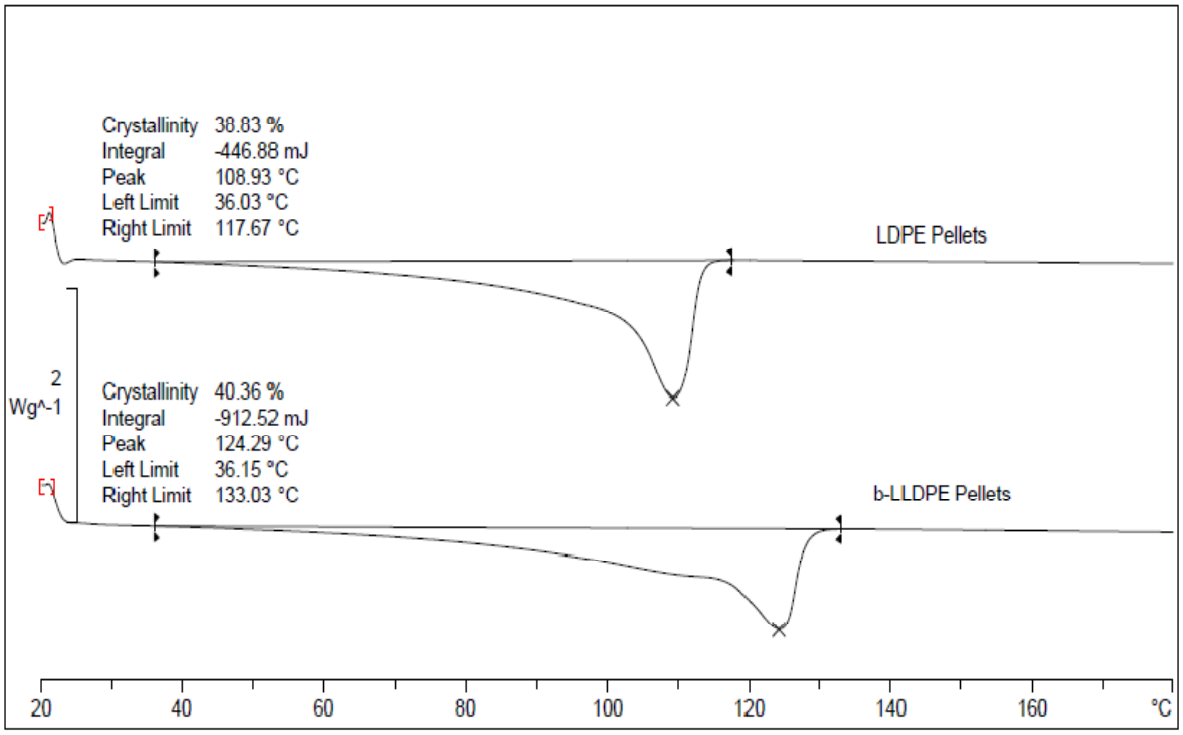

Figure 4.42. Heating cycles of b-LLDPE and LDPE pellets.

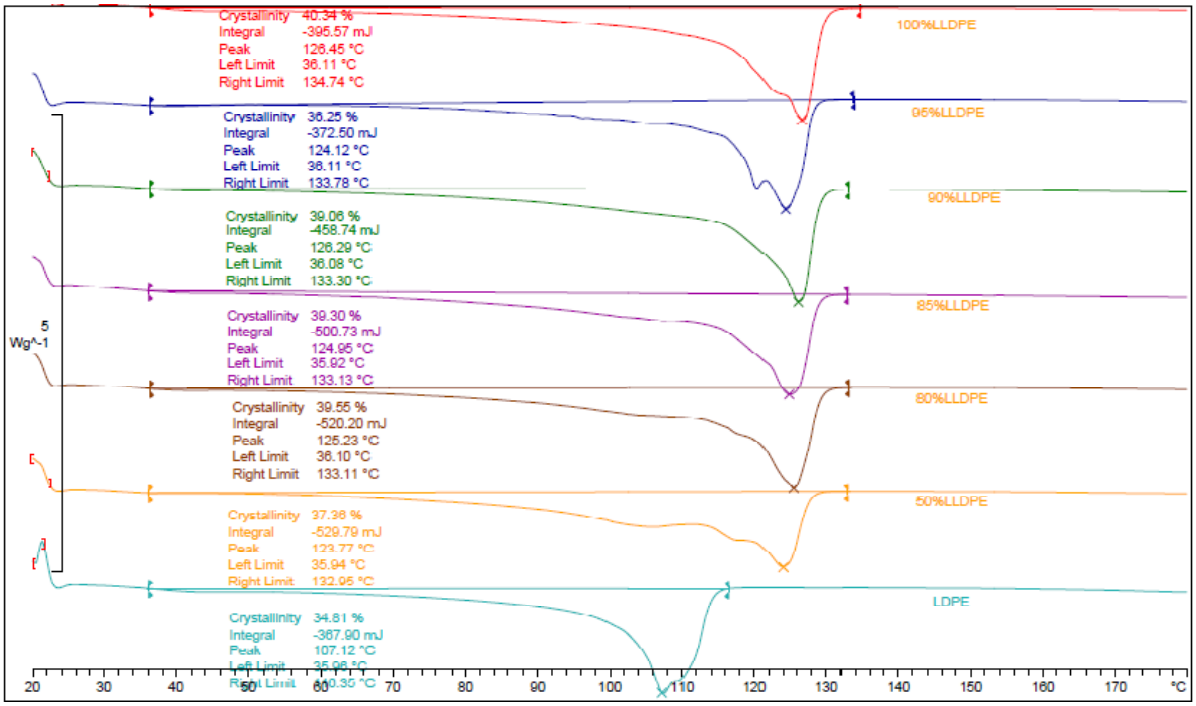

Figure 4.43. Heating cycles of samples at different blend ratios.

Table 4.21. crystallinity percentages at different blend ratios.

%LDPE	% Crystallinity	SD
0	40.3	0.75
5	36.2	1.21
10	39.0	0.05
15	39.3	0.4
20	39.5	1.02
50	37.3	0.33
100	34.5	2.32
Virgin b-LLDPE Pellets	40.4	-
Virgin LDPE Pellets	38.8	-

4.3.5 Orientation.

The birefringence (Δn) values in MD is calculated and listed in table 4.22.

Table 4.22. Birefringence at different blend ratios.

LDPE%	Birefringence ×1000	SD
0	-2.9	0.04
5	-1.6	0.09
10	1.5	0.11
15	2.0	0.02
20	2.5	0.10
50	6.1	0.08
100	3.0	-

CHAPTER FIVE

DISCUSSION

5.1 Effect of Draw Ratio on Mechanical Properties of b-LLDPE Films.

In this section, the aim is to select the optimum draw ratio that provides better mechanical properties of the produced films. As discussed in the previous chapter, the draw ratios used are 21, 36, 49 and 64. These draw ratios were selected to conform to the take up unit limitations and to the processability of the produced films.

5.1.1 Tensile Test.

The crystallinity percent and the orientation of tested films at different draw ratios are shown in figures 5.1 and 5.2, respectively. It seems that the draw ratio has a minor effect on the crystallinity of the films. A draw ratio of 36 provides a film with barely higher crystalline content. According to figure 5.2, all of the draw ratios provide films that are oriented in the transverse direction. A draw ratio of 36 provides a film with slightly higher orientation.

Figure 5.3 shows the effect of changing the draw ratio on the yield strength in machine and transverse directions. In MD, the yield strength has a maximum value at a draw ratio of 21 but drops slightly at a draw ratio of 36 and it continues dropping by almost 30% for the draw ratio of 49 followed by a small increase at a draw ratio of 64. In TD, the yield

strength does not vary that much for 21 and 36 draw ratios, but it increases slightly at draw ratios of 49 and 64. Figure 5.4 shows the effect of changing the draw ratio on the tensile strength in machine and transverse directions. In MD, the tensile strength is maximum at a draw ratio of 21, then it decreases by 50% at a draw ratio of 36 and then it has a small increase at 49 and 64 draw ratios. The tensile strength in TD drops from a maximum value of 40 MPa at a draw ratio of 21 to almost a constant value of 28 MPa for the other draw ratios. Figure 5.5 shows that increasing the draw ratio has no significant effect on the ductility in the transverse direction, while in the machine direction, increasing the draw ratio decreases the ductility. The effect of changing the draw ratio on the toughness of the tested films in both directions is shown in figure 5.6. In Transverse direction, it starts with a high value at a draw ratio of 21, and then drop by almost 15% for 36 and with the same percentage for 49, and have a jump at the end at a draw ratio of 64. In machine direction, it decreases gradually while increasing the draw ratio.

Krishnaswamy et al. [24] proved that for low draw ratios (DR from 6 to 30), the tensile properties are better in machine direction; while at high draw ratios (DR from 30 to 70), the properties are better in the transverse direction. In our present study, we can see that at draw ratios of 21 and 36, the strength is higher in machine direction, while at draw ratios of 49 and 64, the strength is higher in the transverse direction. This is clearly visible in the yield strength profile but not the case in the tensile strength. In their study, they pointed that at low draw ratios, the orientation is enhanced in the transverse direction to some extent, while at high draw ratios, due to the high drawing forces, the molecules are oriented in the machine direction. Their observations, somehow, match with our orientation results. The orientation increased in the transverse direction up to a

draw ratio of 36 and then the molecules started to orient themselves in the machine direction in the draw ratios of 49 and 64.

The crystallinity and orientation studies, shown in figures 5.1 and 5.2, respectively, of the blown films did not comprehensively describe the mechanical behavior of the tested films. Morphological investigations using SEM and TEM might need to be performed in order to fully understand the structure-properties relationship of the tested films. This could be done as a future work of this study.

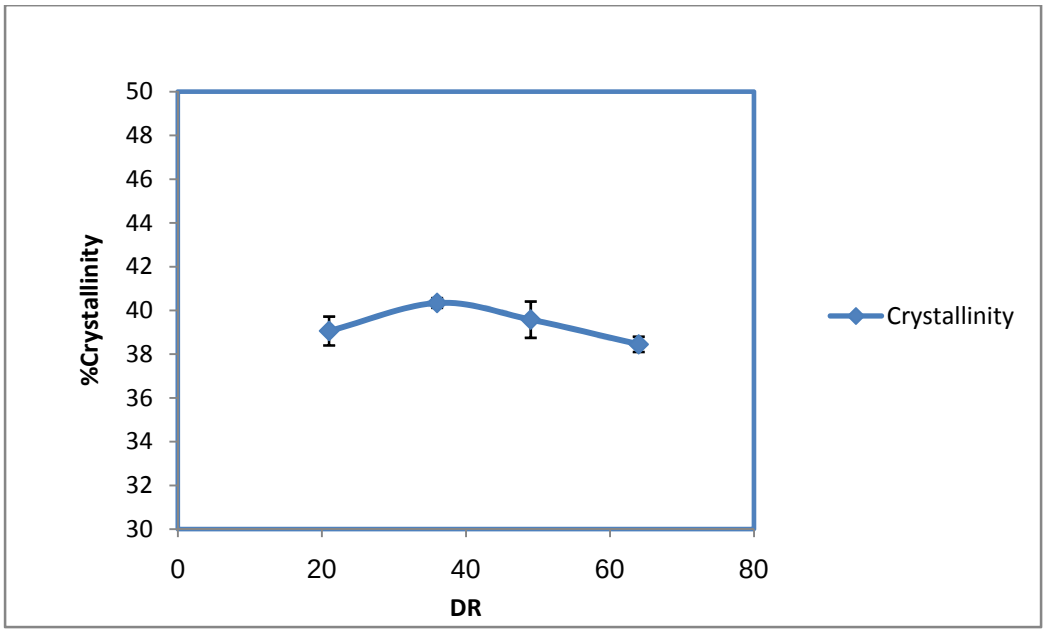

Figure 5.1. Crystallinity of b-LLDPE at different DRs.

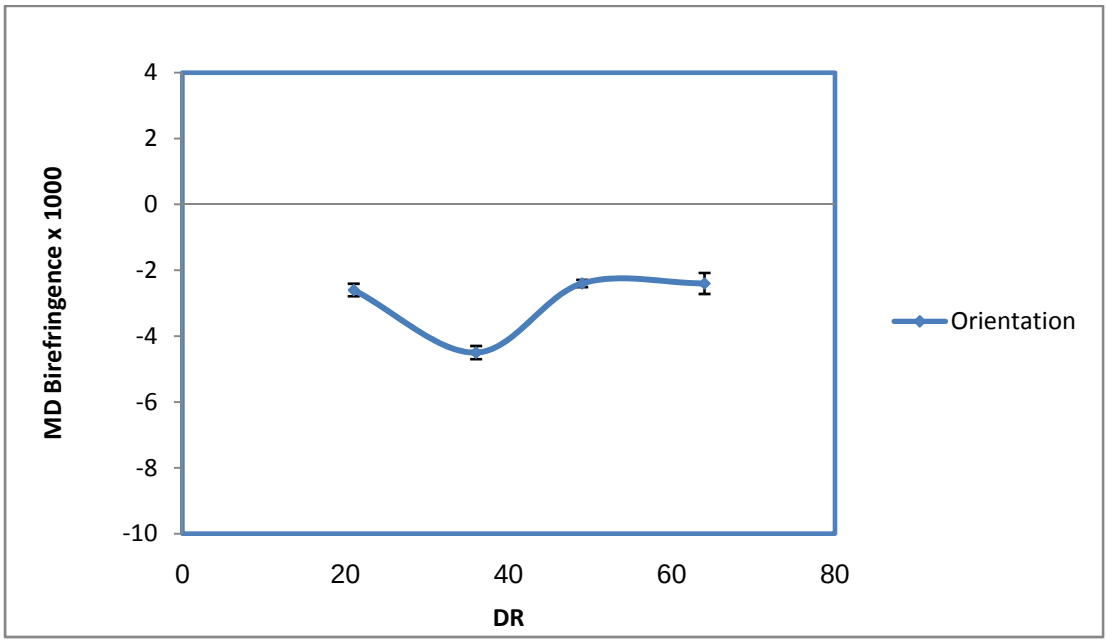

Figure 5.2. Orientation results for 1st order birefringence at different DRs.

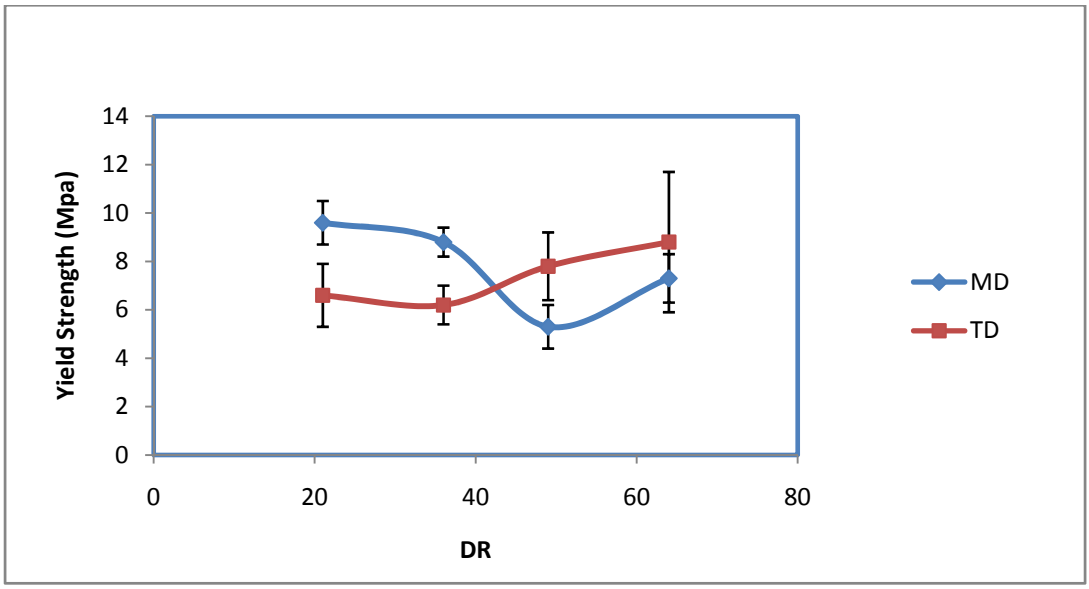

Figure 5.3. MD and TD yield strengths at different draw ratios.

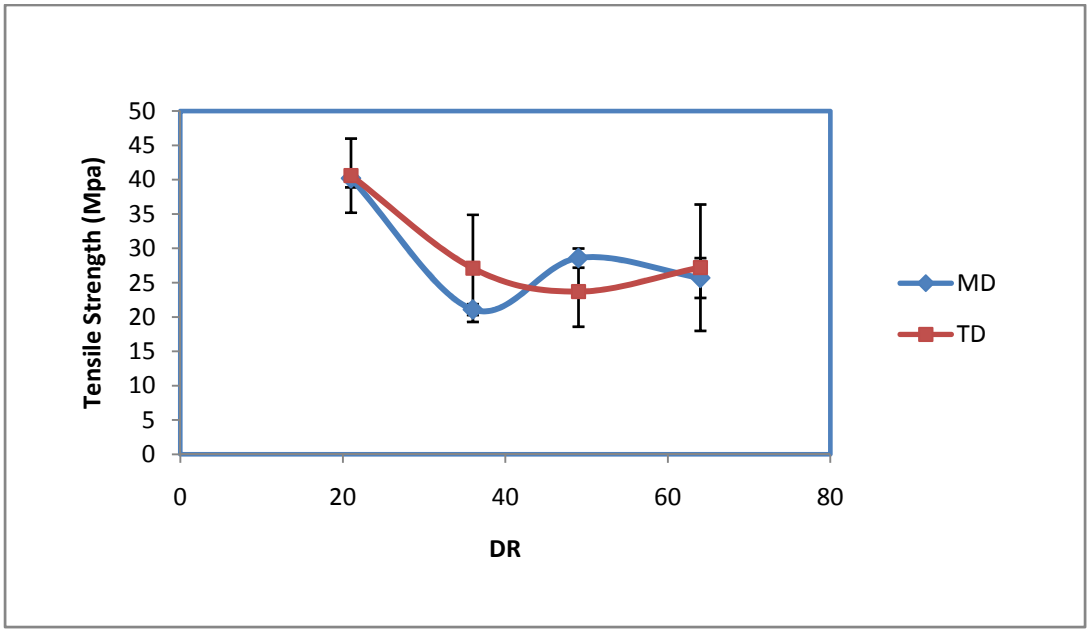

Figure 5.4. MD and TD tensile strengths at different draw ratios.

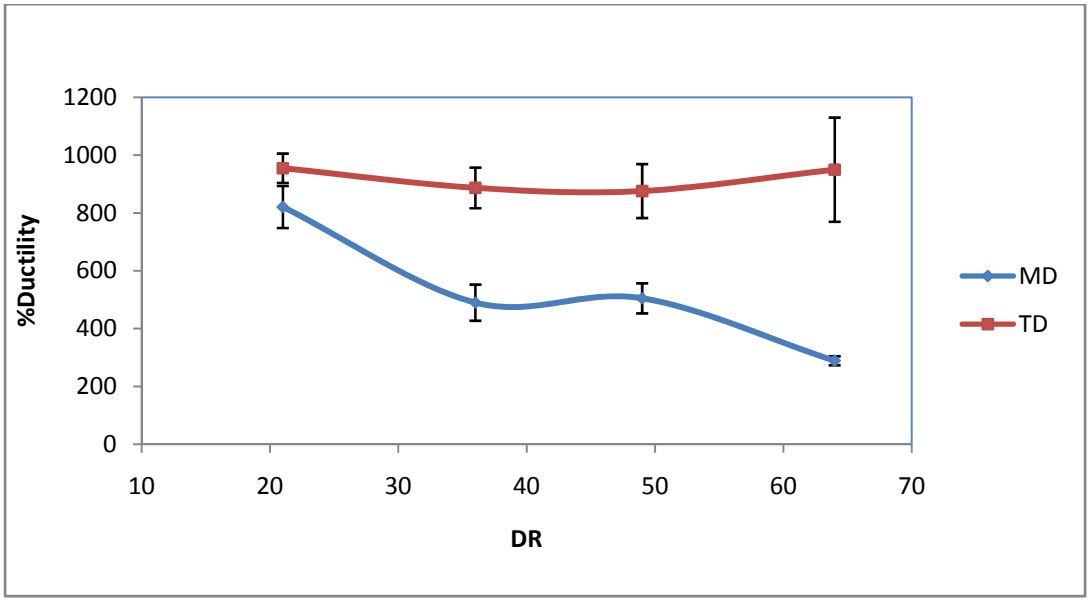

Figure 5.5. MD and TD ductility at different draw ratios.

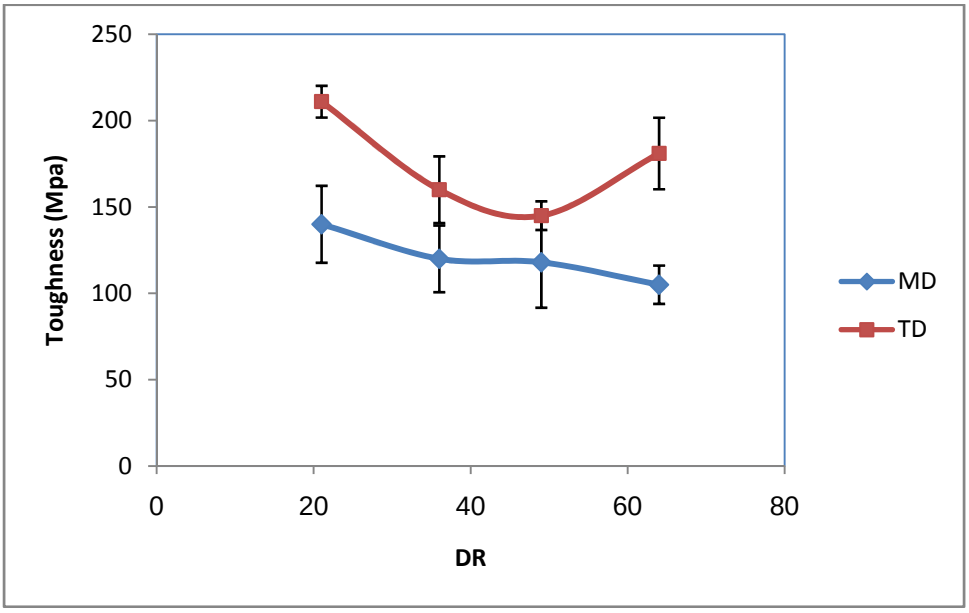

Figure 5.6. MD and TD toughness at different draw ratios.

5.1.2. Impact Test.

Impact tests show that there is a strong relation between impact energies and the draw ratio. Figure 5.7 reveals that a draw ratio of 21 gives maximum impact properties. Then, the energies keep decreasing at 36 and 49. There is no much difference in impact properties between 49 and 64 draw ratios. Therefore, a draw ratio of 21 is the optimum selection. All of the tested samples have the same thickness.

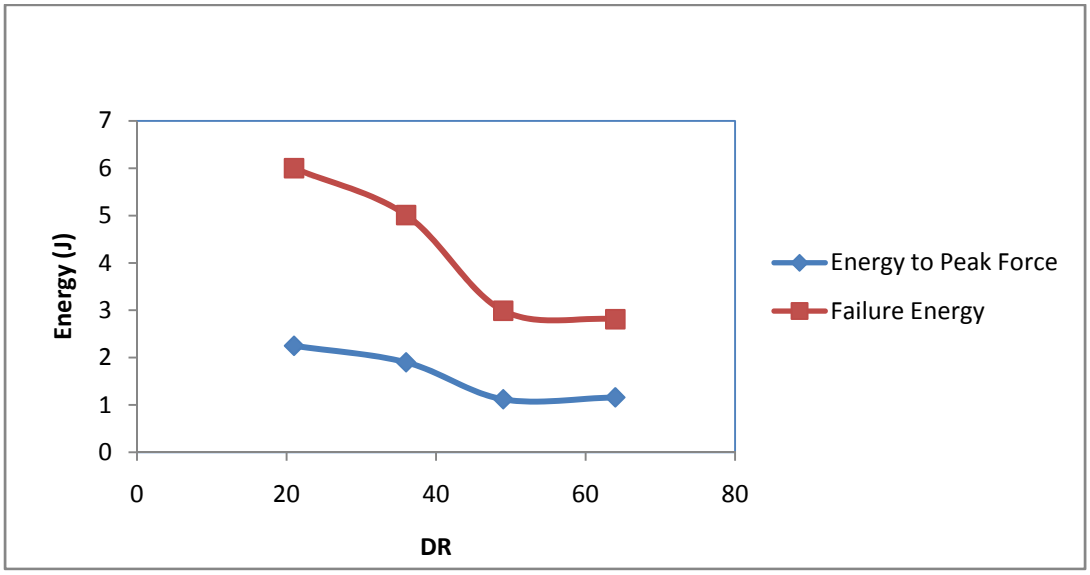

Figure 5.7. Impact Energies at different draw ratios.

5.1.3 Tear Test.

Figure 5.8 shows that tear resistance in transverse direction improves while increasing draw ratio. In machine direction, increasing the draw ratio has no strong effect in tear resistance. Kim et al. [21] pointed that if the molecules are oriented in the machine direction, the TD tear resistance will increase while the MD tear resistance will drop. In our present study, increasing the draw ratio from 36 to 64 enhanced the orientation in the machine direction, as shown in figure 5.2. From figure 5.8, the TD tear resistance is enhanced going from 36 to 64 draw ratios, while the MD tear resistance drops. This is exactly what has been inferred by Kim et al.

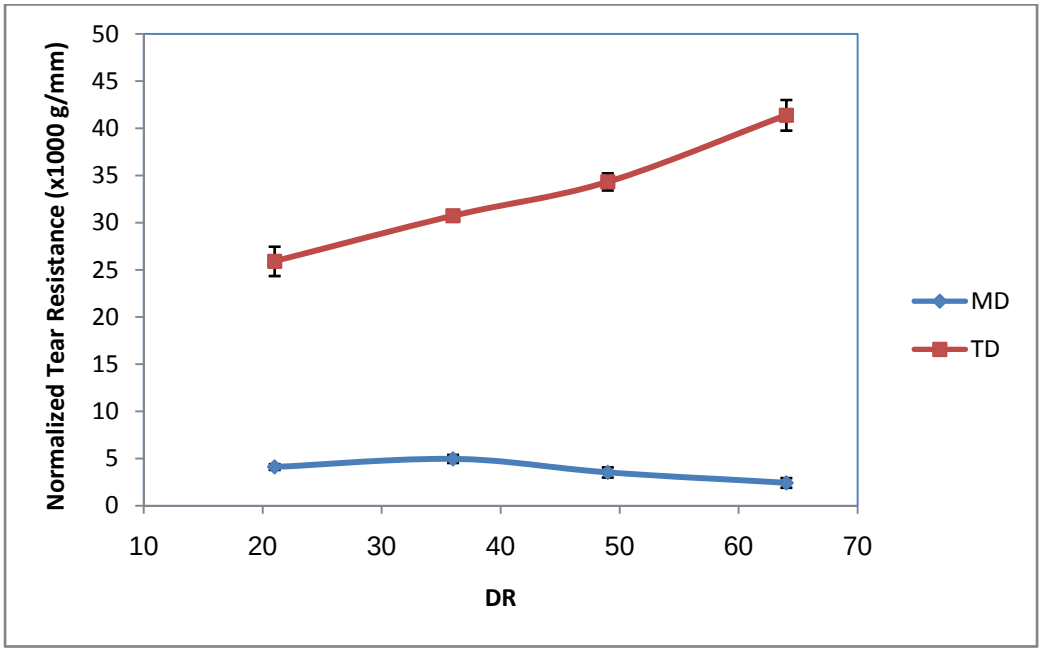

Figure 5.8. Normalized tear resistance at different draw ratios.

From the abovementioned discussion, a draw ratio of 21 gives better impact properties. From the tensile test, draw ratios of 21, 36, and 49 have similar strengths in both

directions but 21 shows much better ductility especially in machine direction. The selection of the optimum draw ratio is based on the impact test as it accounts for both directions of the tested film. Therefore, a draw ratio of 21 is chosen for further analysis, which is the same draw ratio used in the previous study using h-LLDPE by Sarfaraz [27].

5.2 Effect of Blow Ratio on Mechanical Properties of b-LLDPE Films.

The target is to select the optimum blow ratio that gives better mechanical properties of the produced films. As discussed in the previous chapter, the blow ratios used are 1.1, 1.4 and 1.8. These blow ratios were selected conforming to machine and processability constraints.

5.2.1 Tensile Test.

The crystallinity percent and the orientation of tested films at different blow ratios are shown in figures 5.9 and 5.10, respectively. From the orientation curve, it seems that increasing the blow ratio caused the molecules to orient themselves in the transverse direction. The crystallinity is also increased while increasing the blow ratio.

Figure 5.11 shows the effect of changing the blow ratio on the yield strength in machine and transverse directions. In machine direction, the yield strength decreases from a maximum value of 10 MPa at a blow ratio of 1.1 by 17% at a blow ratio of 1.4 and by 10% at a blow ratio of 1.8. In TD, the yield strength has a maximum value at a blow ratio of 1.1 then it decreases by 16% at 1.4 and by 19% at 1.8. Figure 5.12 shows the effect of changing the blow ratio on the tensile strength in machine and transverse directions. The tensile strength in MD has a maximum value at a blow ratio of 1.1. It then decreases by 16% to a minimum value at 1.4. The tensile strength is recovered again in the blow ratio of 1.8. In TD, the tensile strength decreases linearly while increasing the blow ratio. The decrease of yield and tensile strengths and ductility in TD while increasing the blow ratio might be due the increase in the orientation in the transverse direction as shown in figure 5.10.

Figure 5.13 shows that the ductility in machine direction remains unchanged while changing the blow ratio, whereas in the transverse direction, the ductility decreases by almost 30% when increasing the blow ratio from 1.1 to 1.4 or 1.8. Figure 5.14 shows the toughness of the tested films in both directions. For 1.1 and 1.8 blow ratios, the toughness in both directions is almost the same. At a blow ratio of 1.4, toughness has a maximum value at MD and a minimum value at TD.

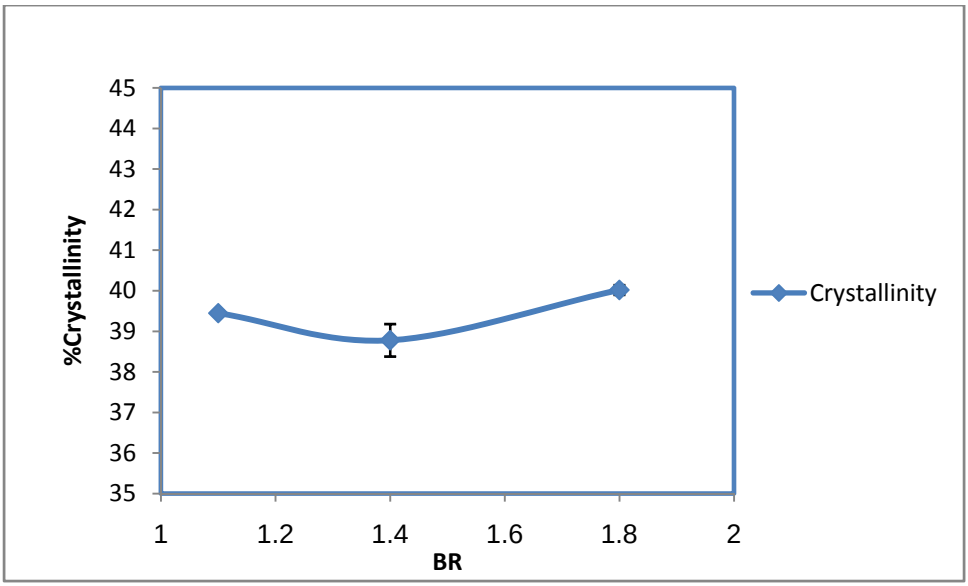

Figure 5.9. Crystallinity of b-LLDPE at different BRs.

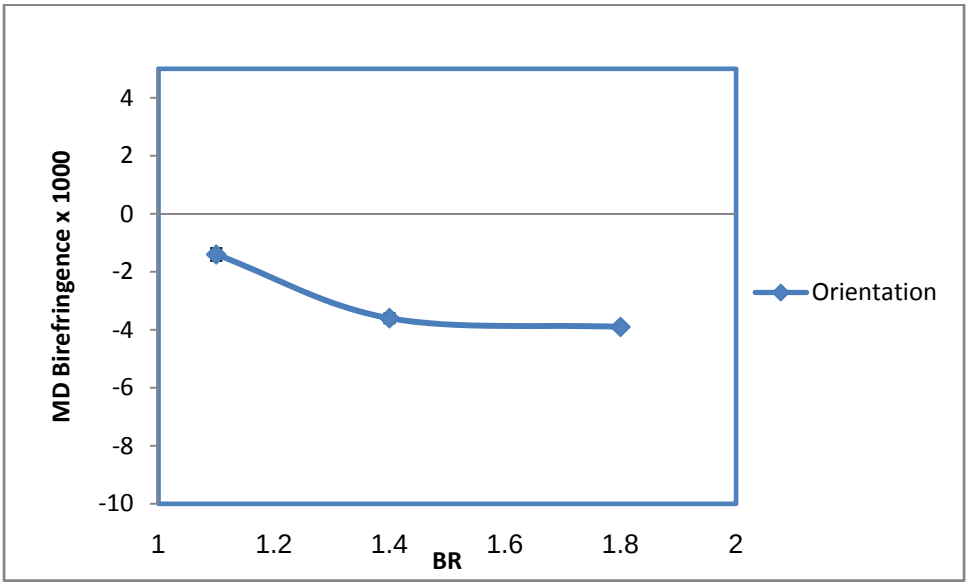

Figure 5.10. Orientation results for 1st order birefringence at different BRs.

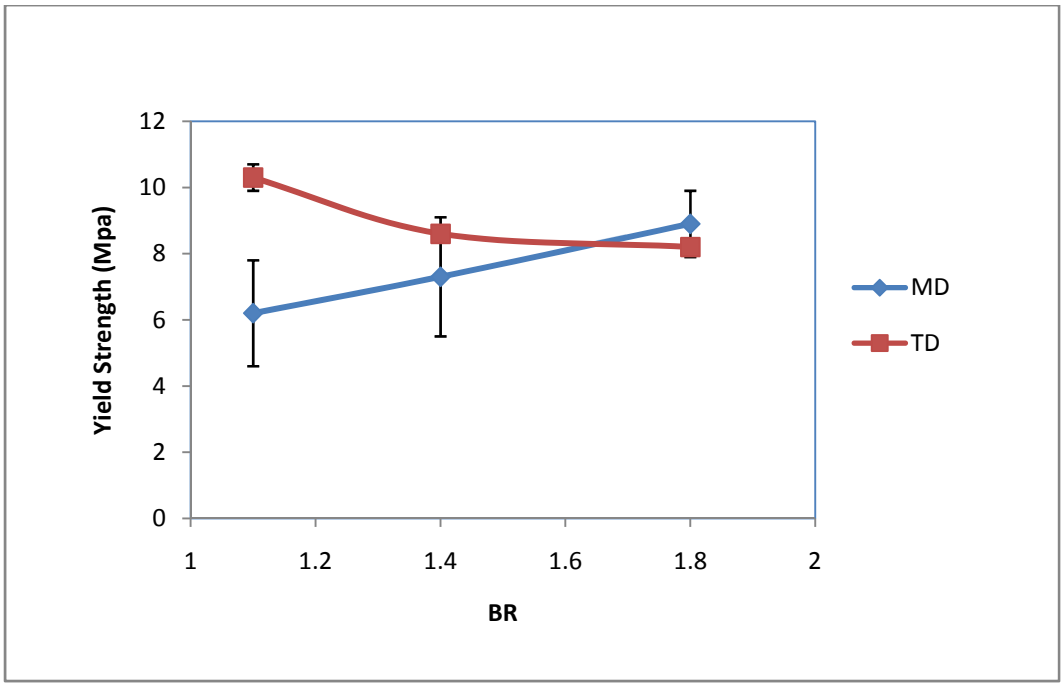

Figure 5.11. MD and TD yield strengths at different blow ratios.

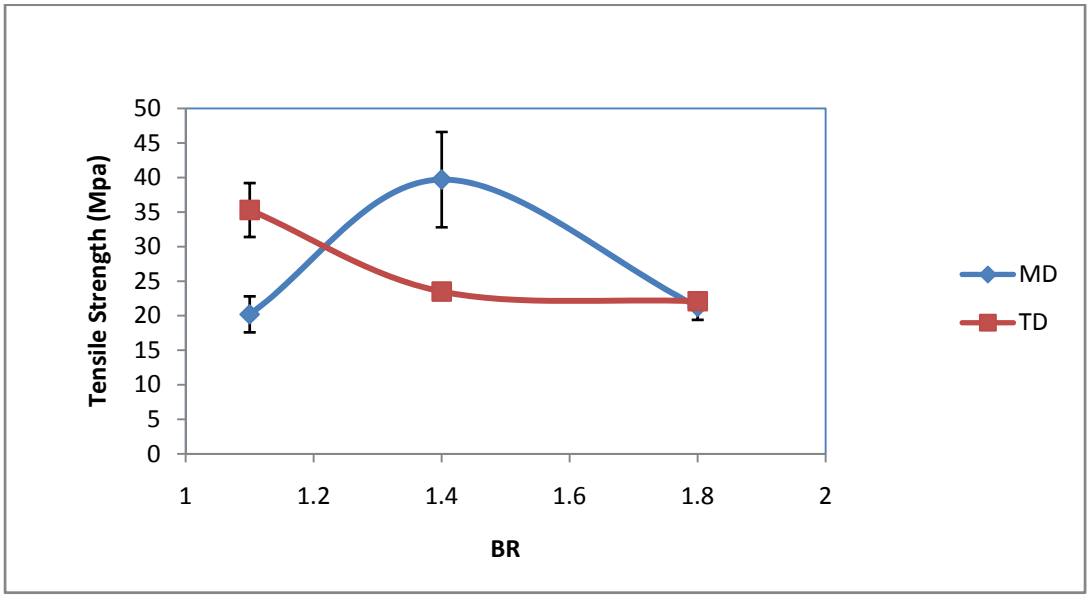

Figure 5.12. MD and TD tensile strengths at different blow ratios.

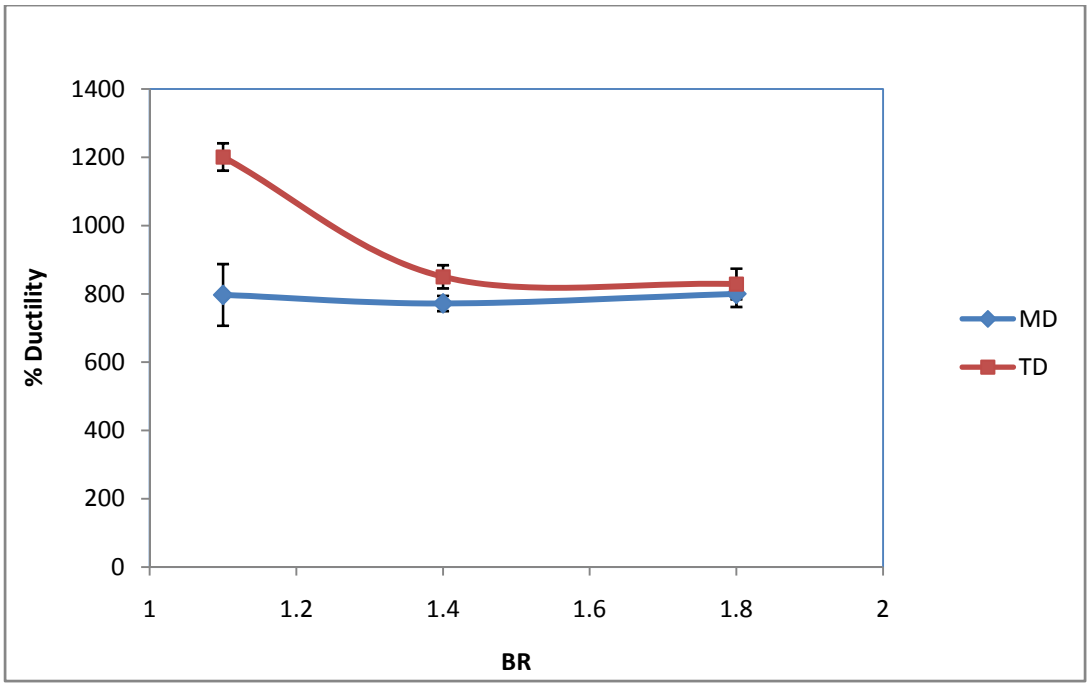

Figure 5.13. MD and TD ductility at different blow ratios.

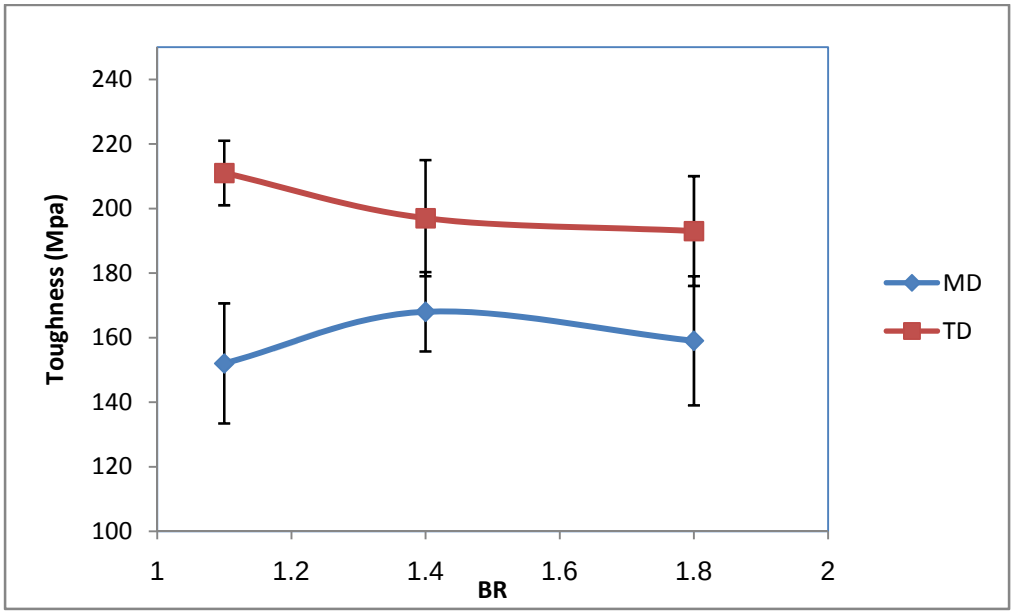

Figure 5.14. MD and TD toughness at different blow ratios.

5.2.2 Impact Test.

Figure 5.15 shows the effect of changing the blow ratio on the impact energies. A blow ratio of 1.4 gives the best impact energies. For 1.1 and 1.8, the impact properties are almost the same. The industrial blow ratios are within the range from 2 to 2.5 which cannot be obtained with our existing setup. In our case, we would choose a draw ratio between 1.4 and 1.8 for optimization purposes, because we need to have wider films as to satisfy commercial needs. The selection of 1.6 blow ratio would be appropriate as it shows moderate mechanical properties and wider films.

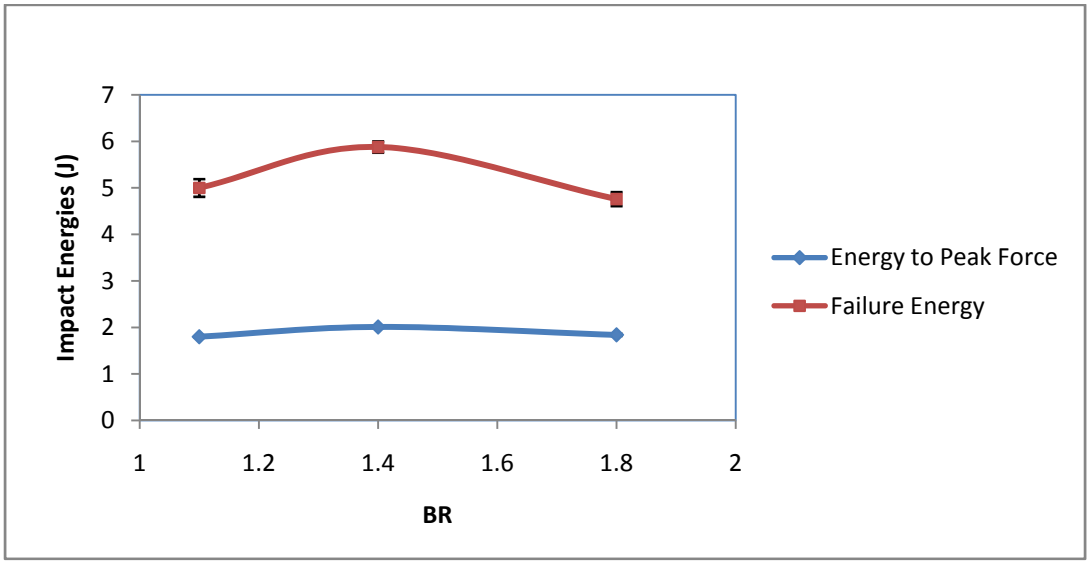

Figure 5.15. Impact Energies at different blow ratios.

5.2.3.Tear Test.

Figure 5.16 shows the effect of changing the blow ratio on the normalized tear resistance in both directions. The blow ratio of 1.4 has the maximum normalized tear resistance in transverse direction and the values of 1.1 and 1.8 are almost the same. In machine direction, the normalized tear resistance decreases with decreasing the blow ratio.

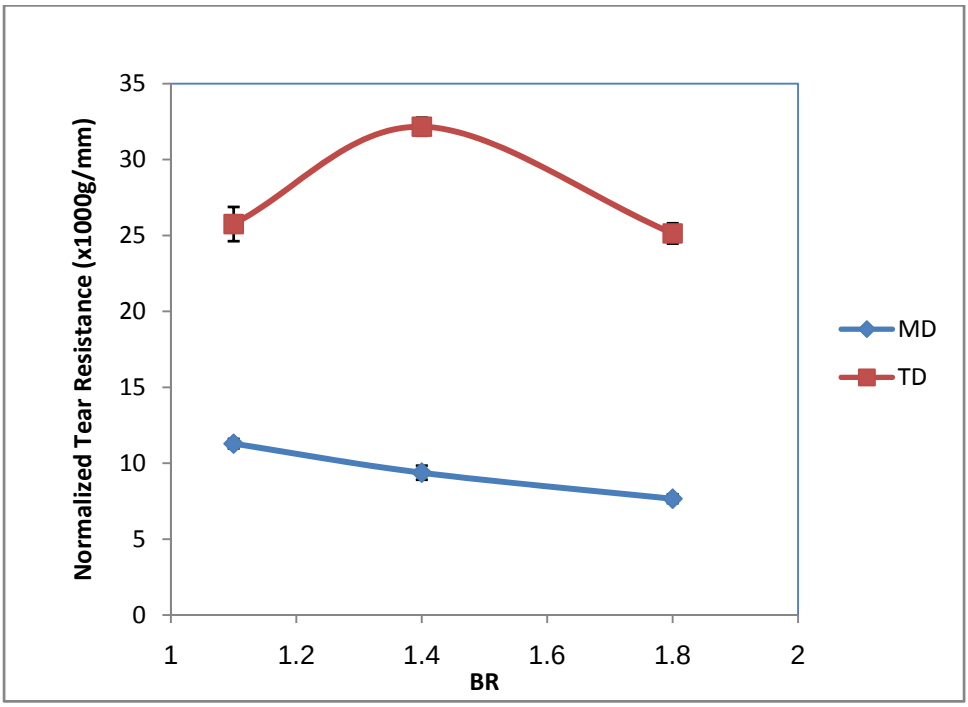

Figure 5.16. Normalized tear resistance at different blow ratios.

From the previous discussion, a blow ratio of 1.6 is selected for further analysis. In industries, a blow ratio of 2.5 is common, but it is beyond the capability of our setup. If the blow ratio exceeds 1.8, the bubble touches the air ring and fractures. Increasing the mass flow rate might solve the problem, but doing so will increase the torque needed to turn the motor. The mass flow rate of 8 g/min is the maximum flow rate can be attained by our existing conditions. From the mechanical properties point of view, a blow ratio between 1.4 and 1.8 is preferred. So, a blow ratio of 1.6 is suitable.

5.3 Effect of Blend Ratio on Mechanical Properties of b-LLDPE/LDPE Blown Films.

b-LLDPE and LDPE were blended together with the help of the two controlled feeders. The different blend ratios are listed in table 4.15. The results of thermal and mechanical tests are presented in this section. A blow ratio of 1.6, a draw ratio of 21 and a mass flow rate of 8.3 g/min are maintained during the blending process.

5.3.1 Tensile Test.

The crystallinity percent and the orientation of tested films at different blend ratios are shown in figures 5.17 and 5.18, respectively. It is clear that increasing the amount of LDPE, orients the molecules towards the machine direction. The effect of changing the blend ratio on the yield strength is shown in figure 5.19. In machine direction, adding up to 20% of LDPE enhances the yield strength except for 5%, then the yield strength decreases while increasing the blend ratio. In TD, adding up to 15%, there is a clear deterioration. The yield strength is almost unchanged when adding 20% of LDPE. Adding more than 20%, the yield strength decreases.

Figure 5.20 shows the effect of blend ratio on the tensile strength of the blended films. In MD, the tensile strength increases up to 15%. With the addition of more than 15%, the tensile strength decreases. In TD, the tensile strength decreases at all blend ratios except for 5%. The machine direction yield strength correlates well with the crystallinity results shown in figure 5.17, as the strength would increase if the crystalline content increases; but the other properties don’t have this nice correlation.

The effect of blending on ductility in both directions is shown in figure 5.21. In both directions, the ductility profiles are similar. There is an enhancement in ductility at blend ratios of 5 and 10 %. At 15 and 20% of LDPE the ductility is almost unaltered. It drops with the addition of more than 20%.

Figure 5.22 shows the effect of blend ratio on the toughness of the films. In machine direction, there is an enhancement of about 60% at blend ratios of 10, 15 and 20%. At 5% LDPE, the increase is with almost 10%. In the transverse direction, there is an enhancement when adding 5 or 10% of LDPE by around 16%, but the toughness decreases slightly when adding more than 10%.

The enhancement of tensile properties with the addition of small amounts of LDPE is incredible. Adding some amount of LDPE decreases the torque needed to turn the motor, which enhances the processability. The usual expectation is that increasing the processability will cause some deterioration in the mechanical properties, but in this analysis we gained both, which is a good achievement. Nouri et al. [30] studied the effect of blending on some properties. They used blend ratios from 25 to 75% LDPE. From their studies, they reported that an addition of LDPE will deteriorate the mechanical properties (stress at break and elongation at break). Our enhancement was when adding up to 20%, but they started at 25% LDPE. This might be the reason why they did not realize the enhancement.

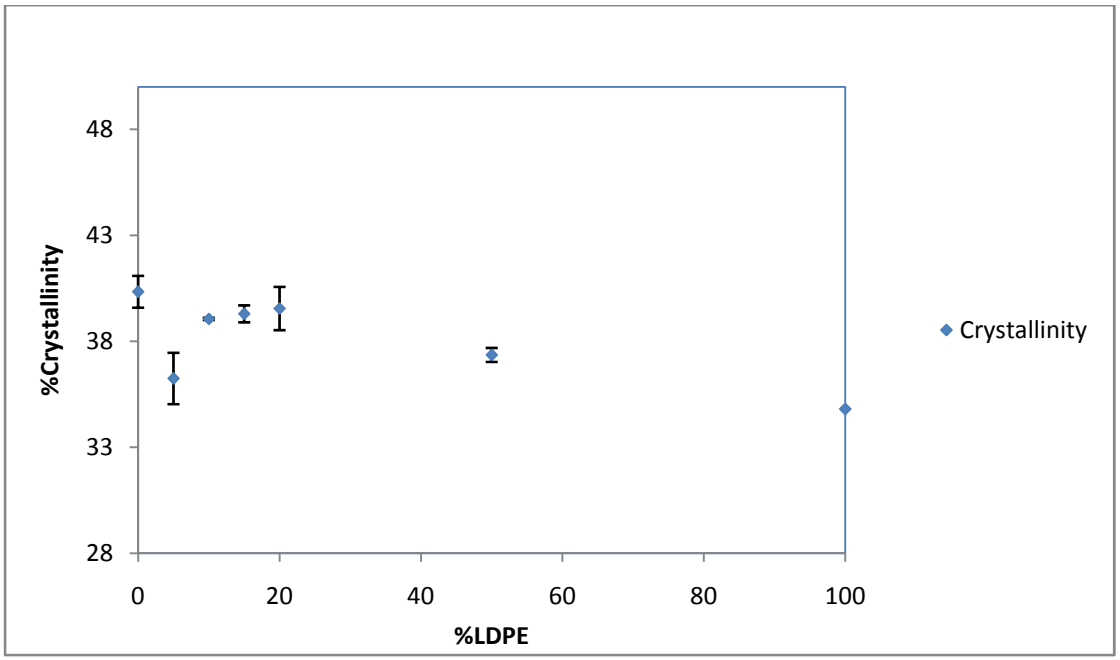

Figure 5.17. Crystallinity of b-LLDPE/LDPE at different blend ratios.

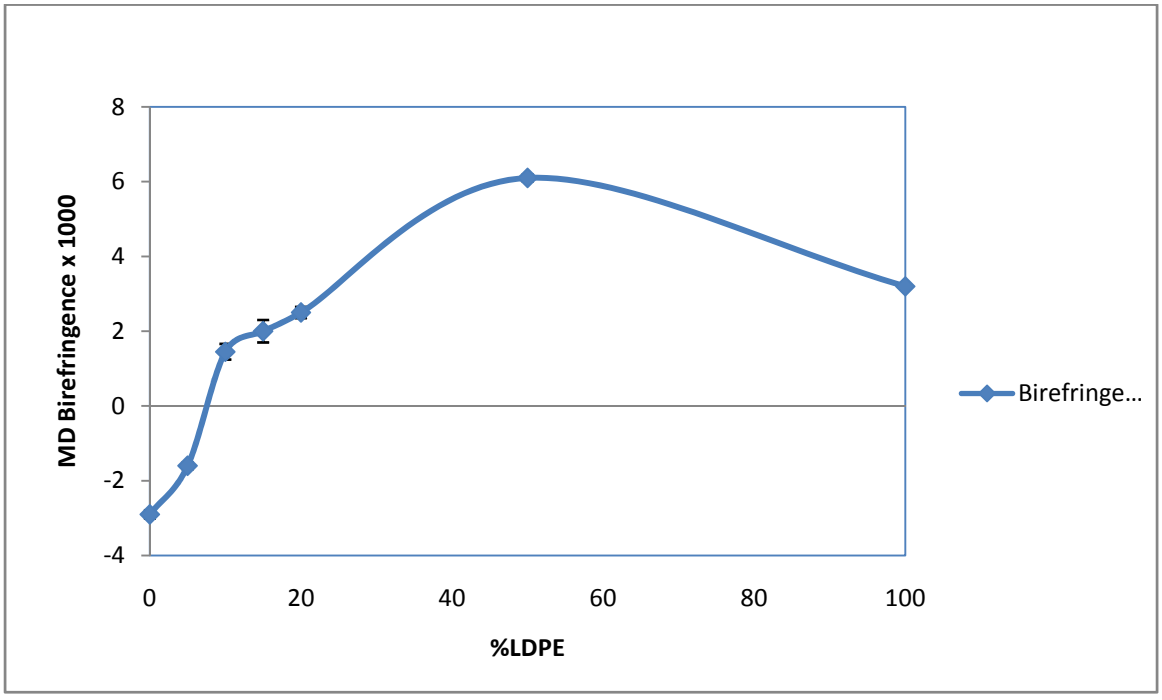

Figure 5.18. Orientation results for 1st order birefringence at different blend ratios.

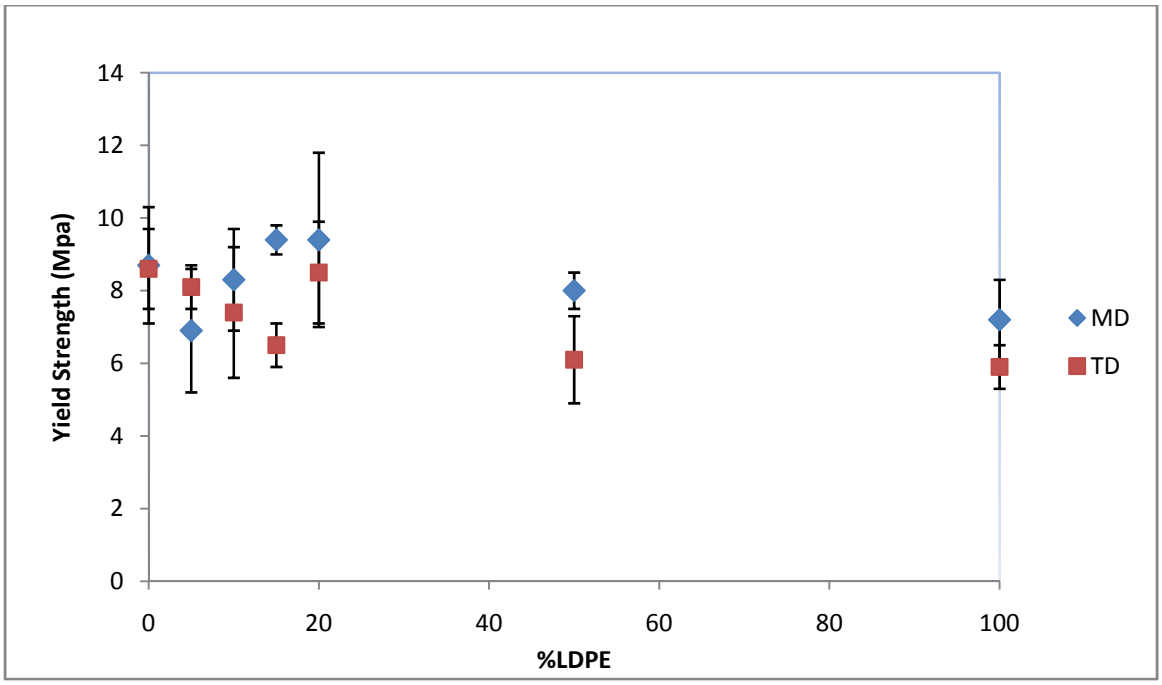

Figure 5.19. MD and TD yield strengths at different blend ratios.

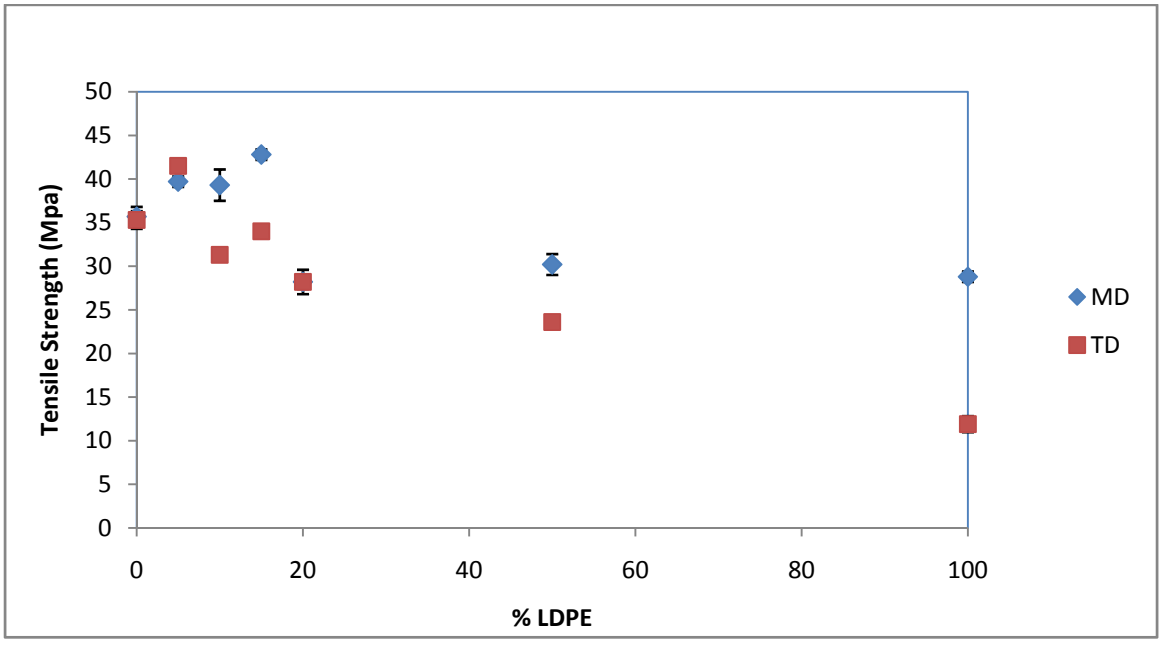

Figure 5.20. MD and TD tensile strengths at different blend ratios.

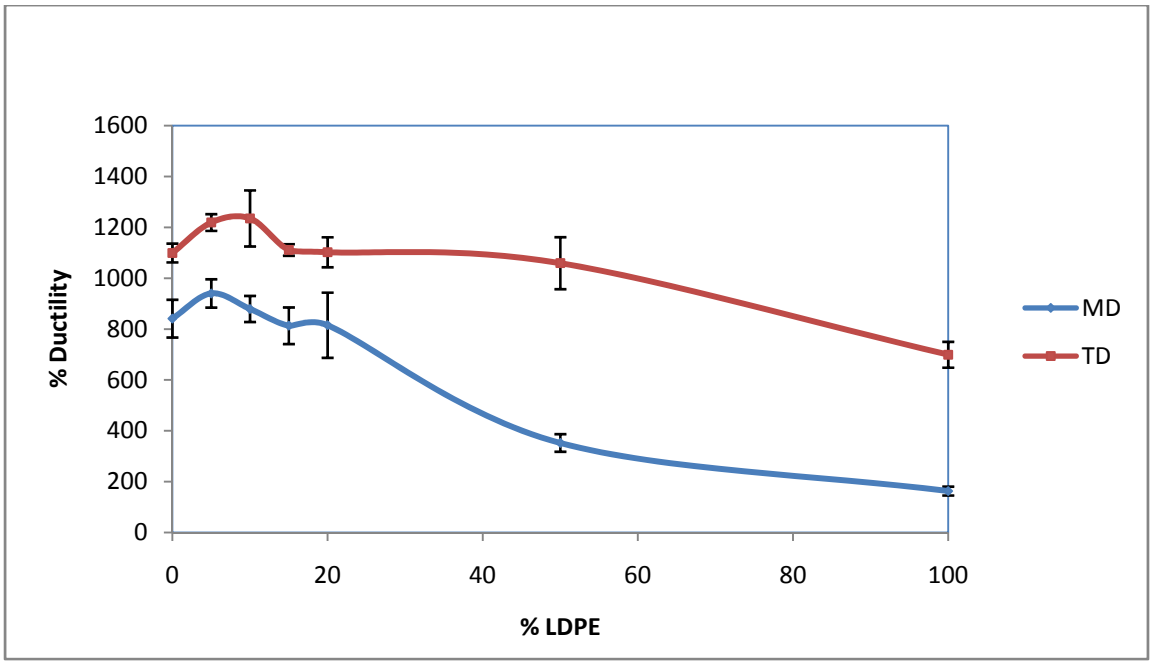

Figure 5.21. MD and TD ductility at different blend ratios.

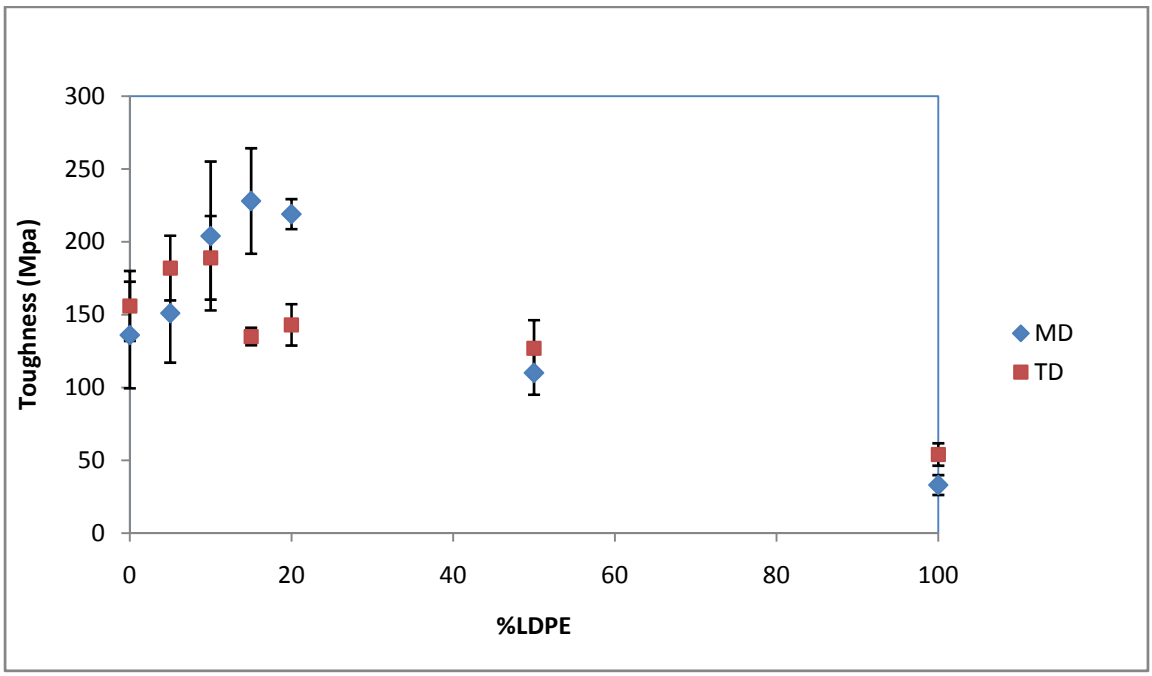

Figure 5.22. MD and TD toughness at different blend ratios.

5.3.2 Impact Test.

The impact properties are affected greatly with the addition of LDPE as shown in figure 5.23. With the addition of only 5% of LDPE, the failure energy and the energy to peak force are increased by almost 25%. Adding 10% of LDPE, shows deterioration in the failure energy but the energy to peak force is enhanced. Adding more than 10% reduces the impact energies. Nouri et al. [30] reported that upon increasing the percentage of LDPE, the Dart Impact energies decrease. Again, they did not study the effect of adding small percentages of LDPE (5-20%). The enhancement in the present study was when adding up to 20% LDPE. Morphological studies are needed to exactly determine the structure-properties relationship. This might be done as a future work of the present study.

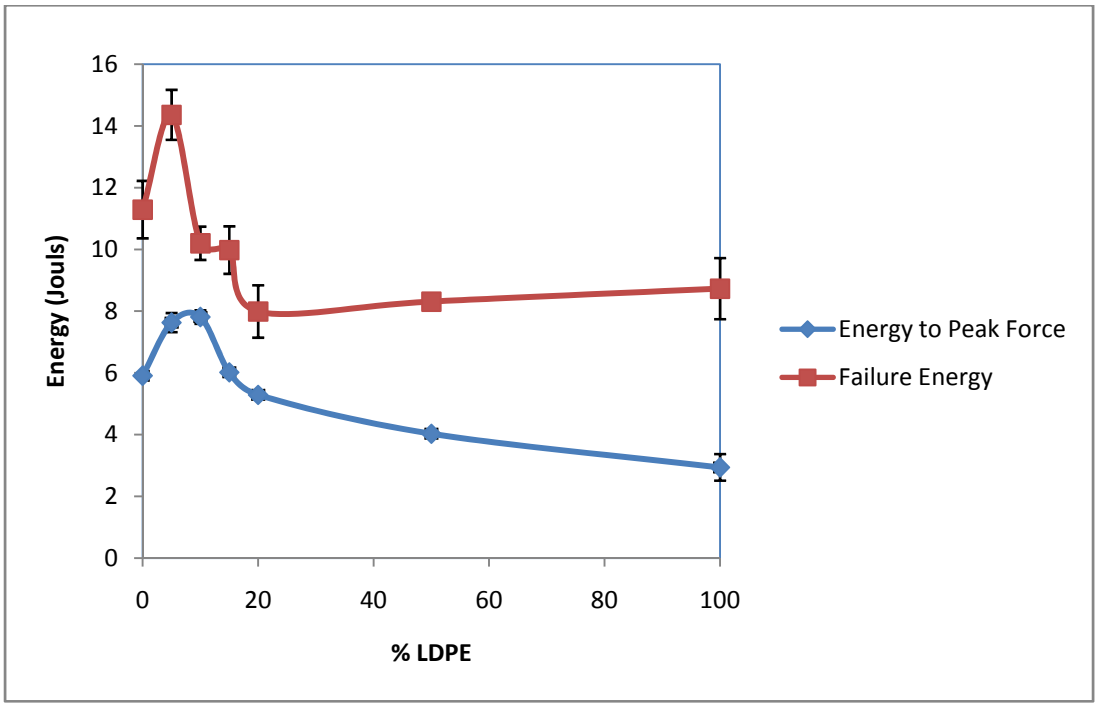

Figure 5.23. Impact Energies at different blend ratios.

5.3.3 Tear Resistance Test.

The effect of blend ratio on the Elmendorf tear resistance is shown in figure 5.24. If 5 or 10% of LDPE is added, the enhancement of TD tear resistance will be around 90%. At 15 and 20% of LDPE the enhancement will be amazingly 115 and 100%, respectively. Above 20% of LDPE, the tear resistance drops dramatically. In machine direction, the tear resistance decreases with increasing the blend ratio up to 15 %, then it remains almost constant. Because the molecules are oriented in the machine direction (figure 5.18), the tear resistance in the transverse direction increases. This trend is the same as what discussed earlier by Kim et al. [21]. Nouri et al. reported that the TD tear resistance decreases while increasing the amount of LDPE between 25-75% LDPE. They did not realize the enhancement since they did not study the effect of adding small percentages of LDPE. Without complete morphological studies, which are out of the scope of the present study, it will be difficult to describe the comprehensive behavior of the material. Anyhow, it is clear that the addition of small percentage of LDPE has a strong influence on the orientation developed within the material as shown in figure 5.18. Because the orientation is enhanced in the machine direction, the tear resistance is improved in the transverse direction and deteriorated in the machine direction for an addition of up to 20% LDPE.

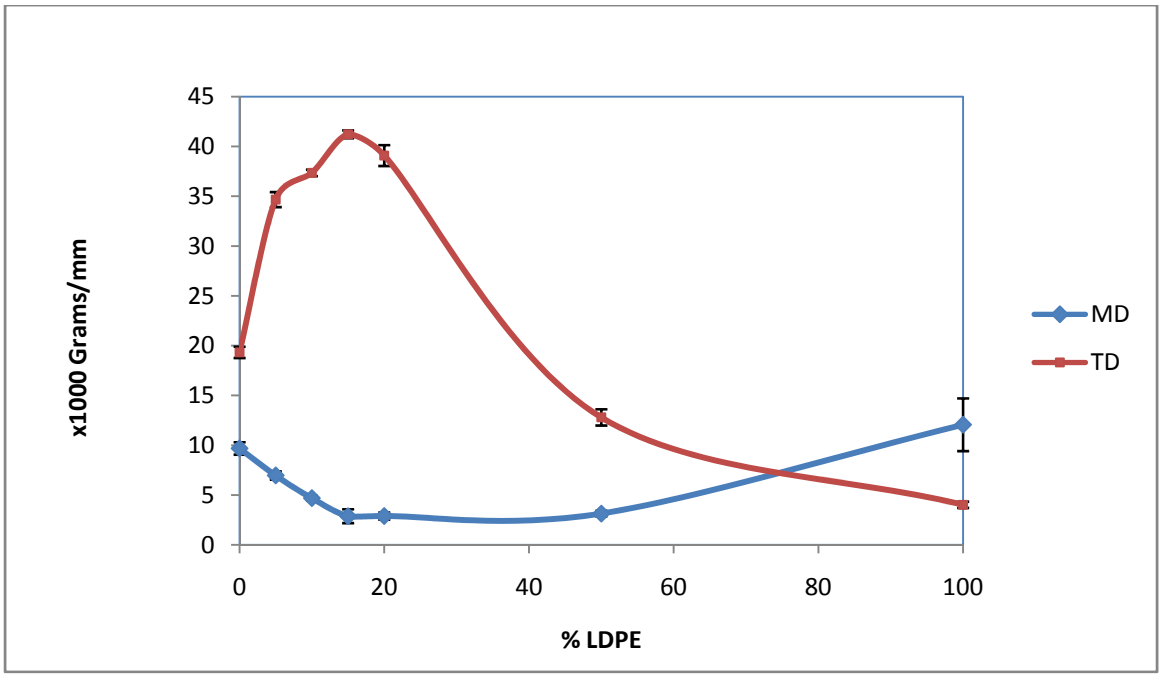

Figure 5.24. Normalized tear resistance at different blend ratios.

From the previous findings, it is clear that having a blend ratio of up to 20% of LDPE with b-LLDPE brought a great achievement to us. Blending with LDPE reduces the torque needed to turn the motor, which lowers the energy consumption and lowers the cost of the process, in turn. From the mechanical tests results, many mechanical properties improved, especially for TD tear resistance and MD toughness.

5.4. Effect of Blend Ratio on the Processability.

Figure 5.26 shows the effect of blending with LDPE on the processability. In the present study, the processability is described in terms of the torque needed to turn the screw of the extruder. As expected, the addition of LDPE enhanced the processability greatly. Reducing the torque means lowering the energy consumption which, in turn, means reducing the cost. Thus, by addition of up to 20%LDPE, we enhance the mechanical properties and improve the processability which is a great achievement.

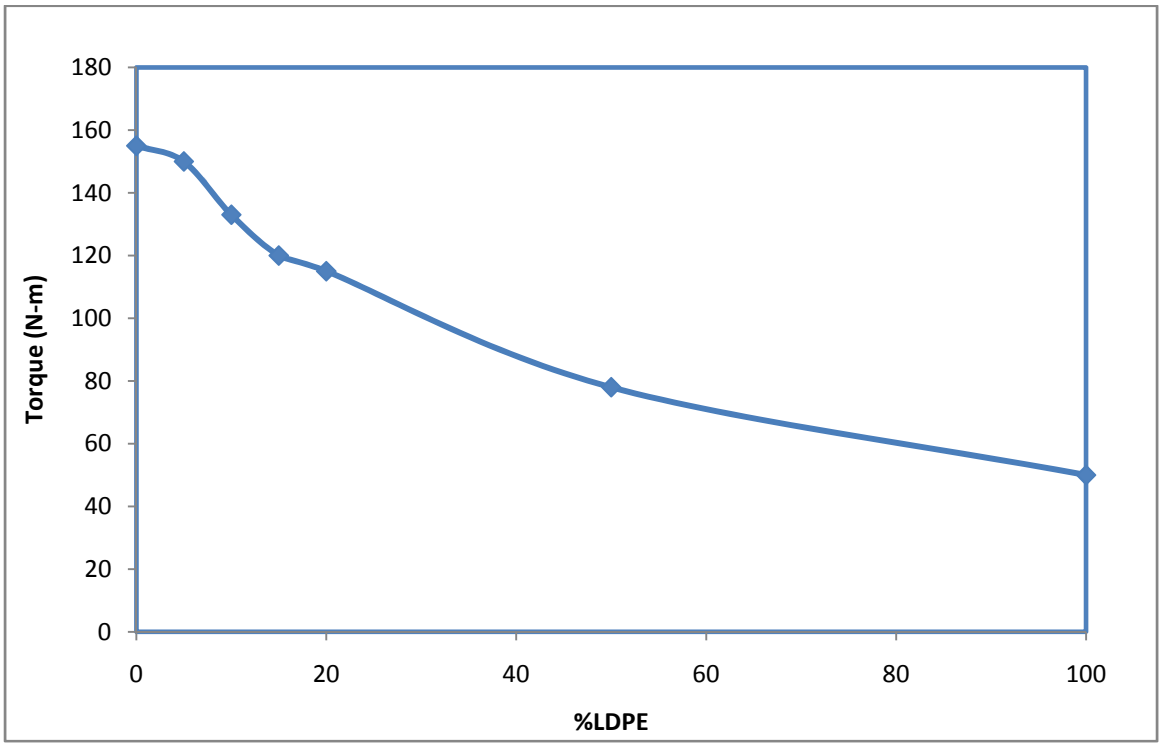

Figure 5.25. Effect of blend ratio on the torque needed to turn the screw of the extruder.

5.5. Comparison between b-LLDPE and h-LLDPE When Blended with LDPE.

Sarfaraz F. [27] did a similar work with the same experimental setup and with the same conditions but with h-LLDPE. The difference between b-LLDPE and h-LLDPE is in the length of the side branches. In b-LLDPE, there are two carbon atoms in the side branch, while in h-LLDPE, there are four carbon atoms. He found that with addition of up to 20% LDPE, there was a 20% enhancement in MD yield strength without any decrement in the MD ductility. The MD toughness also observed an increment of around 43%. The enhancement in TD tensile strength was more than 75%. The TD ductility improved slightly in comparison to pure h-LLDPE. There was 20% enhancement in failure energy due to 5% blend ratio. The TD tear resistance improved by almost 100% by adding 20% of LDPE. With addition of up to 20% many mechanical properties improved. These findings are almost the same as for b-LLDPE, even the percentages of enhancement or deterioration are almost the same. The only difference is that h-LLDPE presents a wider range of draw ratio. Draw ratios of 7 or 86 were not possible for b-LLDPE. This might indicate that the processability of h-LLDPE is somehow better but the mechanical properties are almost identical between the two polymers.

CHAPTER SIX

CONCLUSION

In this study, a twin screw extruder was used to melt and process the polymer. The extruder has an L/D ratio of 40 and it has seven controllable heating zones. A temperature profile of 120/ 150/ 180/ 200/ 200/ 200/ 200 ^{o}C was maintained throughout the extruder. This temperature profile was chosen by putting into account the machine limitations, processability and the degradation of the polymer. The optimized screw speed was 12 rpm. This speed provided the maximum flow rate without overwhelming the motor torque limitation. The pressure at the extruder exit was around 16 bars. The melt pump speed of 10 rpm was optimum as to maintain constant flow rate. The maximum flow rate was 8.3 grams/min. The effect of draw ratio on the thermal and mechanical properties of the blown films was investigated. The draw ratio can be varied by changing the nip rolls speed. In this study, draw ratios of 21, 36, 49 and 64 were used. A draw ratio of 21 was selected because it gave better thermal and impact properties. The effect of blow ratio on mechanical properties of b-LLDPE films was then studied. The blow ratio of 1.6 was chosen based on better mechanical properties. At the end, blending pure LDPE with b-LLDPE was performed with the following percentages: 5, 10, 15, 20 and 50% of LDPE. The effect of blend ratio was studied. Adding up to 20% of LDPE enhanced the yield strength in machine direction except for 5%, then the yield strength decreased while

increasing the blend ratio. In TD, adding up to 15%, there was a clear deterioration. The yield strength was almost unchanged when adding 20% of LDPE. Adding more than 20%, the yield strength decreased. The tensile strength in MD increased up to 15% LDPE. With the addition of more than 15%, the tensile strength decreased. In TD, the tensile strength decreased at all of the blend ratios except for 5%. The machine direction yield strength correlated well with the crystallinity results. In both directions, the ductility profiles are similar. There was an enhancement in ductility at blend ratios of 5 and 10 %. At 15 and 20% of LDPE the ductility was almost unaltered. It dropped with the addition of more than 20%. Figure 5.22 shows the effect of blend ratio on the toughness of the films. Regarding films toughness, there was an enhancement in machine direction of about 60% at blend ratios of 10, 15 and 20%. At 5% LDPE, the increase was with almost 10%. In the transverse direction, there was an enhancement when adding 5 or 10% of LDPE by around 16%, but the toughness decreased slightly when adding more than 10%.

The enhancement of tensile properties with the addition of small amounts of LDPE was incredible. Adding some amount of LDPE decreased the torque needed to turn the motor, which enhanced the processability. The usual expectation is that increasing the processability will cause some deterioration in the mechanical properties, but in this analysis we gained both, which was a good achievement.

The impact properties were affected greatly with the addition of LDPE. With the addition of only 5% of LDPE, the failure energy and the energy to peak force were increased by almost 25%. Adding 10% of LDPE, showed deterioration in the failure energy but the energy to peak force was enhanced. Adding more than 10% reduced the impact energies. Morphological studies are needed to exactly determine the structure-properties

relationship. This might be done as a future work of the present study. The effect of blend ratio on the Elmendorf tear resistance was carried out. If 5 or 10% of LDPE is added, the enhancement of TD tear resistance will be around 90%. At 15 and 20% of LDPE the enhancement was amazingly 115 and 100%, respectively. Above 20% of LDPE, the tear resistance dropped dramatically. In machine direction, the tear resistance decreased with increasing the blend ratio up to 15 %, and then it remained almost constant. Without morphological studies, which are out of the scope of the present study, it will be difficult to describe the behavior of the material. Anyhow, it was clear that the addition of small percentage of LDPE had a strong influence on the orientation developed within the material. Because the orientation was enhanced in one direction, the tear resistance was improved in one direction and deteriorated in the other.

It is clear that having a blend ratio of up to 20% of LDPE with b-LLDPE brought a great achievement to us. Blending with LDPE reduces the torque needed to turn the motor, which lowers the energy consumption and lowers the cost of the process, in turn. From the mechanical tests results, many mechanical properties improved dramatically, especially for TD tear resistance and MD toughness.

The findings of Sarfaraz work with h-LLDPE [27] are almost the same as for b-LLDPE, even the percentages of enhancement or deterioration are almost the same. The only difference is that h-LLDPE presents a wider range of draw ratio. Draw ratios of 7 or 86 were not possible for b-LLDPE. This might indicate that the processability of h-LLDPE is somehow better but the mechanical properties are almost identical between the two polymers.

CHAPTER SEVEN

FUTURE WORK

- Future work could be carried out on morphological structure of the films using rheological instruments.
- Structural development analysis using SEM or TEM should be carried out to comprehensively investigate the structure-properties relationship of b-LLDPE.
- The effect of mass flow rate on the mechanical properties needs also to be studied.
- Effect of extrusion temperature on the size of the operating window could be studied.
- Effect of blending o-LLDPE with LDPE might also be investigated.

REFERENCES

1- A. Peacock, "Handbook of Polyethylene: Structures, Properties, and Applications", 1st Ed., New York: Marcel Dekker, Inc. (2000)

2- J. Pearson and C. Petrie. The flow of a tubular film. Part 1. Formal mathematical representation. Journal of Fluid Mechanics, 40(1):1-19, 1970.

3- J. Pearson and C. Petrie. The flow of a tubular film. Part 2. Interpretation of the model and discussion of solutions. Journal of Fluid Mechanics, 42(3):609-625, 1970.

4- C. Petrie. Computational Analysis of Polymer Processing, Chapter 7, Pages 217-241. Applied science, London, 1983.

5- O. Sweeting, ed., "The Science and Technology of Polymeric Fluids," vol. 1 and 2, wiley, 1971.

6- H. Mark and N. Gaylord, eds., "Encyclopedia of Polymer Science and Technology," Interscience, 1964.

7- R. Farber and J. Dealy, Polym. Eng. Sci., 14,435 (1974)

8- G. Manges and W. Predhol , Polym. Eng. Sci., 15, 394 (1975)

9- S. Goren, S. Middlman, and J. Gavis. Journal of Applied Polymer Science, 3 , 367 (1960)

10- S. Middlman, and J. Gavis, Phys. Fluids, 4 , 355; 4 ,963; 4 1450 (1961)

11- O. Truesdell, Trans. Soc. Rheol., 4 , 9 (1960)

12- W. Ast, "Air Cooling on Blown Films Lines" Kunstoffe 46 , 146 (1974)

13- C. Han, and J. Park, "Studies on Blown Film Extrusion. III. Bubble Instability" Journal of Applied Polymer Science. 19 , 3291 (1975).

14- T. Kanai and J. White, “Kinematics, Dynamics and Stability of Tubular film extrusion of Various Polyethylenes”, Polymer Engineering Science 24 1185 (1984)

15- W. Minoshima and J. White, “Instability Phenomena in Tubular Film, and Melt Spinning of Rheological Characterized High Density, Low Density and Linear Low Density Polyethylenes” Journal of non-Newtonian Fluid Mechanics 19, 275 (1986)

16- A. Ghaneh-Fard, P. Carreau and P. Lafleur, “Study of Instabilities in Film Blowing” AICHE Journal 42, 1388 (1996)

17- A. Beagan and C. Malleja, “The extrusion, performance and characterization of metallocene-catalyzed polyethylene based packaging films”, DAI-C 61/104,

Winter (2000), p.1091.

18- M. Shishesaz and A. Donatelli, “Tensile Properties of Polyethylene Blends”, Polymer Engineering and Science, Vol 21, No 13, pp 869-872(1981).

19- K. Rajendra and J. Lamborn, “Tensile properties of linear low-density polyethylene (LLDPE) blown films”, Polymer Engineering and Science, Vol 40, No 11, 2000, pp 2385-2396.

20- S. Jafari, A. Rana and K. Surya, “Tensile fracture morphology/properties correlation of high-density/linear low-density polyethylene blends”, Iranian Polymer journal, Vol 9, No 3, 2000, pp 133-142.

21- Y. Kim and J. Park, "Effect of short chain branching on the blown film properties of LLDPE”, J. Applied Polymer Science, Vol.61, 2315-2324 (1996).

22- Y .Hong et al. “Film blowing of LLDPE blended with a novel hyperbranched polymer processing aid”, Polymer. Vol,41. 7705-7713 (2000).

23- Y. Fang, P. Carreau, P. Lafleur and S. Ymmel, “Properties of mLLDPE/LDPE blends in film blowing” Polymer Engineering and Science, 343-353 (2005).

24- R. Krishnaswamy and A. Sukhadia, “Orientation characteristics of LLDPE blown films and their implications on Elmendorf tear performance” Polymer, Vol. 41, 9205-9217 (2000).

25- P. Gupta et al. “Does the length of the short chain branch affect the mechanical properties of linear low density polyethylenes? An investigation based on films of copolymers of ethylene/1-butene, ethylene/1-hexene and ethylene/1-octene synthesized by a single site metallocene catalyst”, Polymer, Vol. 46, 8819-8837 (2005).

26- A. Ward and S. Hadley, “An Introduction to the Mechanical properties of Solid Polymers”, Wiley, Chichester, (1993).

27- S. Furquan, " Effect of Blend Ratio of h-LLDPE with LDPE on The Processability and Mechanical Properties of Blown Films" Master Thesis, KFUPM, (2009).

28- J. Mark, "Physical Properties of polymers", American Institute of Physics, AIP Press, (1996).

29- I. Ward and J. Sweeny, "An Introduction to The Mechanical Properties of Solid Polymers", Wiley Interscience. (2004).

30- M. Nouri, J. Morshedian, A. Rabbani, I. Ghasemi and M. Ebrahimi, " Investigation of LLDPE/LDPE Blown Films by Response Surface Methodology" Iranian Polymer Journal vol.15 (2), 155-162, (2006).

VITA

Name: Wael Sulaiman Fallatah

Present and Permanent Address:

Faculty Housing, Al-Ferdaus Court, KFUPM.

P.O.Box 1328, Dhahran 31261.

Saudi Arabia.

Phone: +966 558441101

Email Address: wfallata@gmail.com

Date of Birth: 19 January 1985

Nationality: Saudi

Education: Master of Science (M.S.) July 2010

Department of Mechanical Engineering

King Fahd University of Petroleum and Minerals

Dhahran, Saudi Arabia

Bachelor of Science (B.S.) June 2007

Department of Mechanical Engineering

King Fahd University of Petroleum and Minerals

Dhahran, Saudi Arabia